This is to certify that the

dissertation entitled

Morphologic Analysis of the Terminal End Bud

in the Prepubertal-Pubertal Mouse Mammary Gland

presented by

Susan Marie Ball-Mulcrone

has been accepted towards fulfillment
of the requirements for

Ph.D. degree in Pathology and
Environmental
Toxicology

Robert Leader
Major professor

Date 3-22-93

MORPHOLOGIC ANALYSIS OF THE TERMINAL END BUD IN THE PREPUBERTAL-PUBERTAL MOUSE MAMMARY GLAND

By

Susan Marie Ball-Mulcrone

A DISSERTATION

Submitted to
Michigan State University
in partial fulfillment of the requirements
for the degree of

DOCTOR OF PHILOSOPHY

Department of Pathology
and
Institute for Environmental Toxicology

1993

ABSTRACT

MORPHOLOGIC ANALYSIS OF THE TERMINAL END BUD IN THE PREPUBERTAL-PUBERTAL MOUSE MAMMARY GLAND

By

Susan Marie Ball-Mulcrone

Ultrastructural and histologic analysis of normal terminal end buds (TEB) from Balb/c and athymic nude (Nu/+) prepubertal-pubertal mouse mammary glands confirmed the presence of four cell types and identified a fifth morphologically distinct cell termed the "myocap" cell (MCC). Morphometric analysis showed that undifferentiated cap cells (CC) and intermediate cells (IC) had the largest nuclear and cellular areas followed by the differentiated myoepithelial cells (MEC) and luminal cells (LC).

Analysis of the TEB revealed that CCs possess no visible intercellular junctions or adhesions with neighboring CCs or stromal cells (SC), MECs possess primarily desmosomes, and ICs and LCs display various tight and intermediate junctions in addition to desmosomes. No gap junctions were identified in the cells examined and direct contact between CCs and SCs was not observed.

Asynchronous development of TEB structures was documented in the prepubertal-pubertal mouse mammary gland. The No. 2 and No. 3 thoracic and No. 4 inguinal glands were collected from Nu/+ mice weaned at 21 days of age and fed a high fat non-restricted intake diet for 2 and 3 weeks post-weaning. At 5 weeks of age, the No. 2 and No. 3 gland mean maximum TEB (MTEB) area and mean number of TEBs per gland (NTEB/G) were significantly greater than the No. 4 gland. By 6 weeks of age, the No. 2 gland means significantly decreased, indicating that the largest and greatest number of TEB structures is present at approximately 5 weeks of age. The No. 3 and No. 4 gland means remained relatively constant between 5 and 6 weeks of age.

The effect of body weight and feed consumption on TEB development was examined against mean MTEB area and mean NTEB/G. At 5 weeks of age, mice with higher initial weights and greater total feed consumption had larger TEBs when litter pairs were conserved and threshold limits imposed. By 6 weeks of age, the consistent lack of significance found between dependent and independent variables appeared to be associated with a developmental decrease in the overall size and number of TEBs as well as a decrease in the variation of body weight and feed consumption.

Dedicated with love and appreciation to my husband Jim and to my children Ryan, Patrick and Lauren.

ACKNOWLEDGEMENTS

I sincerely thank the members of my committee for their time and support over the past five years. Each of these individuals had a special role in the pursuit and completion of my dissertation. Dr. Behzad Yamini, my former office mate and dear friend, who encouraged me to pursue my dissertation. Dr. Robert Leader, Chairperson of my committee and coordinator of the National Institutes of Health post-doctoral multidisciplinary training program between the Department of Pathology and the Institute for Environmental Toxicology who accepted me into the program in 1987. Dr. Stuart Sleight, my former instructor in veterinary pathology. Dr. Sleight's knowledge, financial and personal support during the latter 2 years of my program was instrumental in the completion of my degree. Dr. James Trosko, one of my graduate instructors, whose ideas regarding the mechanisms of carcinogenesis captivated me and will remain a focus in my future research. And lastly, Dr. Karen Klomparens, my friend, confidant, teacher and mentor. I owe a great deal of my ability to complete this dissertation to her. Without Dr. Klomparens' academic guidance, personal and financial support I would not have been able to complete this dissertation.

She has been and always will be a true "mentor" to me. I have a tremendous degree of respect for her and aspire to live up to her standard of academic and personal professionalism.

I extend my deepest appreciation to Dr. John Heckman for his guidance, support and assistance during many long hours spent in the Center for Electron Optics; Ralph Common for his technical assistance and contribution of high quality light microscopic prints; Dr. Gregory Fink for his statistical expertise and guidance; and Shirley Eisenhauer for her friendship and clerical contribution to my dissertation.

I acknowledge the contribution of Jane DeHoog, Debbie O'Connor and Vonnie VanderPloeg for their laboratory assistance and Dr. Clifford Welsch for his financial contribution to my research project.

Finally, it is with much love in my heart that I thank the Lord for seeing me through this difficult goal and my family and friends for their love and support over the past several years. For without them, this would be but a bittersweet accomplishment. A special thank you to my loving husband and children, my mom and dad, mother-in-law Helen Mulcrone, aunt and uncle Eileen and Bob Yost, and dear friends Nailah and Greg Orr.

TABLE OF CONTENTS

LIST OF TABLES

LIST OF FIGURES

LIST OF ABBREVIATIONS

AB	alveolar bud
ANOVA	analysis of variance
A°	angstroms
AS	alveolar sac
BL	basal lamina
CC	cap cell
CO	corn oil
C°	degrees celsius
DHA	docosahexaenoic acid
DMBA	dimethylbenzanthracene
DNA	deoxyribonucleic acid
E	estrogen
ECM	extracellular matrix
EFAs	essential fatty acids
EGF	epidermal growth factor
EPA	eicosapentanoic acid
EPF	estrogen potentiating factor
ER	endoplasmic reticulum
EtOH	ethyl alcohol
FGF	fibroblastic growth factor
FPF	fat pad filled
FPP	fat pad precursor tissue
FW	final weight
GAG	glycosaminoglycans
HCTO	hydrogenated cotton seed oil
H_o	null hypothesis
IC	Intermediate cell
IGF	insulin growth factor
IM	indomethacin
IW	initial weight
L	left
LC	luminal cell
LNo	left number
M_2	mean MTEB area of gland number 2
M_3	mean MTEB area of gland number 3
M_4	mean MTEB area of gland number 4
MEC	myoepithelial cell
ml	milliliters
mm	millimeters
MTEB	maximum terminal end bud
nm	nanometers
No.	number

Nu	athymic nude mouse
P	progesterone
PMGF	pituitary mammary gland growth factor
PO	propylene oxide
PDGF	platelet derived growth factor
PUFAs	polyunsaturated fatty acids
R	right
RNo	right number
S_L	slope of the line
TEB	terminal end bud
TED	terminal end duct
TFC	total feed consumed
TGF	transforming growth factor
TSH	thyroid stimulating hormone
TWG	total weight gained
ug	microgram
μm	micrometer
μ^2	microns squared

INTRODUCTION

INTRODUCTION

The American Cancer Society (1992) estimates that over 180,000 new cases of breast cancer will be reported in American women in 1992. Out of the 180,000 new cases, 46,000 women will die from this disease. The increase in the incidence of breast cancer, at a rate of approximately 3% per year since 1980 (from 84.8 per 100,000 in 1980 to 109.5 in 1988), is attributed in part to improved techniques in early detection. However, in spite of this improvement, the overall mortality rate associated with breast cancer has not declined in recent years. In fact, the mortality rate has remained relatively stable over the past 50 years.

The inability to reduce the number of deaths associated with breast cancer lies in the complexity of the disease and in the lack of a clear understanding of its diverse etiology and pathogenesis. Most scientists believe that breast cancer is the result of a combination of intrinsic (genetic and endocrine) and extrinsic (diet and socioeconomic) factors. Currently, the majority of research being conducted in this area focuses on the effects of growth factors and receptor-enzyme complexes on DNA and RNA as they relate to the initiation - promotion - progression phases of carcinogenesis. In addition, the effects of hormones, diet and the immune system remain significant areas of research.

Epidemiologic studies which analyze estrous cycles in pubescent females and monitor the levels of estradiol-17ß in sexually mature females in their teens and twenties, have shown that prolonged stimulation of breast epithelial cells by estrogen (i.e., the amount and length of estrogen exposure via menses) is highly correlated with an increased incidence in breast cancer (Bernstein et al., 1990). The results of these ongoing studies suggest that the onset of menses and the period of time between this onset and the first full term pregnancy may be the window of time in which initiation - promotion of breast cancer occurs. Bernstein and his colleagues found that females who had an early menses, less than 13 years of age, had a greater risk of breast cancer, and women, who had a full term pregnancy prior to 20 years of age, had one-half the risk of developing breast cancer when compared to nulliparous women and women who had their first child after age 35.

Morphologically, researchers have documented that a large number of mammary tumors in rodents and breast tumors in women consist primarily of undifferentiated or less well differentiated cells (Russo et al., 1987). Coincidentally, a large number of undifferentiated cells are present in the TEB structure of the prepubertal-pubertal mouse mammary gland. By the nature of their developmental state, these cells are believed to be more susceptible to initiation and promotion events. However, it still remains to be seen if the susceptibility of the undifferentiated cells is or is not

associated with the level or length of estrogen exposure during these early developmental growth periods.

In 1983, Williams and Daniel reported the findings of an in-depth morphologic examination of the terminal end bud and found that it contained 4 major cell types. The first cell type was a peripherally located undifferentiated cell which they termed the "cap cell". They theorized that the cap cell was the stem cell of the mammary gland. The other cell types described in this structure included a body cell (also referred to as the intermediate cell), which is located under the cap cell layer and believed to be the predecessor of the luminal cell, and the fully differentiated myoepithelial cell, a direct descendent of the cap cell, and the luminal cell.

The target cell associated with initiation is believed to reside in the terminal end bud during the period of ductal expansion (Russo and Russo, 1978) or in the mature duct possessing cells that are not fully differentiated and/or have the ability to dedifferentiate (Williams and Daniel, 1983). Therefore, it is possible that the undifferentiated cell population within the TEB, especially the "cap cells", may not only be the stem cells of the mouse mammary gland but may also be the primary target of initiation of mammary gland carcinogenesis. If one assumes that carcinogenesis is the result of intrinsic and extrinsic factors and is multi-staged, and that cancer is a stem cell disease, cap cells, if indeed they are the stem cells of the mammary gland, should play a

key role in the initiation - promotion - progression sequence of mammary gland carcinogenesis.

The primary purpose of this research project was to examine the normal morphology of the terminal end bud during the prepubertal pubertal growth period and to identify unique cellular and developmental relationships associated with communication and growth. Specifically, the objectives were to, 1) ultrastructurally examine the epithelial cells of the terminal end bud structure in the mouse mammary gland, 2) identify the type and degree of intercellular communication between cap cells and adjacent stromal and ductal epithelial cells, i.e., the ability of cap cells to communicate via gap junctions and the ability of cap cells to come in direct contact with adjacent adipocytes and/or fibroblasts, and 3) investigate the effect of body weight and feed consumption on terminal end bud development, i.e., influence on the overall size of the terminal end bud and the number of cap cells per terminal end bud structure.

CHAPTER 1

LITERATURE REVIEW

Taxonomic Categorization of the Laboratory Mouse

Taxonomy. The rodent ancestors of the present day laboratory mouse date back to the early Pleistocene period. Classification of various extinct as well as present day rodents is based on fossil records which contain information on dentition, enamel composition, and cranial variations in skeletal anatomy. The order Rodentia falls under the class Mammalia. Mammalia is considered to be the highest class of living organisms. It includes all vertebrate animals, monotremes, marsupials, and placentals, that are viviparous and possess mammary glands which produce milk for their suckling young. A summary of the taxonomic classification of the mouse is listed in Table 1.1. The infraclass Eutheria is a subclass of mammals that possesses a placenta; and excludes monotremes and marsupials. The order Rodentia is the largest order of placental animals, and includes mice, rats, guinea pigs, squirrels, and beavers, amongst other species. At the familial level, all mice are placed in the superfamily Muroidea and the family Muridae. Muridae is the largest family in the order Rodentia, and of mammals in general. The laboratory mouse is categorized under the genus Mus. Mus includes approximately 16 species of wild mice and numerous domesticated strains (Bonhomme and Guenet, 1989).

Genetic Strains. There are several genetic strains and

variants of laboratory mice used in research today. This large population of rodents is a direct result of cross matings and genetic manipulation by man. Only information regarding the Balb/c and athymic nude mouse will be reviewed.

The Balb strain of laboratory mouse was obtained by Halsey J. Bagg in 1913 from a supplier in Ohio. The "alb" refers to albino and the phenotypic expression of a white coat in this strain. The "c" was added by Snell in 1932 and refers to the site of the mutation on the c-locus allele (Staats, 1975; Festing, 1989).

The athymic nude (Nu/+) strain used in the present study was derived from the cross mating of a Balb/c female and an athymic nude male (Nu/Nu). The genotype composition of the offspring from this mating were either Nu/Nu or Nu/+, and displayed very different phenotypes.

Briefly, the athymic nude mouse, first discovered at the Ruchill Hospital in Glasgow, Scotland (Green et al., 1989), has a genetic alteration at the Nu locus on chromosome II, which results in an athymic hairless rodent. The autosomal recessive traits expressed phenotypically in the athymic nude mouse require homozygous expression of the Nu gene (Nu/Nu). At birth, the hair follicles are normal, but a lack of keratinization of these follicles prevents the mice from developing a normal hair coat. The athymic presentation is associated with abnormal development of thymic anlage from the ectoderm of the third pharyngeal pouch. This results in the presence of a thymic rudiment at birth which fails to attract

lymphoid cells. Consequently, the affected mice are immune deficient. The degree of immune deficiency is severe and consists of a depletion of thymus-dependent lymphocytes (T cells) from the lymph nodes and spleen, an absolute decrease in the lymphocyte population (which is composed primarily of B cells), failure to reject allogeneic and xenogeneic skin and tumor grafts, and a greater susceptibility to infection (Green, et al., 1989). Unlike their Nu/Nu litter mates, the Nu/+ mice do not express any of the above anomalies because they are not homozygous for Nu at the Nu locus. Phenotypically, they have a white hair coat and possess a normal thymus and are immune competent.

Table 1.1. Taxonomic Classification of the Mouse

Phylum:	Chordata	Subphylum:	Vertebrata
Class:	Mammalia	Subclass:	Theria
		Infraclass:	Eutheria
Order:	Rodentia	Suborder:	Myomorpha
Super-family:	Muroidea	Family:	Muridae
Genus:	Mus - laboratory mouse; Microtus - field mouse		
Species:	musculus - laboratory mouse pennsylvanicus - field mouse		
Strain:	numerous domesticated strains		

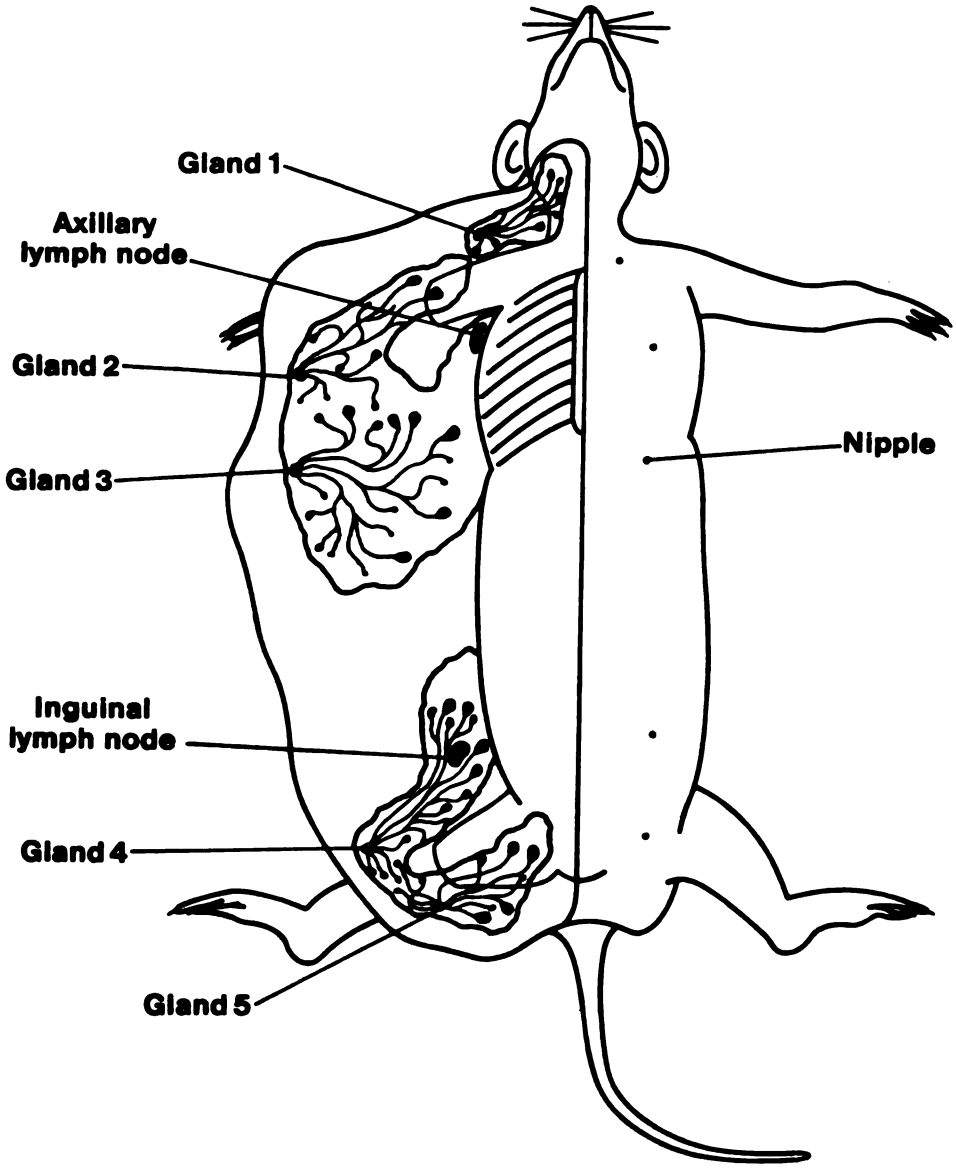

Figure 1.1 Diagram of a mouse to illustrate the number and location of the mouse mammary glands and regional lymph nodes. Gland 1 is a cervical gland, Glands 2 and 3 are thoracic glands and Glands 4 and 5 are inguinal glands.

Macroanatomy of the Mouse Mammary Gland

Number and Location of Glands. The mouse has five pairs of mammary glands (Coleman et al., 1975). The glandular epithelium is located in discrete bilateral subcutaneous fat pads that are numbered according to their cranial to caudal location (Figure 1.1). The number one (No. 1) gland is a ventrolateral cervical gland. It is located in the neck region adjacent to the parotid salivary gland. The No. 2 and No. 3 glands are ventrolateral thoracic glands. The No. 2 gland is the smaller of the two thoracic glands and has a characteristic "U" shape with a centrally placed nipple. The cranial arm of the No. 2 gland lies in a diagonal position over the humeral-axial musculature. The caudal arm extends under the pectoralis superficialis muscle and descends down toward the No. 3 gland fat pad (Thorpe, 1968; Olds, 1979). In some mice, the No. 2 and No. 3 gland fat pads are continuous, and the glandular epithelium may be intertwined. The No. 3 mammary gland is the largest of the five glands with respect to the size of the fat pad. It has a wedge-shaped appearance and extends out from a ventrolateral to a mediodorsal position. The No. 4 and No. 5 glands are ventrolateral inguinal glands. The No. 4 gland has a very distinct "J" shape and, like the No. 3 gland, has a prominent dorsal extension. Because of its defined borders and ease of removal, the No. 4 gland is one of the most widely used glands

for mammary gland analysis in the mouse. The No. 5 mammary gland is the most caudal gland. This gland does not possess well defined borders and is often continuous with the No. 4 fat pad. The majority of the glandular epithelium in the No. 5 gland is located adjacent to the preputial gland and perivulvular fat deposits; in some mice the glandular epithelium can be seen extending into these fat deposits.

Blood, Lymphatic, and Nerve Supply. The rodent mammary glands are highly vascular organs that receive their blood supply from various sources. The specific blood, lymphatic and nerve supply to the mouse mammary gland could not be verified in the literature by this author. Therefore, the following information is based on anatomical descriptions of the rat, mouse and canine mammary gland (Christensen, 1964; Thorpe, 1968; Olds, 1979; Popesko et al., 1992). The No. 1 cervical gland in the mouse is believed to receive arterial blood from a branch of the cervical artery. The No. 2 and No. 3 thoracic glands are nourished by branches from the internal thoracic and mammary arteries and the epigastric arteries and the No. 4 and No. 5 inguinal glands receive arterial blood from the mammary branches of the epigastric and external pudendal arteries (Christensen, 1964; Thorpe, 1968; Popesko, et al., 1992). The major veins draining the thoracic and inguinal mammary glands coincide with their arterial counterparts.

Several lymphatic plexuses are found throughout the mammary gland parenchyma, subcutis, and nipple regions. The

No. 1 cervical gland is believed to drain into the cervical lymph nodes, the No. 2 and No. 3 thoracic glands drain into the axillary lymph nodes, and the No. 4 and No. 5 inguinal glands drain into the superficial inguinal lymph nodes (Olds, 1979).

The primary nerve supply to the cervical and thoracic mammary glands are from the ventral cutaneous nerves, which extend from the brachial nerve plexus. The inguinal glands are innervated by branches of the inguinal, iliohypogastric, and ilioinguinal nerves (Christensen, 1964; Thorpe, 1968; Olds, 1979).

Basic Morphology of the Virgin Mouse Mammary Gland. As in other mammals of the class Mammalia, the mammary gland in the mouse undergoes the majority of its development post-natally. This characteristic makes the mammary gland an excellent model for studying glandular morphogenesis. By late gestation, day 17 of a 21 day gestational period, the basic morphology of the mouse mammary gland is present in the fetus. The mammary gland is composed of a nipple, large primary (1°) duct and several secondary (2°) ducts. At birth, around 21 days in the mouse, the mammary gland consists of 15-20 dichotomously branching ducts (Sakakura, 1987). In some mice, tertiary branching might also be present at this time. The very distal aspect of the 2° or 3° ducts are either blunted terminal end ducts (TED) or rounded terminal end buds (TEB) (Sekhri, et al., 1967). These two structures correspond to opposite degrees of cell proliferation and ductal expansion.

The round, bulbous TEBs are exceedingly mitotically active. They contain a layer of cells called cap cells, which are believed to be the pleuripotential stem cells of the mammary gland responsible for ductal expansion of the mammary gland tree prior to sexual maturity (Williams and Daniel, 1983). The TEBs visible in the mammary glands at birth are present in response to high levels of maternal hormones (primarily estrogen and progesterone) in the circulatory system of the neonatal mouse (Daniel and Silberstein, 1987). Because the TEBs are the result of hormonal stimulation, as the levels of maternal hormones decrease there is a coinciding decrease in TEB size and number during the first few days post-partum. Morphologic analysis of the neonatal (birth to 21 days of age) and juvenile (22 to 28 days of age) growth periods has shown that the TEB structure is absent after maternal hormone withdrawal until the prepubertal-pubertal growth period at 4 to 7 weeks of age (Nandi, 1959). During the prepubertal-pubertal growth period, large numbers of TEBs are present in response to rising levels of ovarian secreted hormones and result in direct ductal expansion throughout the mammary gland fat pad (Williams and Daniel, 1983).

The blunt, tubular TEDs are relatively quiescent structures in the neonate, with little mitotic activity and no cap cell layer (Williams and Daniel, 1983). While they are not as dynamic as the TEBs, the TEDs are present throughout the life of the nulliparous mouse and are hormonally responsive structures as well. They have the potential to

transform into TEBs, alveolar buds (AB), and alveolar sacs (AS) at the appropriate time with the appropriate hormonal stimulus (Cole, 1933; Turner and Gomez, 1933; Wellings et al., 1960). The TEDs are very numerous in the fully developed mature virgin mouse at approximately 9 weeks of age (Sekhri et al., 1967).

The alveolar buds and alveolar sacs are morphologic structures associated with pregnancy and lactation and will not be addressed in detail in this literature review. The ABs proliferate from the sides and ends of TEDs in response to the hormones of pregnancy (Sekhri et al., 1967). Clusters of ABs are present as early as day 12 of gestation in the mature mammary gland, and are seen prior to the development of alveolar sacs. The ASs are present between late gestation and approximately 3 weeks post-partum. The ASs emerge from the ABs and are characteristic of complete secretory development. They produce milk in response to lactogenic hormones such as prolactin prior to involution (Sekhri et al., 1967). The remainder of the literature review will focus on the developmental stages of the murine mammary gland up to and including the mature virgin mouse.

Cellular Composition of the Ductal Structures in the Virgin Mouse Mammary Gland

Extensive postnatal development of the mammary gland coincides with a dynamic cellular evolution in this organ.

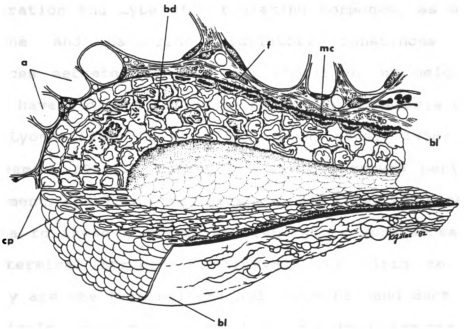

Figure 1.2 Diagram of end bud to illustrate the cap (cp) cells and their relationship to the luminal (bd) and myoepithelial cells (mc). A basal lamina (bl) of varying thickness surrounds the end bud with adipocytes (a) and fibroblasts (f) comprising the cellular stroma. The nature of the extracellular matrix is not shown in this figure, however, it is discussed extensively in the original text. [Adapted from Williams and Daniel (1983) with permission from Academic Press.]

The prepubertal and early pubertal growth periods of the mouse mammary gland prior to sexual maturity are associated with several unique histomorphologic characteristics. In vivo, in vitro and organ culture studies have shown that the concentration and type of circulating hormones, as well as autocrine and paracrine regulatory substances (those substances secreted by the cell itself or by neighboring cells), have a direct influence on the morphogenesis of this gland (Lyons, 1958; Lyons et al., 1958; Nandi, 1958; Topper and Freeman, 1980). During the various growth periods of development, specific structures and cell types are present in response to these hormones and regulatory substances. The major terminal structures observed from birth to sexual maturity are the terminal end bud, terminal end duct and in some animals, small numbers of alveolar buds; which can appear prior to pregnancy in association with the fluctuating hormones of estrous. The specific cell types associated with the TEB are reviewed below.

The Cap Cell. The cap cell was first identified in the early 1980's as an undifferentiated cell present in a single layer lining the peripheral border of the TEB (Williams and Daniel, 1983) (Figure 1.2). Further analysis of this cell in vivo and in vitro produced evidence to support the present theory that the cap cell is the pleuripotential stem cell of the mouse mammary gland and drives ductal morphogenesis during the prepubertal-pubertal growth periods (Bennett et al, 1978; Dulbecco et al., 1982; Williams and Daniel, 1983; Dulbecco et

al., 1983). As such, the cap cell is believed to be the origin of all cell types present in mammary gland. Researchers have found through immunocytochemistry and time-lapse microcinematography that the cap cell definitely gives rise to the myoepithelial and intermediate cells in the TEB structure, as well as various transitional cell types within these two distinct groups of cells (Dulbecco et al., 1982); Williams and Daniel, 1983). A fourth cell type identified in the TEB, the luminal cell (also referred to as the dark cell or body cell), is a fully differentiated cell, and is believed to evolve from the cap cell, via the intermediate cell population (Russo et al., 1987).

The histomorphologic and ultrastructural composition of the cap cell was described in the literature by Williams and Daniel in 1983. They described the cap cell as a low columnar to cuboidal shaped cell, with a large, round euchromatic nucleus and multiple nucleoli. The cytoplasm was described as containing abundant ribosomes, mitochondria and various sized fat vacuoles. Ultrastructural analysis of the basal surface of the cap cell membrane shows that the membrane aligns itself with a dynamic basal lamina which surrounds the entire TEB structure. In addition, the lateral and luminal cap cell membrane surfaces are arranged in irregular cytoplasmic projections that are often surrounded by fluid-filled intercytoplasmic spaces of various sizes. These intercytoplasmic spaces are believed to result from the production of hyaluronate by the cap cell (Silberstein and

Daniel, 1982a), in order to decrease cellular adhesion. Decreasing cellular adhesion, allows cellular expansion within the TEB and advancement of the TEB structure throughout the mammary gland fat pad. Specialized intercellular membranous junctions and adhesions, such as tight, intermediate and gap junctions and desmosomes, have not been positively identified in the cap cell population to date (Williams and Daniel, 1983).

The Myoepithelial Cell. The myoepithelial cell is a direct descendant of the cap cell and has been described in the literature in great detail (Dulbecco et al., 1982; Warburton, et al, 1982; Williams and Daniel, 1983). It lies along the peripheral margin of the TEB and is distinctly visible in the flank region of the TEB structure. The myoepithelial cell is a fully differentiated, elongate, spindle-shaped cell with an irregular, oval-shaped heterochromatic nucleus and variable numbers of nucleoli. Its cytoplasm contains prominent myofilaments, 4-5 nm in diameter, and abundant ribosomes and endoplasmic reticulum (ER) (Pitelka et al., 1973). The basal surface of the myoepithelial cell borders a thick, irregularly folded basal lamina. The lateral and luminal surfaces often contain specialized intercellular adhesions called desmosomes. Desmosomes are present between adjacent myoepithelial cells and underlying intermediate or luminal cells. Hemi-desmosomes are commonly found between the myoepithelial cell and the basal lamina in the mature duct.

It is important to note that, even though the myoepithelial cell is considered to be fully differentiated, Williams and Daniel (1983) believe that it has the ability to "dedifferentiate" and produce a cap cell-like population of cells. This cap cell-like population, in turn, has the ability to give rise to lateral ductal branches which possess a TEB or alveolus at the tip. This is a controversial opinion and other scientists believe a separate population of partially differentiated peripheral cells deep in the mature duct give rise to lateral ductal branches which have the capability of producing TEBs and alveoli (DeOme et al., 1959; Hoshino, 1964; Daniel et al., 1968). The latter theory implies that there are residual populations of undifferentiated cells present in the mature duct that respond to local and hormonal factors which enable them to produce lateral ductal branches ending in TEBs or TEDs.

The Intermediate Cell. Very little has been written about the intermediate cell (IC) in the TEB structure because, unlike the myoepithelial cell, it is not present in the mature end duct. The intermediate cell (IC) was a term coined by Russo and Russo (1987) to describe a partially differentiated cell in the TEB of the rat. The IC had the shortest cell cycle of the 3 cell types (intermediate cell, dark cell and myoepithelial cell) identified by Russo and Russo. Williams and Daniel (1983) described this cell simply as one of the "body cells" which included the luminal cell population. Using time-lapse microcinematographs, Williams and Daniel

suggested that, like the myoepithelial cell, the body cells are descendants of the cap cell layer. Diagrammatically they placed the body cells (i.e. ICs) between the peripheral cap cell and myoepithelial cell layers and the fully differentiated luminal cell layer. In addition, Russo and Russo (1987) have shown that the ICs can reach the lumen of immature TEBs in the rat. The ICs are oval in shape, with an irregular oval heterochromatic nucleus and contain variable numbers of nucleoli. The cytoplasm contains abundant mitochondria, golgi, ribosomes, endoplasmic reticulum and fat vacuoles of various size and number. Their cell membranes are irregular, and contain any of a number of specialized structures such as tufts of microvilli, and intercellular junctions and adhesions.

The Luminal Cell. Because the luminal cell is present at all stages of development in the mammary gland, a great deal of information is available regarding the morphology and physiology of this cell (Pitelka et al., 1973; Williams and Daniel, 1983; Russo and Russo, 1987). The luminal cell is a fully differentiated cell that lines the ductal lumens of the mammary gland in the TEB and in the mature duct. The luminal cell has a cuboidal shape and contains an irregular, oval, heterochromatic nucleus. Its cytoplasm contains abundant mitochondria, golgi, and rough endoplasmic reticulum. Ribosomes, smooth endoplasmic reticulum, and protein-filled vesicles are also present but in lesser amounts. The luminal cells have the largest number and greatest diversity of

specialized membrane structures (Pitelka et al., 1973). The lateral and basal membrane surfaces are primarily linear and often possess desmosomes, gap, intermediate and tight junctions. The distinct reinforcing tight junctions are present at the apical junction between adjacent luminal cells. They serve to maintain alignment of the luminal cells, and the spatial integrity of the lumen itself. The apical or luminal membrane surface of these cells display abundant blunt microvilli, which increase the surface area facing the lumen and the absorptive capacity of the cell.

The primary function of the luminal cell is to produce milk during the postnatal lactation period. The cells lining the alveolar lumen in the pregnant mouse are highly responsive to the hormones of pregnancy and lactation, and undergo their most dynamic histomorphologic and ultrastructural changes prior to milk production (Pitelka et al., 1973).

Developmental Growth Periods in the Mouse Mammary Gland

Embryogenesis. The gestation period for the mouse is 19-21 days (Austin et al., 1969). In 1933, Turner and Gomez, documented the histomorphologic appearance of mammary gland anlage in the mouse between days 10 and 11 of gestation. Histologically, they found that a single layer of ectodermal cells, arranged in a line, extended from the anterior to posterior limb bud. This single layer of cells was termed the mammary streak. Between day 12 and 14 of gestation, there are

major changes in the cellular composition of the mammary streak. In most species, the single layer of ectodermal cells or mammary streak begins to proliferate into a multilayered epidermal line, called the mammary line (Sakakura, 1987). There is marked unequal proliferation of the stratum germinativum in this line, which results in the formation of distinct lens shaped mammary gland anlage. In contrast, Balinsky (1950) found no thickened mammary line in 13-day-old mouse embryos. Using graphic reconstruction of serial sectioned embryos, he found individual epidermal thickenings in 11-day-old embryos, not a thickened epidermal mammary line, from which the lens shaped anlage developed around day 12 of gestation. Balinsky (1950) also discovered that the proliferation index within the mammary anlage was well below that of the neighboring epidermal cells and concluded that the emergence of the mammary buds was the result of cellular displacement and differentiation, which was followed by a relatively quiescent phase. Balinsky's work was later supported by Propper (1978) who revealed the ability of epithelial cells to migrate within the mammary line of the rabbit using a scanning electron microscope. By day 14, the lens shaped anlage develop into bulb shaped structures connected to the epidermal surface by a narrow row of cells, called the mammary bud.

In addition to the appearance of the mammary buds on day 14, the sexual phenotype of the mammary gland is also determined on day 14. The determination of mammary gland

phenotype is directly attributed to sexual differentiation of the rodent gonads and the presence of fetal androgen (Raynaud, 1961). The interaction between fetal androgen in the mesenchyme and the mammary epithelial stalk results in complete separation of the mammary bud from the overlying epidermis and a male mammary gland phenotype. The role of fetal androgen in the mesenchyme surrounding the stalk of the mammary bud is discussed in detail in the section on "The Role of the Basal Lamina and Extracellular Matrix in the Development of the Virgin Mouse Mammary Gland."

In the female mouse, between days 11 and 16 of gestation, the mammary gland is quiescent and said to be in a "resting phase" (Balinsky, 1950; Sakakura, 1987). The resting phase is characterized by slow growth and non-progressive histomorphologic differentiation. However, from late in the 16th day to day 17 of gestation, the cells of the mammary bud begin to proliferate rapidly. The end result is elongation of the mammary bud into a funnel shaped structure called the mammary sprout (Sakakura, 1987). The distal end of the mammary sprout grows downward, through the dense mammary mesenchyme surrounding it, into the mammary fat pad precursor tissue below. The mammary fat pad precursor tissue is composed of immature adipocytes that do not accumulate lipid or resemble mature fat cells until birth (Hausman and Thomas, 1984; Sakakura, 1987). The importance of the mammary fat pad precursor tissue in gestational development of the mammary gland, as well as that of the mature mammary fat pad in

postnatal development, is discussed in the section on "The Role of the Extracellular Matrix in the Development of the Virgin Mouse Mammary Gland."

The proximal end of the mammary sprout is composed of cells containing intracellular vacuoles. These vacuoles have been shown to fuse and form a canal-like opening, which eventually gives rise to the teat canal. Between day 17 and birth, the epithelial cells comprising the mammary sprout continue to proliferate (Sakakura, 1987). As there is further expansion into the mammary fat pad precursor tissue, the elongated single mammary sprout begins to form several lateral extensions or ducts. At birth, 15 to 20 branching ducts are present in each of the 10 mammary glands, and give rise to what has been termed the mammary gland tree (Sakakura, 1987).

Neonatal to Juvenile Growth Periods. The neonatal growth period in the mouse stretches from birth to 21 days of age. At birth, the mouse mammary gland consists of a nipple, primary duct, and 15-20 dichotomous branching secondary ducts. The primary duct is composed of 1 to 3 epithelial cell layers (Sekhri et al., 1967). The secondary and tertiary ducts are at various stages of canalization and, therefore, have variable cell thickness. The canalization process consists of the fusion of successive lumina within a specific ductal structure. The distal aspect of the majority of the 2° and 3°, and in some glands 4° ducts, contain mitotically active TEBs. These bulbous structures are under the control of maternal hormones during this period, and as the hormone levels

decrease in the bloodstream of the neonate, there is a coinciding decrease in size and number of TEB structures until there is complete disappearance of these structure (Daniel and Silberstein, 1987). During the neonatal period, the ductal system within the mammary glands continues to elongate and grow isometrically, with respect to the rodent (Knight and Peaker, 1982) and is ovary dependent; as are all of the subsequent growth periods (Rugh, 1968).

The period of growth following the neonatal period is called the juvenile growth period. This period extends from approximately 21 to 28 days of age in the mouse, and is characteristic of a change in mammary gland growth potential. The most significant change observed here is a shift from isometric growth to allometric growth (Cowie, 1949). The growth shift is characterized by an increase in the rate and degree of dichotomous ductal branching and a reappearance of the TEB structure at the distal aspect of the advancing ducts (Nandi, 1958). It is the TEB structure, present from the mid- to late phase of the juvenile growth period throughout the pubertal growth period, that directs and propagates the expansion of the mammary gland tree in the mammary gland fat pad (Williams and Daniel, 1983). This expansion is under the influence of endocrine, autocrine, and apocrine factors, which will be discussed in greater detail in the section on "The Influence of Hormones and Local Factors on the Development of the Virgin Mouse Mammary Gland."

Prepubertal-Pubertal Growth Periods. The prepubertal growth period is that period of growth prior to the onset of estrous, between 4 to 5 weeks of age (Topper and Freeman, 1980; Williams and Daniel, 1983). Estrus usually occurs some time around 5 weeks of age in the female mouse, and can be easily identified by vaginal smear cytology (Austin, 1969). The period of pubertal growth coincides with the onset of sexual maturity (around 5 weeks of age) up to approximately 7 - 9 weeks of age (Rugh, 1968). During this growth period, there is a rapid expansion of the mammary gland tree throughout the mammary gland fat pad accompanied by a large increase in the number of TEB structures (Williams and Daniel, 1983). Williams and Daniel (1983) described the bulbous TEBs as varying in size according to their location within the expanding ductal tree and ranging from 0.2 to 0.8 mm (no clarification was given as to whether these were length or width measurements). Histologically, they reported that the cap cell and body cells (ICs) were highly mitotically active. In addition, they measured the progression of the TEB structures through the mammary gland fat pad and found that they advanced approximately 0.5 mm per day during these growth periods. As the advancing ducts reach the limits of the mammary fat pads, the TEB structures, which Williams and Daniel believe drive ductal morphogenesis, become less mitotically active and regress into TEDs. Typically, the largest percentage of TEDs in the prepubertal-pubertal mammary gland is found at the lateral edges and deep within the

mammary ductal mass of the fat pad (Faulkin and DeOme, 1960). The consistent location of the TEDs in these areas supports the theory by Williams and Daniel (1983) that a minimal amount of space is required for maintaining TEB structures. When this spatial relationship is lost, the cap cells in the TEB are somehow signaled to stop dividing and eventually the TEBs regress into a mitotically inactive TEDs.

Mature Virgin. The virgin mouse mammary gland is believed to reach sexual maturity by 9 weeks of age (Topper and Freeman, 1980). The mammary gland at this stage is composed of a complex array of dichotomously branched ducts that have primarily TEDs at their distal ends. The TEDs do not contain cap cells and are relatively quiescent (Williams and Daniel, 1983). Histologically, the TEDs are 1 to 2 cell layers thick, and consist of a luminal cell layer surrounded by a discontinuous myoepithelial cell layer (Pitelka et al., 1973). While the TEDs are not as mitotically active as their counterparts, the TEBs, they are very responsive to the fluctuating hormones of estrous, and the hormones of pregnancy and lactation (Topper and Freeman, 1980; Pitelka et al., 1973). Under the right hormonal influence, the TEDs of the mature virgin mouse will develop into the alveolar buds and alveolar sacs of pregnancy and lactation, respectively. This transformation results in complete differentiation of the mouse mammary gland and in the production of milk for suckling pups (Pitelka et al., 1973).

The Role of the Extracellular Matrix and the Basal Lamina in the Development of the Virgin Mouse Mammary Gland

The Mesenchyme and Extracellular Matrix Proteins. There are two distinct types of mesenchyme present in the embryonic mouse mammary gland. One type is dense mesenchyme which is present on day 13 of gestation, consists of 2 to 3 layers of fibroblasts, and surrounds the mammary epithelium. The second type of mesenchyme is mammary fat pad precursor tissue (FPP) which is present on day 14 of gestation and lies beneath the dense mesenchyme (Sakakura, 1987).

The dense mesenchyme has been shown to play a key role in determining phenotypic sexual dimorphism and in regulating cytodifferentiation and early morphologic development (organogenesis) (Kratochwil, 1969). In the 13- to 14-day-old male fetus, the dense mesenchyme surrounding the stalk of the mammary bud contains androgen (Kratochwil, 1977). The androgen present in this region is believed to be the result of epithelial induced androgen receptors in the adjacent mesenchyme (Heuberger et al., 1982). Stromal bound androgen results in condensation of the dense mesenchyme around the epithelial stalk. The stalk eventually becomes very narrow and ruptures on day 15 of gestation (Sakakura, 1987). The rupture results in an isolated mammary gland rudiment in the mammary FPP tissue that is left to develop with no external opening or to degenerate depending on the species. In the

Balb/c male mouse, approximately 50% of all males lack mammary glands, and in the male rat the mammary gland will develop to various degrees (Sakakura, 1987).

The interaction between mesenchyme and mammary epithelium is also evident in the pattern of dichotomous branching of the ductal elements in the mouse mammary gland. Significant levels of sulfated glycosaminoglycans, particularly chondroitin sulfate, and the extracellular matrix protein, tenasin, have been found in the mesenchyme adjacent to the flank and neck regions of terminal end buds and in clefts between ductal branches (Silberstein and Daniel, 1982a; Bernfield et al., 1984). The presence of these substances not only functions to induce tissue stabilization, but also appears to regulate interductal spacing by inducing the deposition of collagen which in turn influences the dichotomous branching of the expanding mammary gland tree (Bernfield et al., 1984).

The role of dense mesenchyme in regulating early morphologic development was first associated with the identification of an extracellular matrix glycoprotein called tenasin (previously known as myotendinous antigen) in the dense mesenchyme (Chiquet and Fambough, 1984b; Chiquet-Ehrismann et al., 1986). Tenasin has been found in the mesenchyme surrounding the epithelium of many organs, such as the tooth, hair follicle, kidney, and mammary gland during early embryogenesis. Inaguma and his colleagues (1988) isolated tenasin in fetal and juvenile mammary glands and in

malignant mammary tumors. Using immunohistochemical studies they showed that, in the fetal gland, between day 13 and 16 of gestation, tenasin was present in the dense mesenchyme immediately surrounding the epithelial stalk of mammary buds and sprouts. During the juvenile growth period at 3 weeks of age, tenasin was also found surrounding the early ductal end buds. However, once the end bud began to elongate tenasin disappeared. In mammary gland adenocarcinomas (type A or B) from C3H mice, tenasin was present in the stroma surrounding the malignant epithelium. Inaguma and his colleagues believe that both embryonic and neoplastic epithelium induce tenasin synthesis in the surrounding mesenchyme. The function of tenasin during the early stages of morphogenesis is thought to be an inductive one. It has been theorized that tenasin is part of a complex interactive sequence between the mesenchyme and mesenchymal epithelium, in which the primary role of tenasin is to alter the mesenchyme in such a way as to induce the morphogenesis of the mammary gland (Chiquet-Ehrismann et al., 1986).

In culture, there is evidence that tenasin functions as both a growth promoter and an inhibitor of cell attachment depending on the substrate. In <u>in vitro</u> experiments by Inaguma and his colleagues (1988), CMT 315 mammary tumors cells, derived from a C3H/HeN^{+} mouse, were grown on tenasin coated and non-coated plates. Those cells grown on tenasin coated plates displayed greater proliferation than those grown on non-coated plates. However, in <u>in vitro</u> experiments by

Chiquet-Ehrismann and her colleagues (1988), tenasin was also found to inhibit mammary tumor cell adherence to fibronectin. Therefore, it appears that there is more than one factor involved determining the role of tenasin in the ECM.

The Mammary Gland Fat Pad. The mammary gland fat pad is white adipose tissue derived from histologically distinct mammary fat pad precursor tissue which is visible around day 14 as a condensed tissue mass lying well below the dense mesenchyme (Sakakura, 1987). By day 17 of gestation, the FPP tissue consists of preadipocytes and has been penetrated by the descending mammary sprout. Numerous organ culture experiments have shown that the presence of the FPP tissue is necessary for normal organotypic development of the mammary gland (Sakakura et al., 1976, 1979, 1982). When mammary epithelium from fetal mice and postnatal mice was removed and placed in dense mesenchyme versus mammary FPP tissue, those samples in the mammary FPP tissue developed normal linear ductal extensions. However, those mammary epithelial tissues placed in the dense mesenchyme developed ductal hyperplasias and had minimal linear ductal extension (Sakakura et al., 1976).

From day 17 of gestation up to 2 to 3 days postpartum, the mouse mammary gland fat pad contains preadipocytes, or immature "brown" fat cells (Sakakura, 1987). The preadipocytes contain variable amounts of lipid vacuoles, which eventually coalesce into fully developed "white" fat cells, or mature adipocytes (Hausman and Thomas, 1984). The

FPP tissue and subsequent mammary fat pad serves as the major substrate for the expansion and normal morphologic development of the mammary gland tree (Hoshino, 1967, 1978). The fat pad, itself, provides a boundary for ductal expansion during the prepubertal-pubertal growth periods (Hoshino, 1964) and the adipocytes provide energy and nutrients for cell proliferation at all stages of growth and during lactation (Pitelka et al., 1973; Bartley, 1981).

The Basal Lamina. The basal lamina (BL) in the TEB of the mouse mammary gland is a dynamic, specialized membrane structure. Histologically, the BL consists of an anionic lamina externa and a two dimensional globular lamina interna (Gordon and Bernfield, 1980; Williams and Daniel, 1983). The lamina externa is composed of irregular filaments extending out toward the extracellular matrix collagen. The lamina interna is composed of an inner filamentous layer and a lamina densa. The inner filamentous layer adheres the lamina densa to the underlying epithelial cells.

In the mouse mammary gland the BL varies in its chemical composition and morphologic appearance, depending on its location within the duct. The BL at the tip of the TEB structure is produced by the cap cell layer. Histologically, it appears smooth and is reported to be approximately 104 nm thick (Williams and Daniel, 1983). Most basal laminas are composed of laminin, type IV collagen, proteoglycans and glycoproteins (Bissell and Hall, 1987). The TEB basal lamina contains two types of proteoglycans (protein-glycosaminoglycan

complexes), hyaluronate and chondroitin sulfate (Gordon and Bernfield, 1980). Extensive histochemical and autoradiographic studies, using [N^3] glucosamine and $^{35}SO_4$ incorporation, have shown that the major proteoglycan at the tip of the TEB (including the ECM) is hyaluronate (Silberstein and Daniel, 1982a). Hyaluronate is a salt or ester of hyaluronic acid and is associated with decreased intracellular adhesion and cell migration. The presence of hyaluronate in high concentrations at the tip of the TEB is believed to be directly associated with the structure's ability to penetrate the mammary gland fat pad. Within the TEB, there is also a significant degree of intercellular spacing between adjacent cap cells and the underlying intermediate cell population. This is attributed to the production of hyaluronate and the degradation of the epithelial basal lamina glycosaminoglycans by the mesenchymal cells (Smith and Bernfield, 1982; Williams and Daniel, 1983).

In the flank or "transition" region of the TEB, the BL changes character, both chemically and morphologically. The thin, smooth lamina at the tip of the TEB becomes abruptly thick and corrugated. Williams and Daniel (1983) reported that the BL in the flank region was approximately 1,462 nm thick (14 times greater than at the tip), and was composed of sulfated glycosaminoglycans, primarily chondroitin sulfate, not hyaluronate.

In addition to chemical and physical changes in the BL, there is also an abrupt change in the primary cell type

present in the extracellular matrix and in the TEB bordering the flank BL. In the flank region, which corresponds to the maximum diameter of the TEB structure, the primary GAG, chondroitin sulfate, is believed to contribute to cap cell-myoepithelial cell cytodifferentiation and thereby propagate mammary duct morphogenesis (Silberstein and Daniel, 1982a; Williams and Daniel, 1983). In the extracellular matrix, there is a sudden and abundant deposition of collagen and numerous fibroblasts adjacent to the BL. This change in the composition of the extracellular matrix is also believed to be associated with the presence of sulfated GAGs.

In the neck region, defined as that area preceding the completed duct, the BL remains corrugated but is much thinner, approximately 130 nm in width (Williams and Daniel, 1983). The corrugated appearance of the BL in both the flank and neck regions is thought to be directly related to a decrease in surface area from the bulbous TEB tip to the narrow differentiated terminal end duct (Williams and Daniel, 1983). Quantitatively, the neck region contains less sulfated glycosaminoglycans than the flank region (Silberstein and Daniel, 1982a).

The Influence of Hormones and Growth Factors on the Development of the Virgin Mouse Mammary Gland

The Effect of Maternal Hormones. The primary maternal hormones circulating through the blood stream during the later

part of gestation are progestins, estrogens and prolactin (Lyons et al., 1958 and Nandi, 1958). From day 16 of gestation, which marks the end of the "resting phase" (day 11 - 16 of gestation) throughout the remainder of gestation, it has been hypothesized that the presence of both maternal hormones and fetal hormones from the developing ovary influence the morphogenesis of the mammary gland. This hypothesis is supported by information gathered from in vitro experiments in rodents due to the lack of technologic ability to extract hormones from embryos in utero (Ceriani 1970a, 1970b; Topper and Freeman, 1980; Du Bois and Elias, 1984). Ceriani (1970a), using fetal analgen in organ culture and 17 day old embryologic mammary epithelium, documented the response of several hormones on the development of the embryologic rodent mammary gland. He looked at the effects of insulin, d-aldosterone, prolactin, progesterone, estrogen (estradiol 17-ß) and testosterone. The results of these studies showed that insulin was a requirement for in vitro growth and development, and a combination of hormones was necessary for optimum morphogenesis and secretion of casein. Specifically, Ceriani found that insulin (5 µg/ml) stimulated growth and development, of the fat pad, and lumen formation in ducts. Prolactin (2 µg/ml) enhanced the growth response to insulin by producing terminal cell accumulations and influencing the mesenchyme. Aldosterone (0.25 µg/ml) induced ductle branching, and with the addition of insulin and prolactin the appearance of secretions. The addition of

progesterone further increased cell proliferation and the secretory response. He also discovered that when progesterone was added alone, at 1 μg/ml, to insulin, ductles were produced similar to those observed with prolactin and aldosterone alone. But when a combination of estrogen and progesterone was added to the aforementioned hormones, the mammary gland analgen developed morphologic patterns identical to those of newborn rats. These experiments established the role of maternal hormones in the development of the prenatal mammary gland. In addition, he discovered that when estradiol - 17ß was added alone it had no effect or only a slight stimulatory effect on granular secretion and, in fact, was toxic to the analgen resulting in epithelial necrosis at concentrations of 0. 001 μg/ml or greater. When testosterone was added it inhibited fetal analgen development but did not inhibit maintenance of the fetal analgen.

In their review on the effect of multiple hormones on the development of the mammary gland, Topper and Freeman (1980) stated that estradiol - 17ß was elevated at parturition and may be partially responsible for neonatal epithelial proliferation. They also found that "it stimulates thyroid stimulating hormone (TSH) and prolactin secretion by cultured pituitary cells" thereby revealing its indirect effect on the mammary gland via its interaction with other hormones in the periparturient animal. In addition, maternal plasma progesterone, which had an antilactogenic effect, was decreased around parturition and therefore, they concluded

that it was unlikely that progesterone influenced the periparturient mammary gland.

The Effect of Pubertal Hormones. The onset of puberty in the mouse occurs between 4 to 6 weeks of age (Topper and Freeman, 1980). This two week time period, known as the prepubertal-pubertal growth period, is associated with TEB development and extensive expansion of the ductal tree throughout the mammary gland fat pad (Williams and Daniel, 1983). Several factors influence this allometric growth period including systemic hormones, growth factors, nutrients and genetics. In general, the hormones present during the prepubertal-pubertal growth period play a significant role in stimulating cell proliferation. Studies using endocrinectomized female rodents and hormonal replacement therapy protocols identified the three major hormones required for ductal expansion (Flux, 1954; Topper and Freeman, 1980). The results of these studies showed that during the prepubertal-pubertal growth period, estradiol-17β, growth hormone, and glucocorticoids are necessary for maximum ductal proliferation. In contrast insulin, though required for *in vitro* growth, was not required for *in vivo* growth. Topper stated that "cell replication associated with ductal expansion in the immature female, as well as cell maintenance in the mature nonpregnant female, are in fact insulin insensitive."

In vitro studies by Elias (1959) and Du Bois and Elias (1984) examined the epithelial heterogeneity of the mammary gland tree during the prepubertal-pubertal growth period. By

using organ cultures and labeling index measurements, Du Bois and Elias found that different regions of the expanding mammary gland tree (the primary duct, secondary and tertiary ducts and TEBs) had different hormonal requirements. Maintenance of the epithelial integrity of the primary duct required insulin. However, the maintenance of the TEBs required deoxycorticosterone acetate or aldosterone and growth hormone, prolactin or placental lactogen. The hormones shown to be necessary for growth and development of the mammary gland *in vivo*, i.e., estrogen, growth hormone and glucocorticoids, did not result in the incorporation of [^{3}H] thymidine in mammary glands in organ culture. In fact, none of the protocols examined by Du Bois and her colleagues had labeling index values numerically similar to the control gland indices of the primary duct, secondary duct, tertiary duct or TEBs.

The Effect of Growth Factors. Growth factors are polypeptides produced by a wide variety of organs and cells. Identification of growth factors which are believed to affect the growth and development of the mammary gland are limited and are primarily derived from *in vitro* studies (Tonelli and Sorof, 1980; Yang, et al, 1980; Taketani and Oka, 1983b; Smith et al, 1984; Dembinski and Shiu, 1987). What is known about the effects of estrogen potentiating factor (EPF), insulin growth factor 1 and 2 (IGF-1 and IGF-2), pituitary mammary gland growth factor (PMGF), epidermal growth factor (EGF), fibroblastic growth factor (FGF), transforming growth

factor (TGF) and other mitogens on the growth and development of the mammary gland will be reviewed.

The effect of many of the well known growth factors on immature mammary gland development in vivo is not known. However, in 1987, Newman and her colleagues using in vivo based studies, investigated the effects of human pituitary extracts on mammary gland development. Hypophysectomized and castrated immature male rats (20-23 days old) and rhesus monkeys were given estradiol to imitate the follicular phase of estrous. The animals were then treated with whole or stripped pituitary extract (which contained very low levels of prolactin or growth hormone) for 8 days. At the end of this period, the mammary glands were removed and evaluated for ductal development. The data showed that estradiol administration in the control rats (nonhypophysectomized) resulted in significant mammary gland development compared to the hypophysectomized rats in which mammary gland development was significantly inhibited. They also found that both whole and stripped pituitary extracts had a stimulatory effect on mammary gland development when rats were given estradiol. Newman concluded that there was "evidence for the existence of a non-prolactin, non-growth-hormone mammary mitogen derived from the human pituitary." Her theory was based on the fact that the stripped human pituitary extract, which contained very low levels of prolactin and growth hormone, resulted in significant mammary gland development in both rats and monkeys.

In an *in vitro* study three years earlier, Smith and his colleagues (1984) discovered that a pituitary derived substance they named PMGF, (pituitary mammary gland growth factor) stimulated cell division in the cuboidal cell population of the mammary gland.

The effect of known growth factors on cell proliferation, invasion, and metastasis has been well documented *in vitro* and by *in vivo* injection studies using various mammary gland and breast cancer cell lines. EPF (estrogen potentiating factor), believed to be of endocrine origin, has been shown to potentiate the growth of human breast cancer cells in the presence of estradiol both *in vivo* and *in vitro* (Dembinski et al., 1985; Shiu et al., 1986a).

IGF-1 and IGF-2 which have 47% homology to insulin, required for growth and development of mammary gland cells *in vitro*, have been shown to be potent mitogens for mammary tumor cells (T-47D) which carry receptors for these growth factors (Furlanetto and DiCarlo, 1984; Myal et al., 1984). No information could be found regarding the effect of IGF-1 and IGF-2 *in vivo*.

EGF, which is similar to insulin and relaxin, is a single polypeptide, 53 amino acids long. Receptors for EGF are found on both normal and malignant epithelial cells (Taketani and Oka, 1983c). *In vitro* studies have shown that EGF is a potent mitogen and although it stimulates the synthesis of type IV collagen by mammary epithelial cells and cell proliferation, it inhibits cell differentiation.

FGF outside the nervous system is a cationic, heparin binding, mitogenic growth factor. Very little is known about FGF however, Smith and his colleagues (1984) found that bovine pituitary FGF stimulated growth in normal rat mammary myoepithelial and stromal cells, and Shiu (1981) found FGF to stimulate growth in human breast cancer cells (T-47D).

Welch and his colleagues (1990) conducted an in vitro study in which pretreatment of rat mammary adenocarcinoma clone MTLn3 cells, in the presence of serum with TGF-β_1, did not significantly alter the growth of the cells. However, the same cell line in a serum-free medium treated with TGF-β_1 resulted in inhibition of cell growth. Therefore, TGF-β_1 is believed to be cytostatic or slightly inhibitory in cell culture. In addition, they also found that TGF-β_1, as opposed to TGF-α, IGF-I and PDGF (platelet derived growth factor), had a stimulatory effect on metastasis when pre-treated MTLn3 cells were injected into 6 to 7 week old rats and the lungs were evaluated for metastasis.

Finally, mammostatin, a heat sensitive protein, with homology to the progesterone receptor, ß-inhibin and cystatin, causes inhibition of cell mitosis in mammary and non-mammary gland cell lines. Production of this normal growth regulator is evident in the presence of high estrogen, an indirect stimulant of epithelial proliferation. However, cell numbers are decreased in culture and mammostatin production has been shown to decrease with increased tumor metastasis (Ervin et al., 1989).

The above information on growth factors, while presumed to be accurate, does not necessarily reflect, nor can it be extrapolated to, the in vivo environment. However, it does provide a basis for further experimentation using in vivo protocols which examine the prepubertal-pubertal growth period.

The Influence of Diet on the Development of the Virgin Mouse Mammary Gland

Much of the interest in the effect of diet, especially diets containing high concentrations of unsaturated fatty acids, on mammary gland development stems from epidemiologic studies in women which showed a significant correlation between mammary gland carcinomas and the average daily consumption of fat (Carroll et al., 1968; Wynder, 1968). As early as 1950, Silverstone and Tannenbaum examined the effect of dietary fat on mammary gland carcinogenesis in mice. During the 1970's and 1980's rats and mice were used to study the effect of diets containing high concentrations of unsaturated fatty acids on tumorigenesis and mammary gland development (Rao and Abraham, 1976; Chan et al., 1977; Abraham et al., 1984). The results of these studies supported the epidemiologic findings of Carroll et al., (1968) and Wynder (1968) and led to a series of studies in the 1980's which examined the effect of diets deficient in essential fatty acids (EFA), such as linoleic acid, a polyunsaturated

fatty acid, on mammary gland development.

In 1980, Knazek and his colleagues studied the effect of EFA deficient diets on weanlings (1-2 weeks post-weaning) and on the offspring of mice fed an EFA deficient diet from mid-pregnancy through lactation and the post-weaning period. Both groups of C3H mice were fed an EFA deficient diet containing coconut oil. The weanling group (weaned at 4 weeks of age) was fed the EFA-deficient diet for up to 32 weeks. Whole mount evaluation of the mammary glands showed a significant decrease in the volume of the fat pads, but the rate of alveolar development was equal to that of the control group at 17 weeks on the diet. However, by 32 weeks on the diet, no alveoli were detectable in the EFA-deficient glands while the control group maintained their alveoli through 32 weeks. Knazek concluded that EFAs were "necessary for the maintenance of established alveolar structures." Glands devoid of alveoli were also discovered in multiparous female mice fed an EFA deficient diet from mid-pregnancy through post-weaning (33 weeks). The offspring from the EFA-deficient dams also had a decreased rate of alveolar and ductal development when compared to mice fed EFA-adequate diets 1-2 weeks post-weaning. Knazek suggested that EFA deficiency and its effect on mammary gland development could be associated with altered cell membranes (modified hormone-receptor complexes) and their inability to respond to hormones, since EFAs play a key role in maintaining structurally normal lipid bilayers.

Knazek's findings were supported by a series of experiments in Balb/c mice done by Miyamoto-Tiaven and her colleagues in 1981. Both virgin Balb/c mice and transplanted mammary cells from syngeneic Balb/cf C3H mice were used in this study. In one experiment, the mice were fed diets containing 15% corn oil (CO), 15% hydrogenated cotton seed oil (HCTO) and 15% CO plus indomethacin from 4.5 to 8.5 weeks of age. Additional experiments examined the effect of a complete dietary absence of linoleate from birth to 8 weeks of age and the effect of 1) no fat, 2) no linoleic acid, 3) low linoleic acid and 4) high levels of linoleic acid on mammary duct growth between 4.5 to 9 weeks of age. The effect of no fat and/or linoleic acid on the growth of transplanted mammary gland cells was also examined. No. 4 mammary glands were assessed for growth and development of mammary ducts via whole mount analysis. The results were recorded as the percentage of total fat pad in which the ductal mammary tree filled $\geq$ 50% of the fat pad, i.e., fat pad filled (FPF). In all the animal experiments, EFA deficient diets and the indomethacin (IM) diet were associated with a slower rate of ductal growth. In the transplant experiments, the EFA-deficient hosts had less successful transplants and less duct growth than the CO fed hosts. Miyamoto-Tiaven and her colleagues (1981) concluded that EFA-deficient diets affected Balb/c mice in a way similar to C3H mice, in spite of the fact that Balb/c mice have fewer alveoli than C3H mice. Their experiments showed that ductal development was retarded by a complete lack of EFAs or a low

level of EFAs (linoleic acid) and that normal mammary gland development requires a minimum amount of EFA and may have a dose-response relationship. She stated, "within some as yet unknown range of EFA levels there is a direct correlation between amount of dietary EFA and rate of growth and degree of development of the normal gland." They also demonstrated the importance of prostaglandins in ductal development using indomethacin. Indomethacin (IM), a prostaglandin inhibitor, when added to a diet containing polyunsaturated fatty acids (PUFAs) had similar but temporary effects on ductal growth as observed in EFA deficient diets. The relationship between decreased ductal growth associated with IM and that associated with an EFA deficient diet lies in the fact that EFA deficient diets result in decreased arachidonate which results in decreased prostaglandin synthesis. Hence, EFA deficiency and inhibition of prostaglandin synthesis have similar negative effects on mammary gland growth.

From 1985 to 1989, the effect of the "level" of dietary fat as well as the "type" of dietary fat on the development of the mammary gland and their effect on hormone responsiveness was explored by Welsch et al., (1985), Welsch and O'Connor, (1989); and Faulkin et al., (1986). Welsch et al. (1985) examined the effect of diets containing 0%, 5%, and 20% fat corn oil on Balb/c mice. Beginning at 21 days of age, the mice were fed one of the above diets for a 3 month period of time. In addition, 10 days prior to euthanasia, he injected 50% of the mice in each group with saline and the other 50%

with 1 μg of estradiol-17β and 1 mg of progesterone daily, in order to examine the effects of hormones in association with the 3 levels of dietary fat. Whole mounts of the No. 4 mammary glands were evaluated for duct growth, degree of branching and the presence of end buds or lobuloalveolar structures. The No. 2 mammary glands were sectioned (the anterior 3mm tip) at 5 microns and used for [^{3}H] thymidine-autoradiographic analysis and/or collected for organ culture analysis. In the organ culture experiments, one No. 2 gland was exposed to basal medium and the contralateral gland was exposed to basal medium plus mammogenic hormones (for 6 days) to determine the "differential growth response" between the 2 groups. The results of this study showed a significant reduction in mammary gland development in those mice fed a 0% fat diet when compared to those mice fed a 5% or 20% fat diets in groups given either the saline or estradiol:progesterone (E:P). No significant differences were observed in mice fed 5% or 20% fat diets and injected with saline, but a near significant ($p \leq .07$) increase was observed in the E:P. However, when the mice injected with saline were compared to the mice injected with E:P a significant increase in mammary gland development was observed in the latter group. In both groups, the [^{3}H] thymidine autoradiographic analysis showed a linear increase between the number of mammary epithelial cells labeled and increasing fat content in the diet. The results of the organ culture analysis showed that in those mice fed between 0-5% and 5-20% fat and injected with saline there were

significant increases in mammary gland development in the basal medium plus mammogenic hormones when compared to the basal medium alone . However, in those mice injected with E:P, developmental significance was only detected at the 0-5% fat level. Epithelial area analysis in mice injected with saline and fed a diet between 0-5% fat showed a significant increase in epithelial area in the basal medium plus mammogenic hormones group when compared to the basal medium alone. In the mice given E:P, a significant increase was observed between 0-5-20% fat in the diet for epithelial area. Welsch concluded that those mice fed a fat-free diet had significantly "atrophic" mammary gland development compared to those fed a 5% or 20% fat diet irregardless of the presence or absence of mammogenic hormones. He stated, "the mammae from mice fed a fat-free diet appear to be incapable of responding morphologically to hormonal mammogenic growth stimulus." Welsch found that a higher fat diet (20% vs 5%) in the mice injected with E:P resulted in "slightly enhanced" mammary gland development ($p \leq .07$) and significantly greater epithelial area. Welsch concluded that, "mammae derived from mice fed high fat diets (20%) responded greater to a hormonal mammogenic growth stimulus than mammae derived from mice fed a standard level of dietary fat (5%) however, ... not as nearly as striking as the difference observed when comparing hormone responsiveness of mammae derived from mice fed the 0% and 5% fat diets."

Faulkin and his colleagues (1986) examined the effect of

dietary fat on "differentiated stages" of mammary development using transplanted ducts in adult mice. The two diets used in this study contained 10% CO (a source of polyunsaturated fat) or 10% HCTO (a source of saturated fat) added to a stock diet consisting of 9% fat. The stock diet contained 44% linoleate prior to the addition of CO which was high in linoleate or HCTO which was devoid of linoleate. Balb/c mice, at different stages of maturation, were fed the diets at the time of duct transplantation for up to 6 weeks. Faulkin examined the effect of diet on transplants in immature mice during ductal expansion (from 3 - 7 weeks and 3 - 9 weeks of age) and mature mice (from 8 - 11 weeks, 8 - 14 weeks and 17 - 20 weeks of age). Specifically, they recorded the percentage of fat pad filled by the transplanted mammary tissue as a measure of mammary growth. The results of these experiments showed that only those groups in which the mammary gland was developing was affected by the diet, i.e., those immature mice fed the stock plus HCTO diet had slower growing mammary glands. Faulkin then examined the effects of CO and HCTO diets on, 1) ovary development in 3 - 9 week old and 3 - 13 week old mice, 2) mammary gland development during pregnancy, 3) hormone stimulated male mice, 4) ovariectomized immature female mice supplemented with estrogen, and 5) intact female mice given progesterone. He found no significant difference in mammary gland development in pregnant mice fed either diet. The hormone stimulated neutered male mice, used to examine the effects of estrogen and estrogen plus progesterone on ductal

growth, demonstrated that E alone was insufficient to stimulate ductal growth but when progesterone was added significant ductal growth was observed by 6 weeks on the diet. Findings in ovariectomized immature female mice given E were similar to those in neutered male mice. Faulkin concluded that "the effect of dietary fat was mediated through the endocrine system rather than acting directly on the mammary epithelium." When examining the effect of CO or HCTO in the ovariectomized immature female mice given E, either for 3 weeks or 5 weeks, he found no significant difference between the effects of CO and HCTO diets and concluded that "estrogen could overcome the effects of HCTO on mammary gland development." When intact virgin female mice were given progesterone (at 3 weeks of age) and fed CO or HCTO diets for 6 weeks, a reverse in the inhibition of ductal growth in the HCTO diet group, resulting in lobulo-alveolar development, was observed. Finally, Faulkin examined the effects of CO and HCTO diets on the development of the ovary. After 10 weeks on diet, the mice in each group were euthanatized and their ovaries were examined for follicles and corpora lutea. The results of this examination showed that the number of primary, secondary and mature follicles was the same between diet groups at 6 weeks of age. However, by 10 weeks of age, the HCTO group had no corpora lutea and the CO group averaged 2 per ovary. Faulkin's overall conclusions in this study were that the effect of dietary fat on the development of the mammary gland was 1) dependent on the age of the mouse when

the test diet was initiated, 2) not a direct effect of the diet on the ductal structures but an indirect effect via the altered function of the ovary; which resulted in inhibition of mammary gland development from altered hormone levels, 3) associated with the interval in which the diet was fed, and 4) was directly associated with the negative effect of the EFA deficient diet (HCTO diet) on the development of the ovary and the production of hormones by this organ.

In 1989, Welsch and O'Connor expanded on previous studies which analyzed the influence of dietary fat on mammary gland development by examining the effect of different types of fat on immature and mature female Balb/c mice. A total of 12 different diets consisting of 5% corn oil, 20% corn oil, 20% olive oil, 20% linseed oil, 19% coconut oil + 1% corn oil, 20% lard, 19% beef tallow + 1% corn oil, 19% menhaden oil +1% corn oil, 15% corn oil + 5% menhaden oil, 10% corn oil + 10% menhaden oil, 4.5% corn oil + 15.5% menhaden oil, and 19.75% corn oil + 10.25% menhaden oil. The immature mice were fed the diets from 21 to 45 days of age. At 35 days, the mice were ovariectomized and at 42 days each mouse was injected with estradiol-17ß plus progesterone to provide a uniform hormonal environment. The mature mice were fed the diets from 28 to 128 days and divided into 2 groups. The first group was sacrificed between 118 - 128 days during estrus and the second group was given estrogen plus progesterone injections between 118 - 128 days. The results of this extensive study showed that no significant difference was found in the degree of

ductal expansion between the vegetable oils and/or animal fat diets in immature mice, but there was a significant decrease in ductal expansion in those immature mice fed the fish oil diet. The mice fed 5% corn oil diet had less ductal growth than the mice fed 20% corn oil diet and when comparing the 5% corn oil + fish oil diet to the 20% corn oil diet the growth was significantly less. However, when comparing the mice fed 5% corn oil to the mice fed the fish oil diet there was no significant difference indicating that low corn oil diet had the same effect as fish oil diet. The results of this experiment showed that when corn oil was less than 20% of the diet, i.e., 10% and 4.5%, and fish oil was at least 10%, a significant decrease was observed in the degree of ductal expansion when compared to mice fed 20% corn oil.

In the mature group of mice, epithelial area was used to determine the influence of dietary fat on the mammary gland as well as subjective mammary gland developmental scores. There was no significant difference in epithelial area between the non-E:P injected mice fed vegetable oils and/or animal fats. The non-E:P injected mice fed corn oil + fish oil diets also showed no significant developmental or epithelial area differences. However, mice fed the 20% corn oil, olive oil, and lard diets showed significantly higher developmental scores (the degree of ductal-alveolar epithelial development) when compared to the mice fed the fish oil diet. When the mature mice were injected with estrogen and progesterone, a very different developmental pattern was observed. As in the

non-hormone treated group, there was no significant difference between mice fed vegetable oils and animal fats, except when comparing 5% corn oil to 20% corn oil. But a significant difference in both epithelial area and development scores was noted between those hormone treated mice fed fish oil + vegetable oil diets and fish oil + animal fat diets when compared to those mice fed 20% corn oil or coconut oil. In those hormone treated mice fed corn oil + fish oil, the developmental scores and epithelial areas were significantly decreased when compared to mice fed 20% corn oil. Hormone treated mice fed diet combinations of corn oil + fish oil containing 4.5% or greater corn oil and 10% or greater fish oil had significantly lower developmental scores than mice fed 20% corn oil diet, and even less than those mice fed a 5% corn oil diet when the level of fish oil was 15.5%. Therefore, the level of corn oil is not significant as long as the diet includes 10% or more fish oil with the greatest reduction in epithelial area and developmental scores observed in the group of mice consuming the largest percent fish oil in the diet. Welsch and O'Connor (1989) concluded that only mice with actively proliferating mammary epithelium were sensitive to alterations in dietary fat. Of the diet groups tested, only those mice fed the fish oil diets and the 5% corn oil diet consistently showed a decrease in development when compared to mice fed a 20% corn oil diet. All of the other diets tested caused no significant difference in development. Welsch and O'Connor (1989) suggested that it was the change in dietary

fat composition that influenced mammary ductal cell proliferation. This theory is supported by previous work done by Miyamoto and her colleagues (1981), who speculated that mammary gland development was altered by the percent of dietary fat and its direct effect on prostaglandin synthesis. It is well known that increased fish oil in the diet alters the arachidonic acid cascade. Fish oil is rich in n-3 fatty acids (EPA 20:5 and DHA 22:6) which modify linoleic acid (18:2) and arachidonic acid (20:4) metabolism. It is possible that these fatty acids when incorporated into cell membranes alter hormone - receptor relationships in the cell or the ability of the cell to respond to hormone - receptor complexes resulting in decreased cell proliferation and hence decreased mammary gland development. Welsch and O'Connor (1989) speculated that, "the inhibitory effect of dietary menhaden oil on the developmental growth of the mouse mammary gland ... is manifested via an inhibition of linoleic acid utilization by way of interference from large amounts of EPA and DHA in the diet." They also point out that no correlation was found between the level of linoleic acid and mammary gland development in the mouse. Therefore, the effect of fish oil on mammary gland development lies with the effect of EPA and DHA, and not solely on the utilization of linoleic acid. This "effect" relates to altered prostaglandin synthesis and may be associated with "abnormal" hormone - receptor complex activity and cell metabolism such that mammary gland development is either directly or indirectly inhibited.

CHAPTER 2

ULTRASTRUCTURAL ANALYSIS OF THE EPITHELIAL CELLS IN THE TERMINAL END BUD OF THE MOUSE MAMMARY GLAND

Abstract

From late embryogenesis, day 17 of gestation, up through the first few days after birth, and during the prepubertal-pubertal growth period, from 4 to 7 weeks of age, a unique structure called the terminal end bud (TEB) is present in the mouse mammary gland. The primary function of the TEB is to drive ductal morphogenesis, which results in expansion of the ductal network throughout the mammary gland fat pad. Four distinct cell types previously identified in the TEB using light microscopy and ultrastructural analysis (namely, the cap cell, myoepithelial cell, body or intermediate cell and the luminal or dark cell) were confirmed in this study. In addition, a transitional cell type, termed the "myocap cell" was identified near the flank region of the TEB. The myocap cell resembles the cap cell morphologically but contains myofilaments in the cytoplasm which are associated with the myoepithelial cell. Morphometric analysis of the 4 major cell types in the TEB, as measured by area in micrometers squared, showed the undifferentiated cap cells and the moderately differentiated intermediate cells to be the largest cells and the fully differentiated myoepithelial and luminal cells to be the smallest cells.

Introduction

The first published ultrastructural analysis of the postnatal mouse mammary gland dates back to studies by Hollman (1969) and Wellings et al., (1960) in which they analyzed milk secretion in the mammary gland of C3H/Crgl mice. In 1967, Sekhri et al., using transplanted mammary gland tissues from C57BL/Crg 1 mice, analyzed the cytomorphology of the normal mammary gland. Tissue samples from 19 day prenatal to 30 day post-partum mice were examined by light and electron microscopy. This was the first ultrastructural study to examine the epithelial components of the prepubertal-pubertal mouse mammary gland. Sekhri and his colleagues (1967) analyzed the primary (1^0), secondary (2^0), and tertiary (3^0) duct regions in the mature virgin gland. In addition, a chronologic description of the presence or absence of the TEB structures, their location, shape and cellular content was also reported. Sekhri stated, "the terminal end-buds were pear-shaped or sac-like, with deeply stainable, crescentic caps at their distal ends." These caps would later be described in more detail by Williams and Daniel (1983) as the "cap cell" layer or pleuripotential stem cells of the mammary gland. Sekhri's ultrastructural description of the TEB was very basic and did not distinguish between the four histologically distinct cell types known to exist today. In fact, when describing the cytoplasmic organelles found within the cells comprising the TEB, they described them as though

they were describing one cell type, i.e., the "end-bud cell". In this study, electron microscopic samples from only two mice (out of a total of 8 mice) were used to examine the tertiary duct region where the TEB structure resides. Nonetheless, the results from this study, laid the foundation for future morphologic analysis of the TEB structure.

In 1973, Pitelka and her colleagues published a detailed ultrastructural analysis of the cell contacts in the mouse mammary gland. This study not only described the intercellular contacts present during the postnatal developmental period but also gave a detailed ultrastructural description of the different cell types comprising the various duct regions. Unfortunately, only two neonatal (newborn - 2 day) and three juvenile (3 weeks of age) immature C3H/Crg 1 mice were used for ultrastructural analysis and once again the analysis focused on the 1°, 2°, and 3° ducts, and the peripheral myoepithelial and inner luminal cells. During the 1980's the focus of ultrastructural analysis of the mammary gland shifted to the TEB structure and to defining the peripheral cells lining the TEB of the rodent mammary gland.

Prior to the first detailed ultrastructural analysis of the TEB by Williams and Daniel (1983), Gordon and Bernfield (1980) examined the chemical content and structural organization of the basal lamina surrounding the TEB structure. The basal lamina from pregnant and prepubertal mammary glands was analyzed by histologic and autoradiographic techniques. In addition, the mammary glands from 10, 11, and

13 day pregnant mice were collected for ultrastructural analysis. The information gathered in this study would later be used by Williams and Daniel (1983) as a basis of comparison between the basal lamina in the TEB and that of the mid-pregnant duct.

In 1982, Silberstein and Daniel (1982a) further defined the chemical content of the basal lamina at the tip of the end bud using histologic and autoradiographic techniques. The data showed that the primary chemical component of the basal lamina, hyaluronate, was produced by a distinct outer layer of epithelial cells they termed "cap cells", i.e., these were the same cells described by Sekhri (1967) some 15 years earlier as "deeply stainable crescentic caps". They also found that hyaluronate was secreted into the extracellular environment and theorized that it most likely played a key role in decreasing cellular adhesion thereby facilitating the penetration of the TEB through the mammary gland fat pad. Minimal or no hyaluronate was found near the neck or flank regions of the TEB and Silberstein and Daniel (1982a) concluded that the posterior region of the TEB was the site of ductal morphogenesis and tissue stabilization. The work done by Silberstein and Daniel (1982a) was followed by the first and only detailed ultrastructural analysis of the TEB in the mouse mammary gland conducted by Williams and Daniel in 1983. The primary focus of this study was to further define the dimensional variations in the width of the basal lamina along the entire TEB and to describe, in detail, the

undifferentiated "cap cell", which they believed was the stem cell of the mammary gland. An undisclosed number of 6 week old Balb /c and C57 Black strain of mice were used in this study. Mammary glands were collected for whole mount analysis, transmission and scanning electron microscopy, and time-lapse microtelevideo recordings. The size of the TEB structure measured from whole mounts was reported to range from 0.1 to 0.8 mm. Williams and Daniel (1983) reported that the cap cell was located directly beneath the basal lamina and was slightly separated from other surrounding cap cells but continuous with the myoepithelial cells in the TEB flank region. They described the cap cells as having several features which distinguished them from the other cell types within the TEB, namely: 1) a lack of specialized cell junctions or adhesions and 2) frequent intercellular spaces on their lateral borders associated with cell processes. Ultrastructurally, they reported the cells to be low columnar with round to oval nuclei, prominent nucleoli and sparse heterochromatin. The cytoplasm was described as containing abundant free ribosomes, moderate numbers of mitochondria, small numbers of endoplasmic reticulum and variable numbers of lipid droplets. The undifferentiated cellular profile reported by Williams and Daniel (1983) supported their theory that the "cap cell" population was in fact the stem cell population of the mammary gland and hence gives rise to all of the cell types comprising the mature duct. The results of their time-lapse microcinematography experiments, using end

buds incubated in petri dishes, showed that the cap cells were mitotically active, mobile and appeared to migrate directly or divide and migrate into the deeper regions of the end bud; further supporting their stem cell theory. Since the results of this study were published in 1983, there has been very little research in the area of ultrastructural analysis of the TEB structure. Other researchers, such as Dulbecco and his colleagues (1982,1983) have examined the evolution of cell types in the rat mammary gland using radioactive thymidine and immunological markers. The results of these studies support the cap cell - stem cell theory of Williams and Daniel (1983).

The purpose of the present study was to verify the four cell types previously identified in the TEB and describe them in detail, identify and describe "transition" cell types, and calculate cell and nuclear morphometric values of the four major cell types in the TEB structure.

Materials and Methods

Animals. One hundred and eighteen mice, consisting of Balb/c and athymic nude (Nu/+) strains, were used in this study. They ranged in age from 28 to 42 days old. Prior to euthanasia, the mice were housed in a temperature controlled environment at $21^0 \pm 1^0C$ on a 12 hour light, 12 hour dark exposure cycle. They had unlimited access to water and were fed a standard laboratory rodent chow diet.

In Vivo Terminal End Bud Identification. The standard identification procedure most often cited in the literature for visualization of ductal epithelium in the mammary gland is an intralactiferous duct infusion technique using aqueous Trypan Blue dye (Humason, 1979). This procedure requires a great deal of skill and can be difficult to adequately accomplish in young mice with small openings in the nipple. In addition, the pressure required for complete infusion of dye throughout the entire mammary gland tree can be associated with internal epithelial damage. Therefore, it was necessary to develop a less invasive technique that would not disrupt or damage the internal epithelial cells. The SIVS (subcutaneous injection of a vital stain) technique used in this study was developed from an *in vitro* staining technique in which different concentrations of Methylene Blue Chloride (MBC) were tested for toxicity on monolayers of human mammary tissue (Buehring and Jensen, 1983).

SIVS Technique. The success or failure of the SIVS technique depends on correct subcutaneous placement of the MBC vital stain. Therefore, prior to injection the mice are anesthetized intraperitoneally with approximately 0.05 mg of sodium pentobarbital. Once the mice are successfully anesthetized, the nipple associated with the gland to be injected is located and a 25 gauge needle is placed in the subcutaneous tissue adjacent to the nipple. Approximately 0.5 mls of a 100 - 200 ug solution of MBC per ml of Hank's Buffered Salt Solution is then injected into the subcutaneous

region. The solution is allowed to diffuse into the mammary gland fat pad for approximately 2.0 to 2.5 hours. At the end of this time, the mice are re-anesthetized with ether and a ventral midline incision is made to expose the light blue stained ducts and TEB structures. Prior to excision of the TEBs, the mice are perfused, through the left ventricle, with a modified Karnovsky's fixative for approximately 5 minutes to initiate fixation. Using a Nikon photomicroscope or a dissecting microscope, the TEBs are then isolated, excised with a 3.0 mm punch biopsy, placed on a 4.0 mm dacron raft to prevent curling of the tissue sample, and put in a modified Karnovsky's fixative .

Transmission Electron Microscopy

Sample Fixation. Control tissue samples, in which TEBS were collected "blind" from the No. 4 inguinal gland, and SIVS tissue samples collected from the No. 2, No. 3 and No. 4 glands, in which the TEBs stained light blue, were placed in a modified Karnovsky's fixative consisting of 2.0% glutaraldehyde - 2.0% formaldehyde - 1mM calcium chloride - 0.2 M cacodylate (Karnovsky, 1965; Glauert 1975) immediately upon excision. The samples were fixed at room temperature for 2 to 3 hours and washed in 0.1 M cacodylate buffer for a total of 3 15 minute washes. Prior to post-fixation, using a dissecting microscope, the SIVS samples were trimmed into triangular shapes. This procedure resulted in 1 to 3 TEB

structures per sample placed in longitudinal or cross-sectional orientation. The buffer washed samples were post-fixed in a 50:50 solution of 2.0% osmium tetroxide - 2.0 M cacodylate buffer for 2 hours at room temperature. The post-fixed samples were washed in 0.1 M cacodylate buffer for a total of 2 15 minute washes and one 15 minute wash in triple distilled water. In order to increase the contrast in the samples, the tissues were *en bloc* stained in 0.5% uranyl acetate for 8 hours or overnight, at room temperature, and washed in triple distilled water for up to 1 hour. Samples were dehydrated using a graduated series of ethyl alcohol (ETOH) solutions beginning at 25% ETOH up to 100% ETOH for 15 minutes each (25%, 50%, 75%, 95%, and 100% (2 times)). The dehydrated samples were then placed in a graduated series of ethanol:propylene oxide (EtOH:PO) solutions (3:1, 1:1, and 1:3), a transition solvent, for 15 minutes each and transferred to 100% PO for two 30 minute washes. In order for the samples to be compatible with the Epon-Araldite-Spurrs resin, they were placed in a graduated series of PO:resin solutions (2:1 and 1:2) for 3 hours each at room temperature and then transferred to 100% resin for 8 hours or overnight (Dawes, 1971; Klomparens et al., 1986). All of the above procedures were carried out on a rotation device to aid in the infiltration or extraction of chemicals across the mammary gland fat pad. The resin infiltrated samples were placed in capsular molds and oriented so the longitudinal or cross-sectional axis of the TEB was adjacent to the block face. The

capsules were filled with 100% resin and baked in a convection incubator at 65^{0}C for 48 hours.

Serial Sectioning and Positive Staining. One to two micron thick "monitor" sections were trimmed in 15 - 30 micrometers increments from the block face with a glass knife and stained with a 1.0 - 2.0% solution of Toluidine Blue for light microscopy (Kiernan, 1990). At the level where the mid-portion (largest diameter) of the TEB was positively identified, 80 - 100 nm thin sections were serially trimmed from the block face with a Du Pont diamond knife. Approximately half of the sections in each ribbon were picked up on a thin bar hexamesh grid or a formvar coated oval slotted grid for positive staining. The positive staining procedure, which adds electron density to the cellular structures, consisted of a 1 hour immersion in uranyl acetate followed by a 3 to 5 minute exposure to lead citrate.

Ultrastructural and Morphometric Analysis. Selected grids containing representative sections of TEB structures were photographed on a Philips 201 transmission electron microscope. The micrographs were used to study the ultrastructural characteristics of the TEB and to determine the cellular and nuclear areas (in micrometers squared) of the four major cell types in the TEB structure. The cells selected for morphometric analysis were randomly chosen from the micrographs. The cells were carefully traced onto a sheet of clear acetate and measured on a computer assisted image analyzer (Pesce, 1987).

Results

SIVS Technique. The mechanism by which MBC delineates the TEB structure is not clearly understood. Previous researchers have shown that the uptake of MBC by epithelial cells was primarily cytoplasmic, as evidenced by the presence of dense cytoplasmic inclusions of blue dye in frozen sections and observed with phase - contrast microscopy. However, MBC inclusions were not detectable in the cytoplasm of cultured cells in ultrathin sections when viewed under a transmission electron microscope by Buehring and Jensen (1983) or by this author. Buehring and Jensen reported that the MBC dye leaches out of the tissue during the alcohol dehydration step of TEM fixation and therefore, is not present in the ultrathin sections.

In the present study, at concentrations of 100 - 200 μg of MBC per ml of Hank's Buffered Salt solution, the adipocytes and connective tissue stained a very pale blue, the TEB structures a moderate blue and the nerves, an intense blue (Figure 2.1.). A mild degree of subcutaneous edema was occasionally observed at the injection site when the higher concentrations (near 200 μg/ml) were used. Ultrastructurally, MBC at concentrations of 100 - 200 μgs does not appear to alter or damage mammary gland epithelial cells when compared to control tissue samples collected from unstained No. 4 mammary glands. The optimum post-injection time for

Figure 2.1. Light micrograph of a No. 2 thoracic mouse mammary gland. The gland was injected with a 200 μg/ml solution of MBC using the SIVS technique. Note the multiple blue stained ducts in the fat pad (arrow). X10.

Figure 2.2. Light micrograph of a No. 4 inguinal mouse mammary gland. The gland was injected with a 300 μg/ml solution of MBC using the SIVS technique. Note the lack of clearly defined ducts associated with overstaining (arrow). X19.

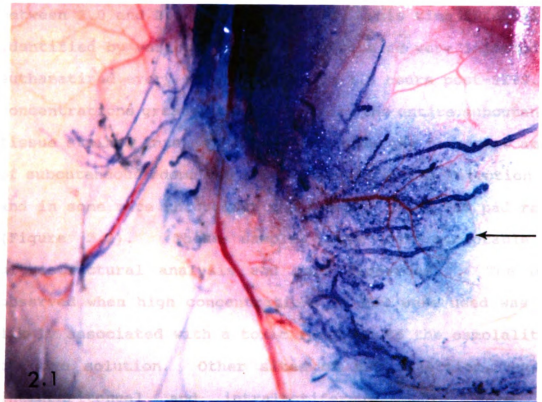

2.1

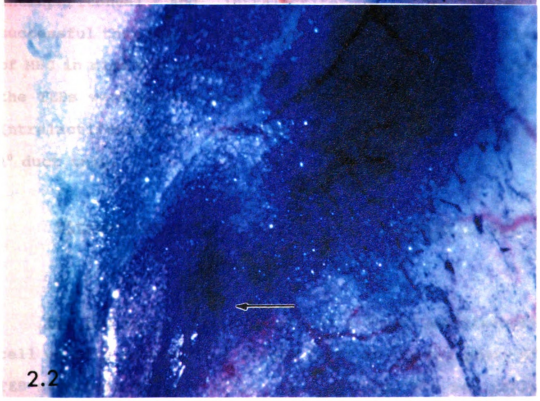

2.2

identifying the TEBs in the present study was found to be between 2.0 and 2.5 hours post-SIVS. This time interval was identified by various trials in which mice were injected and euthanatized every 30 minutes up to 3.5 hours post-SIVS. At concentrations greater than 250 μg/ml, the entire subcutaneous tissue stained intensely blue and a moderate to severe amount of subcutaneous edema was often observed at the injection site and in some mice throughout the mammary gland fat pad region (Figure 2.2). These samples were not acceptable for ultrastructural analysis and were discarded. The edema observed when high concentrations of MBC were used was most likely associated with a toxic reaction to the osmolality of the dye solution. Other sites of MBC injection, such as intraperitoneal and intralactiferous duct, were less successful than the SIVS technique. Intraperitoneal injection of MBC in mice was associated with a higher mortality rate and the TEBs were either poorly stained or not stained at all. Intralactiferous duct infusion resulted in delineation of the 1^0 duct only.

Ultrastructural and Morphometric Analysis of TEB Epithelial Cells

The Cap Cell. The cap cell is a large undifferentiated cell usually located in a single layer at the periphery of the TEB structure (Figure 1.2). In some TEBs, the cap cells can be two or more cell layers deep; especially at points where

Table 2.1 Nuclear and Cellular Areas of TEB Epithelial Cells

	Nuclear Area		Cellular Area	
	Mean	Range	Mean	Range
Cap Cell	37.8[a] n=34	17.2-57.3	94.3 n=14	45.0-164.2
Intermediate Cell	34.3 n=70	19.2-63.7	62.0 n=14	41.9-88.4
Myoepithelial Cell	29.6 n=16	16.0-49.9	51.8 n=3	37.5-66.7
Luminal Cell	16.2 n=5	10.2-22.0	41.9 n=3	24.9-54.3

a= Area measures from longitudinal ultrathin sections in μm^2.
n= Number of nuclear or cellular areas measured.

the TEBs divide or branch. On longitudinal section, the cap cells have an oval to cuboidal shape with a round to oval, centrally located, euchromatic nucleus (Figure 2.3). Focal areas of peripheral heterochromatin and variable numbers of nucleoli are also present. The cap cell cytoplasm contains an array of organelles. There are variable numbers of lipid droplets and microvesicles (both coated and uncoated). The most abundant organelles are mitochondria and free ribosomes. Smaller numbers of endoplasmic reticulum and occasional golgi complexes were also observed. Computer assisted morphometric analysis of the cap cell revealed a mean nuclear area of 37.8 μm^2 and a mean cellular area of 94.3 μm^2 (Table 2.1).

The cap cell membrane is a dynamic structure that varies in its morphologic presentation. The lateral and internal membranes contain multiple intercytoplasmic processes (ICP) of various size and shape. The ICPs are associated with intercytoplasmic spaces (ICS) and the degree of spacing between adjacent cap cells and underlying intermediate cells varies from TEB to TEB (Figure 2.4). The internal IC spacing is believed to result from the secretion of hyaluronate by the cap cells (Silberstein and Daniel, 1982a).

The basal cell membrane is relatively linear and lies adjacent to a very thin, continuous basal lamina which is produced by the cap cell layer. The basal cell membrane engages in both endo- and exo-micropinocytotic activity which is traditionally associated with the exchange of cellular material between cells and between cells and the extracellular

Figure 2.3. Transmission electron micrograph of a cap cell from the tip of a TEB in a mouse mammary gland (a longitudinal ultrathin section). Note the oval euchromatic nucleus (N), prominent intercytoplasmic spaces (ICS) and processes (arrow), thin basal lamina (Bl-*) and numerous mitochondria (M) and ribosomes (R), and lipid vacuole (Lv). The sample was prepared using a standard TEM procedure consisting of a modified Karnovsky's fixative, followed by O_sO_4 and an *en bloc* UA. Scale bar = 1.0 μm.

Figure 2.4. Transmission electron micrograph of a TEB near the flank region in a mouse mammary gland (a longitudinal ultrathin section). Note the intercytoplasmic processes and spaces (arrowheads) between adjacent cap cells (CC) - intermediate cells (IC) - myoepithelial cells (arrow) and luminal (LC) cells. (Fibroblast (F), basal lamina (Bl), and collagen (C) are also labelled). Scale bar = 1.0 μm.


R
ICS
N
Bl
M
Ly
2.3
F
MEC
CC
LC
2.4
IC

Figure 2.5. Transmission electron micrograph of a cap cell membrane at the tip of the TEB in a mouse mammary gland (a longitudinal ultrathin section). Note the prominent extracellular space (double-sided arrow) between the adipocyte (A - tip only shown) and basal lamina (Bl) surrounding the cap cell. The CC membrane is engaged in endo- and exo-micropinocytosis (En-mv and Ex-mv) with the extracellular matrix (arrows). Prominent intercellular spaces (ICS) and processes (ICP), the nucleus (N), endoplasmic reticulum (ER), ribosomes (R) and mitrochondria (M) are also labelled. The sample was prepared using a standard TEM procedure consisting of a modified Karnovsky's fixative, followed by O_sO_4 and an *en bloc* UA. Scale bar = 1.0 μm.

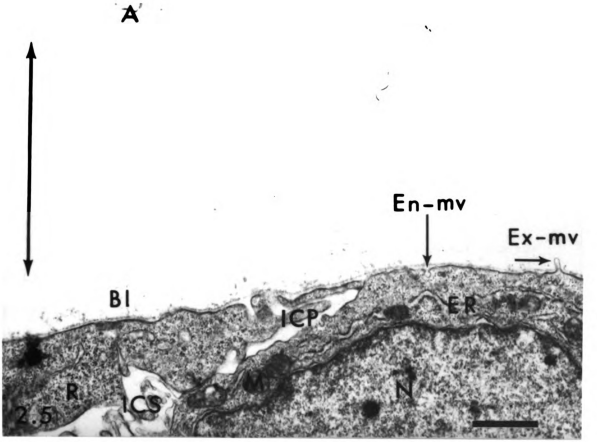
A
En-mv
Ex-mv
Bl
ICP
ER
R
2.5
LCS
N

environment (Figure 2.5). No specialized intercellular junctional complexes were observed between cap cells and any of the adjacent stromal or ductal epithelial cells.

Whole mount and light microscopic analysis of the TEB structure has shown that the larger, more active TEBs are typically at the peripheral leading edge of the advancing ductal tree. In the present study, the large TEBs had more prominent ICS between the cap cell layer and the intermediate cells (Figure 2.6). When prominent intercellular spacing was present below the cap cell layer, an equally distinct space was often present between the TEB and the adjacent stromal cells in the ECM. This space has been termed the "clearance zone" by the author and will be discussed in more detail in Chapter 3.

The Myoepithelial Cell and Myocap Cell. The fully differentiated myoepithelial cell is a peripheral spindle shaped cell, located distal to the cap cell layer in the flank region of the TEB structure (Figures 1.2 and 2.16). The flank region is that area of the TEB, just posterior to the largest diameter of the TEB structure. In the larger more active TEBs this region is very distinct. However, in the smaller TEBs the shape of the bud is often more linear making this region less distinct. Two consistent features present in the ECM which aid in the identification of MECs within the TEB are 1) the sudden and significant presence of collagen bundles and fibroblasts in the extracellular matrix (Figure 2.7a and 2.7b) and 2) the thickness of the basal lamina (Figure 2.8). The

Figure 2.6. Histologic section (5 μm) of a whole mount preparation from a Nu/+ mouse mammary gland. Note the prominent intercellular spaces between the cap cell layer and the underlying intermediate cells (IC) in the TEB (*). An equally distinct space is present at the tip of the TEB (arrow); H and E. X20.

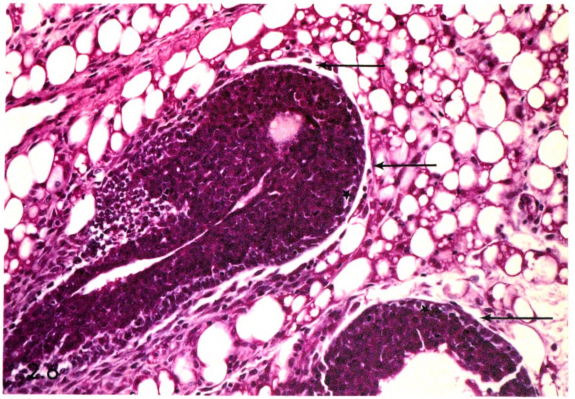

Figure 2.7a. Histologic section (5 μm) of a whole mount preparation from a Nu/+ mouse mammary gland showing two different sized TEBs. Note the distinct cap cell layer (arrow) in each TEB. Both TEBs have a distinct collagen-fibroblast collar in the flank and neck regions (*); H and E. X10.

Figure 2.7b. Close up of the larger TEB in Figure 2.7a. Note the distinct collagen-fibroblast collar (*), cap cell layer (arrow), and clear space (double arrow) between the CC layer and the ECM at the tip of the TEB; H and E. X40.

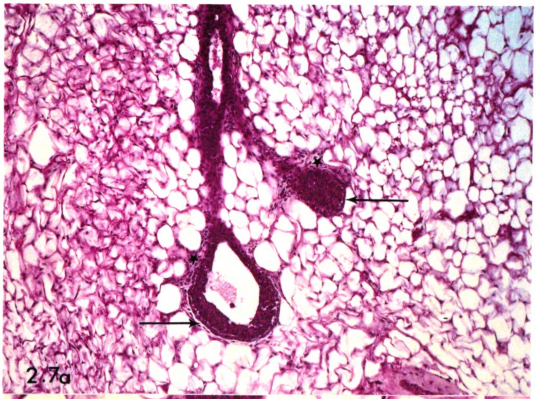

2.7a

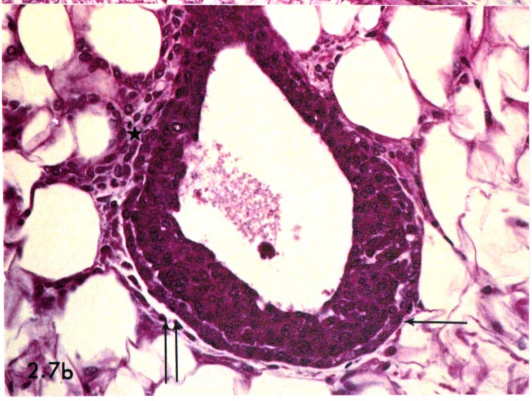

2.7b

Figure 2.8. Transmission electron micrograph of a myoepithelial cell (MEC) near the flank region in the TEB of a mouse mammary gland (a longitudinal ultrathin section). Note the thick and undulating basal lamina (Bl-arrow) between the MEC membrane and adjacent fibroblast (F) in the ECM. Collagen (C) bundles are also labelled. The sample was prepared using a standard TEM procedure consisting of a modified Karnovsky's fixative, followed by O_sO_4 and an *en bloc* UA. Scale bar = 0.5 μm.

Figure 2.9. Transmission electron micrograph of a MEC in the TEB of a mouse mammary gland (an ultrathin cross-section). Note the two desmosomes (arrows) adhering the MEC to the underlying IC. The electron dense material between the two distinct plate-like structures in the intercellular space and the anchoring cytoplasmic filaments are visible. Myofilaments (mf) are present in the cytoplasm along the basal cell membrane border. Scale bar = 0.5 μm.

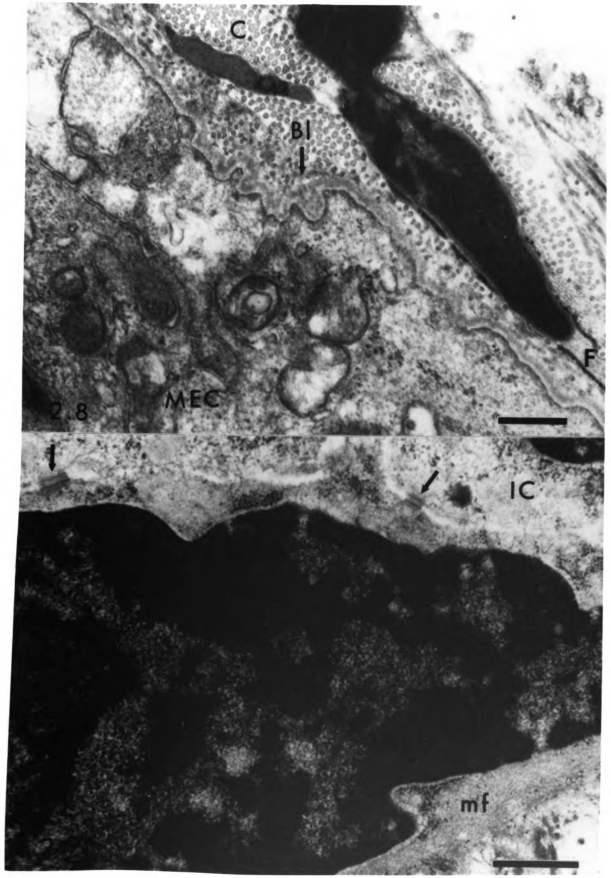
C
Bl
F
2.8
MEC
IC
mf

disposition of collagen in the flank region not only serves as a visual marker for MECs but is thought to be directly associated with the transition of cap cells to myoepithelial cells (Silberstein and Daniel, 1982a; Howlett and Bissell, 1990). In contrast to the tip of the TEB, where the basal lamina is very thin, the basal lamina adjacent to the MECs in the flank region is very thick and undulating (Figure 2.8). The lateral and luminal or internal membrane surfaces have small focal intercytoplasmic projections and occasional micropinocytotic activity was observed on the internal membrane surface. Desmosomes, which are membrane specializations for adhesion, are readily apparent between adjacent MECs and underlying intermediate or luminal cells (Figure 2.9). The desmosomes consist of plate-like structures with anchoring cytoplasmic filaments. The intercellular space between the desmosomal plates is approximately 250 A°, (Gilula, 1974; Rhodin, 1977). Hemi-desmosomes reportedly found between MECs and the basal lamina in mature ducts (Pitelka et al., 1973) were not observed in the prepubertal-pubertal TEB region. The MEC cytoplasm contains an oval to spindle shaped nucleus with moderately irregular borders. The nuclear chromatin pattern is primarily heterochromatic and a single nucleolus is often present. Abundant, longitudinally oriented myofilaments, 4 to 5 nm in width (Pitelka et al., 1973), the hallmark of this cell, course throughout the cytoplasm primarily along the basal membrane border (Figure 2.10). Large numbers of free ribosomes and multifocal

Figure 2.10. Transmission electron micrograph of a MEC in the TEB of a mouse mammary gland (an ultrathin cross-section). Note the abundant myofilaments (mf) in the cytoplasm primarily along the basal cell membrane border. The sample was prepared using a standard TEM procedure consisting of a modified Karnovsky's fixative, followed by O_sO_4 and an *en bloc* UA. Scale bar = 0.5 μm.

Figure 2.11. Transmission electron micrograph of a "myocap" cell (MCC) in the TEB of a mouse mammary gland (a longitudinal ultrathin section). The two "myocap" cells contain intercytoplasmic processes (ICP) separated by an intercellular space (ICS). Note the perpendicular orientation of the euchromatic nucleus (N), mitochondria (M), abundant ribosomes (R) and bundles of myofilaments (mf). Scale bar = 1.0 μm.

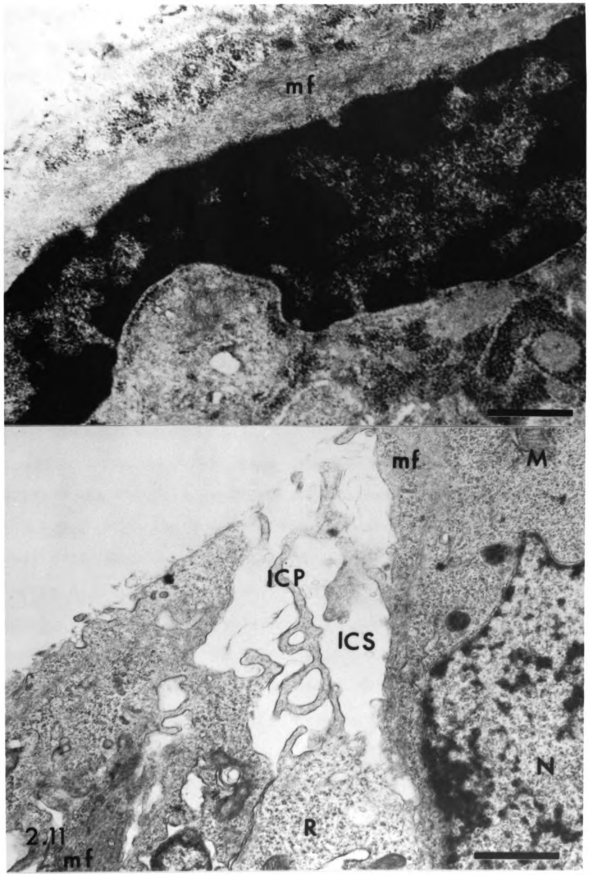
mf
mf
M
ICP
ICS
N
R
2.11
mf

endoplasmic reticulum are also present. The mean nuclear area of the MEC was 29.6 μm^2 and the mean cellular area was 51.8 μm^2.

Posterior to the cap cell and anterior to the fully differentiated myoepithelial cell in the flank region, a transitional cell type with features of both cell types was identified on ultrathin section in this study. The "myopcap cell", as termed by this author, varies somewhat in its shape and orientation but commonly is rectangular with a perpendicularly placed euchromatic nucleus (Figure 2.11). The cytoplasm contains abundant ribosomes and mitochondria, which are characteristic of the cap cell, and focal bundles of myofilaments, which are characteristic of the MEC.

The Intermediate Cell. The intermediate or body cell has a large round to oval shape (Figure 2.12a) and is located between the cap cell layer and the luminal cell layer (Figures 1.2 and 2.16). As a group, the intermediate cells have the most variable nuclei in terms of size and shape. The nuclei occupy a significant amount of space in the cell and can be round, oval or kidney shaped with irregular borders. This variation in shape is most likely associated with the evolution or progression of the IC cell into a fully differentiated luminal cell. The chromatin pattern is also variable and ranges from primarily euchromatic with one or more nucleoli to moderately heterochromatic with no nucleoli. The cytoplasm contains a large number of organelles. Mitochondria, ribosomes, rough and smooth endoplasmic

Figure 2.12a. Transmission electron micrograph of an intermediate cell (IC) in the TEB of a mouse mammary gland (an ultrathin cross-section). Note the large euchromatic nucleus (N), small intercytoplasmic processes and spaces (arrows), small amount of cytoplasm and abundant cytoplasmic organelles (*). The sample was prepared using a standard TEM procedure consisting of a 2.5 % glutaraldehyde fixative, followed by O_sO_4. Scale bar = 1.0 μm.

Figure 2.12b. Close up of Figure 2.12a. Note the diverse array of cytoplasmic organelles in the cytoplasm of the IC. Prominent nuclei (N), golgi complexes (G), small cytoplasmic vesicles (v), abundant ribosomes (R), endoplasmic reticulum (ER) and mitochondria (M) are labelled. Scale bar = 0.5 μm.

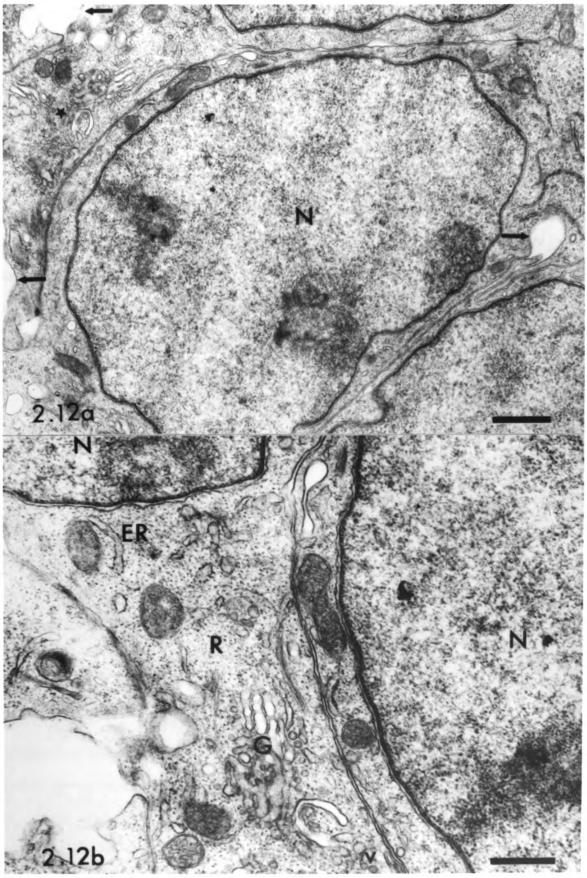
N
2.12a
N
ER
R
N
G
2.12b

reticulum, golgi, occasional lipid droplets and microvesicles are found throughout the cytoplasm (Figure 2.12b). The mean nuclear area of the intermediate cell is 34.3 μm^2 and the mean cellular area is 62.0 μm^2.

Posterior to the flank region, ICs can be observed between MECs and LCs and occasionally occupy a luminal position adjacent to a more differentiated LC. The ICs anterior to the flank region span several cell layers and comprise the largest and most morphologically diverse cell population in the TEB structure. The ICs directly adjacent to the cap cell layer are less differentiated than the ICs adjacent to the luminal cell layer. A moderate number of ICs lying directly above the luminal cell layer have specialized membrane alterations characteristic of LCs such as microvilli, junctional complexes (tight and intermediate) and intercellular adhesions (desmosomes) (Figure 2.13). The IC cells adjacent to the luminal cell layer are most likely destined to become luminal cells in the mature duct and are in the process of migrating to their luminal position in the TEB structure.

The less differentiated ICs have membranes that are primarily void of membrane specializations, except for occasional desmosomes. In addition to the variation in IC membrane morphology, there are two regions where they form intercytoplasmic projections and spaces. The first region is between cell layers, i.e., between the cap cell and the intermediate cell layers and between the ICs themselves and

Figure 2.13. Transmission electron micrograph of intermediate cells (IC) in the TEB of a mouse mammary gland (a longitudinal ultrathin section). Note the orientation of the ICs in relationship to the lumen (L) of the TEB. Tight and intermediate junctional complexes (arrow), and desmosomes (double arrow) are present between the cells. Focal tufts of microvilli (Mv) are present on the apical border of the ICs and abundant microvilli are present on the apical border of the luminal cells (LC). The sample was prepared using a standard TEM procedure consisting of a modified Karnovsky's fixative, followed by O_sO_4 and an *en bloc* UA. Scale bar = 1.0 μm.

Figure 2.14. Transmission electron micrograph of a TEB near the flank region in a mouse mammary gland (a longitudinal section). Note the two regions where ICs form intercytoplasmic processes and spaces. There are distinct spaces between the CCs and ICs (arrow), and between the ICs and MEC and the ICs and LCs (double arrow). Scale bar = 1.0 μm.

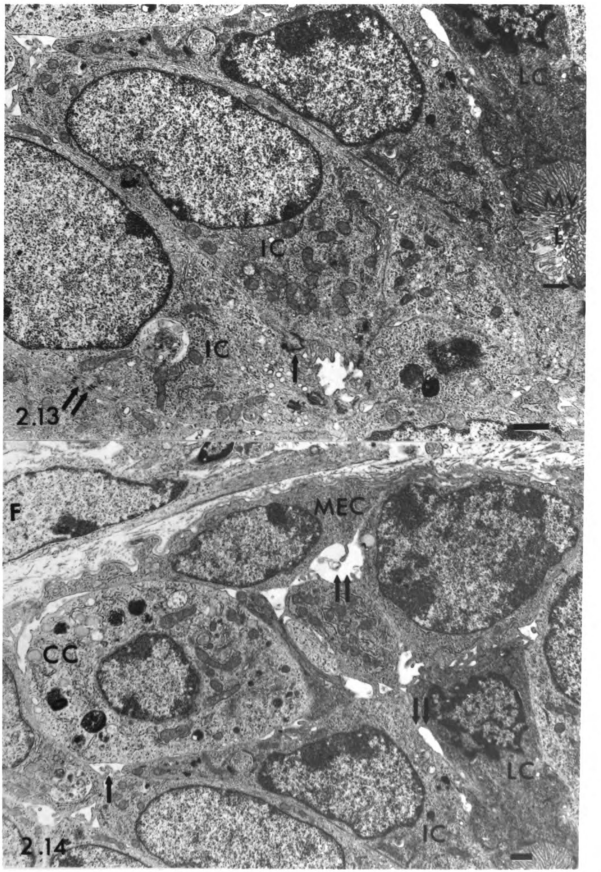
LC
MV
IC
IC
2.13
F
MEC
CC
LC
IC
2.14

Figure 2.15a and 2.15b. Transmission electron micrographs of intermediate cells (IC) in the TEB of a mouse mammary gland (an ultrathin cross-section). Note the sporadic micropinocytotic activity in the cell membranes of adjacent ICs (arrows). The sample was prepared using a special TEM procedure consisting of an alcian blue-lanthanum nitrate fixative. Scale bar = 0.5 μm.

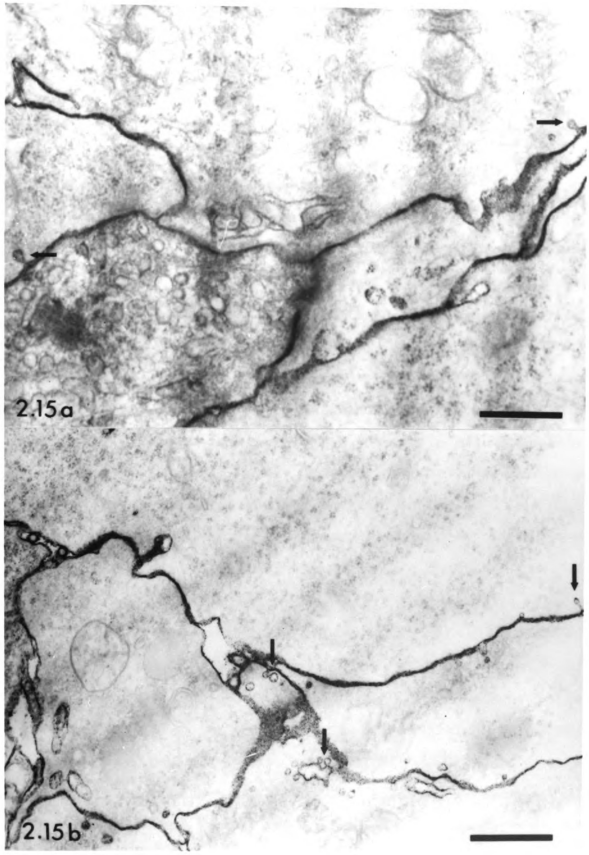
2.15a
2.15b

the second region is where the cell membranes of several different cells meet, i.e., intermediate - myoepithelial - luminal cell membranes (Figure 2.14). Sporadic micropinocytotic activity is also present in the membrane of adjacent intermediate cells within the body of the TEB (Figures 2.15a and 2.15b).

The Luminal Cell. The luminal cells, so named because of their location next to the lumen of the TEB, are highly differentiated and contain many specialized membrane alterations (Figure 2.16). They have a distinct low columnar to cuboidal shape with an angular orientation; i.e., the apex of the luminal cell is narrower than the base and reflects the radial placement of the luminal cells around the TEB lumen. The apical cell membrane contains abundant regularly arranged microvilli. The lateral and basal membranes are primarily linear with occasional small intercytoplasmic projections interdigitating between adjacent intermediate and luminal cells. Tight junctions, intermediate junctions and desmosomes are commonly observed between the lateral borders of the luminal cells near the apex of the cells (Figure 2.17). These junctions function primarily as points of intercellular adhesion, preventing cell separation and the seepage of proteinaceous material from the TEB lumen into intercellular regions (Pitelka et al., 1973). The luminal cell cytoplasm contains abundant ribosomes, endoplasmic reticulum, golgi complexes and mitochondria with variable numbers of microvesicles. The nuclei are predominately heterochromatic

Figure 2.16. Transmission electron micrograph of a TEB near the flank region in a mouse mammary gland (a longitudinal ultrathin section). Note the placement of the luminal cell (LC) in relation to all of the other epithelial cells in the TEB structure. The LC has a low columnar, angular shape and is oriented perpendicular to the lumen. The apical membrane border contains abundant microvilli (Mv) and marks the luminal opening. (Fibroblasts (F), adipocyte (A), intermediate cells (IC), myoepithelial cells (MEC), cap cells (CC), lipid vacuoles (Lv), endoplasmic reticulum (ER), golgi (G), mitochondria (M), intercytoplasmic spaces (ICS) and processes (ICP), the basal lamina (Bl), and junctional complexes (arrowheads) are also labelled). The sample was prepared using a standard TEM procedure consisting of a modified Karnovsky's fixative, followed by O_sO_4 and an *en bloc* UA. Scale bar = 1.0 μm.

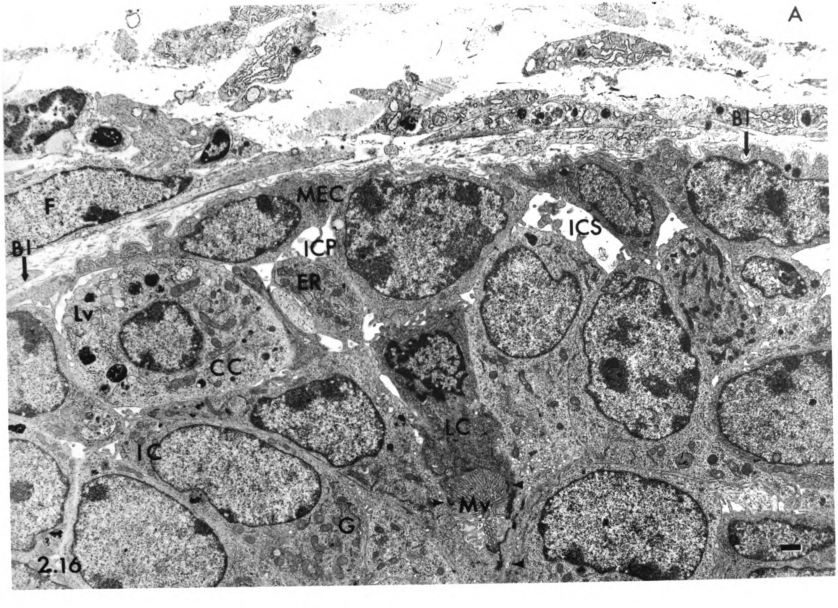
A
F
MEC
ICP
ICS
BI
BI
ER
Lv
CC
LC
IC
Mx
G
2.16

Figure 2.17. Transmission electron micrograph of a luminal cell (LC) in the TEB of a mouse mammary gland (an ultrathin cross-section). Note the complex array of tight junctions (T), intermediate junctions (I), and desmosomes (D) between adjacent LCs at the junction of the apical membrane borders (arrowheads). Mitochondria (M), ribosomes (R) and microvilli (Mv) are also labelled). The sample was prepared using a standard TEM procedure consisting of a modified Karnovsky's fixative, followed by O_sO_4 and an *en bloc* UA. Scale bar = 0.5 μm.

Figure 2.18. Transmission electron micrograph of the intermediate cell (IC) and luminal cell (LC) layers in the TEB of a mouse mammary gland (an ultrathin cross-section). Note the irregularly shaped, deeply clefted, heterochromatic nuclei in the LC layer. In contrast, the ICs have a mixed chromatin pattern with prominent nucleoli (Nu) and a round to oval shape. The lumen is also labelled (L). Scale bar = 1.0 μm.

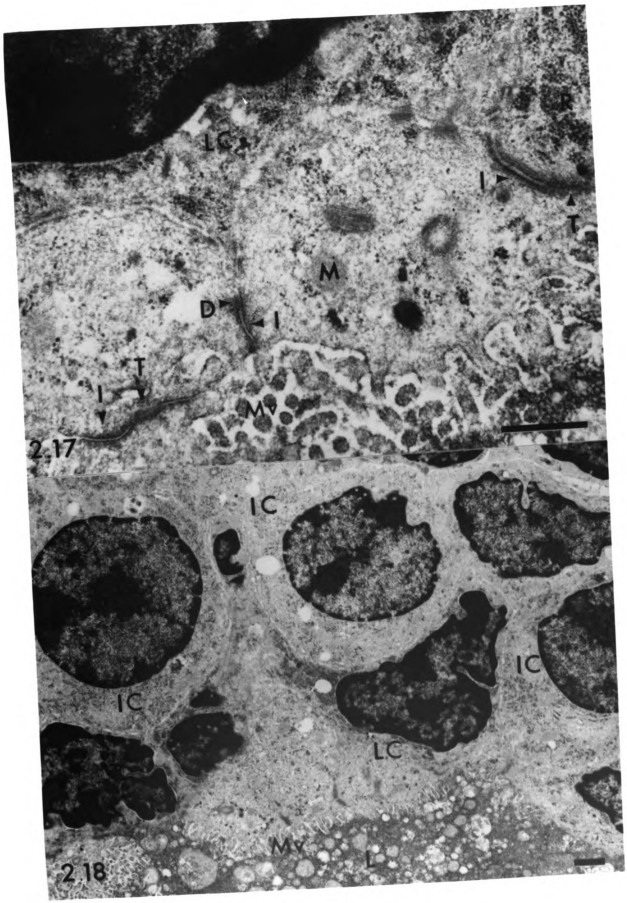
LC
I
T
M
D
I
T
I
MP
2.17
IC
IC
IC
LC
MP
L
2.18

and have highly irregular shapes with large clefts dissecting many of them (Figure 2.18). The mean nuclear area is 16.2 μm^2 and the mean cellular area is 41.9 μm^2.

Discussion

Several hundred TEB structures were collected from the No. 2 and No. 3 thoracic and No. 4 inguinal mammary glands of Balb/c and athymic nude (Nu/+) mice at 4 and 5 weeks of age. As an alternative to intralactiferous duct injection for TEB visualization *in vivo*, the SIVS (subcutaneous injection of a vital stain) technique was developed. The SIVS technique is based on diffusion of Methylene Blue Chloride (MBC) solutions across the mammary gland fat pad into the epithelial cells of the mammary gland tree. A 100 - 200 μg solution of MBC stains the TEB structures light blue within 2 to 2.5 hours post-injection. The advantages of this technique are 1) it is easy to do, 2) is less invasive than the intralactiferous duct technique and 3) has excellent repeatability. The major disadvantages are the various degrees of dense staining and subcutaneous edema present in the subcutis at concentrations greater than or equal to 200 $\mu g/ml$ of solution (Hank's Buffered Salt Solution). The subcutaneous edema present at concentrations greater than 200 $\mu g/ml$ in most likely associated with the osmolality of the solution. This was not addressed by Buehring and Jensen (1983) who used the dye in cell cultures. However, they did notice a dose dependent

toxicity and concluded that the toxicity of MBC to cells was associated with the uptake capacity of the cell lines analyzed.

The present study was divided into two parts: 1) a qualitative analysis of the cell types composing the TEB structure, and 2) a quantitative analysis of the nuclear and areas of each of the 4 major cell types in the TEB.

The four morphologically distinct cell types previously documented in the literature, were confirmed by ultrastructural analysis. The undifferentiated cap cells, occupying the most peripheral cell layer in the TEB, had the largest mean cellular area (94.3 μm^2) and the largest mean nuclear area (37.8 μm^2) of any of the cells in the TEB (Table 2.1). Mitotic cell division was routinely observed in the cap cell layer and within the intermediate cell layers of the TEB. On longitudinal section, the cap cells were oval to cuboidal in shape with a centrally placed euchromatic nucleus and single or multiple nucleoli. No specialized intercellular junctional complexes were observed in the cap cell membranes. However, multiple intercytoplasmic processes of various size and shape were prominent on the lateral and internal membranes. The basal membrane was primarily linear and adjacent to a thin continuous basal lamina. All of the membrane surfaces had various degrees of micropinocytotic (endo- and/or exo-micropinocytosis) activity.

The largest TEB structures were consistently found at the peripheral leading edge of ductal expansion, and distinct

intercellular spaces between the cap cell layer and the underlying intermediate cell layer were often present. However, not all large TEBs had this distinct spacing and the presence and degree of spacing is believed to be associated with the degree of hyaluronate secretion by the cap cells (Silberstein and Daniel, 1982a). A clear space (the "clearance zone", see Chapter 3) between the basal lamina at the tip of the TEB and the stromal cells was consistently present in the larger TEBs with prominent intercellular spacing distal to the cap cell layer. Intracytoplasmically, the cap cells contained abundant mitochondria and free ribosomes and smaller numbers of endoplasmic reticulum and golgi.

The myoepithelial cell is a direct descendent of the cap cell and is peripherally located in the flank and neck region of the TEB and the mature duct (Williams and Daniel, 1983). The myoepithelial cells are among the smallest cells in the TEB with a mean cellular area of 51.8 μm^2 and a mean nuclear area of 29.6 μm^2, (Table 2.1). On longitudinal section, the myoepithelial cells are spindle shaped and have a spindle to oval shaped heterochromatic nucleus. The cell membranes possess desmosomes, with an average of 3 or 4 in any given plane, between adjacent myoepithelial cells and intermediate or luminal cells. In addition to the intercellular junctions, the cell membranes have small intercytoplasmic processes between adjacent cells and focal micropinocytotic activity. Intracellularly, the myoepithelial cells contain distinct

bundles of myofilaments, 4-5 nm in diameter (Pitelka et al., 1973), along the basal membrane, large numbers of ribosomes and multifocal endoplasmic reticulum. The transition of the cap cell to the myoepithelial cell is not only marked by cytologic changes but also by the presence of a thicker more corrugated basal lamina. Williams and Daniel (1983) proposed that this anatomical change was associated with the narrowing of the TEB and an excess of basal lamina in the region. In addition, a distinct increase in collagen and fibroblasts is also present in the adjacent stroma near the flank region. This stromal transformation is believed to influence the transition of the cap cell to the myoepithelial cell (Silberstein and Daniel, 1982a).

In the flank region of some TEBs a transitional cell type, termed the "myocap" cell by the author, was visible without the aid of special markers. The "myocap" cell has features of both the cap cell and myoepithelial cell. It is a large cuboidal cell with an oval nucleus and focal bundles of myofilaments in the cytoplasm.

The intermediate cells, which span several layers, are the most diverse cell type in the TEB in terms of morphologic structures. However, the mean cellular area, 62.0 μm^2 and the mean nuclear area, 34.3 μm^2, are not significantly different from those of the cap cell. This morphometric similarity is not coincidental and reflects the morphologic similarity observed in the intermediate cell layer directly adjacent to the cap cell layer. Overall, there is a decrease in the

cell:nucleus ratio in the intermediate cell population from the peripheral to inner cell layers. The cells in the peripheral layer are very large and on longitudinal section can be larger than the neighboring cap cell. The intermediate cells adjacent to the luminal cells are more differentiated. They are smaller and contain a larger number and more different types of organelles as well as specialized membrane alterations. In this region, the intermediate cells have intermediate junctions and desmosomes on their lateral borders as well as focal tufts of microvilli on their apical or internal borders. As a whole, the intermediate cells have round to oval shaped nuclei with various degrees of heterochromatin and nuclear clefting. The character of this heterogenous looking cell population is a direct reflection of the degree of cell differentiation taking place in this group of cells. Intracytoplasmically, the intermediate cells have numerous mitochondria and ribosomes and increased numbers of endoplasmic reticulum and golgi. Occasional lipid droplets are visible in the peripheral intermediate cells and microvesicles are more prominent in the cells adjacent to the luminal cell layer. Researchers believe that the intermediate cells eventually become fully differentiated luminal cells in the mature duct (Williams and Daniel, 1983; Russo and Russo, 1987).

The luminal cells are the smallest, most differentiated cell in the TEB. They have a mean cellular area of 41.9 μm^2 and a mean nuclear area of 16.2 μm^2. The cells have a

distinct low columnar to cuboidal shape with a narrow apex containing abundant microvilli projecting into the lumen of the duct. The nuclei are heterochromatic and irregular in shape with several large clefts. Tight junctions, intermediate junctions and desmosomes which line membrane surfaces are commonly observed between adjacent luminal cells and neighboring intermediate cells. Intracytoplasmically, their organelles reflect the high metabolic activity of the cell, with abundant ribosomes, endoplasmic reticulum, golgi and mitochondria. Variable numbers of microvesicles containing what has been previously documented as proteinaceous material in other studies are also present (Pitelka et al., 1973 and 1977; Sekhri et al., 1967).

In conclusion, ultrastructural analysis of the prepubertal-pubertal TEB confirmed the presence of 4 distinct cell types; namely, the cap cell or "stem cell", the myoepithelial cell, the intermediate or body cell, and the luminal or dark cell. A fifth cell type the "myocap", located near the flank region of the TEB, is visible without the aid of special markers and supports the results of time-lapse microcinematography experiments by Williams and Daniel (1983) which show that the myoepithelial cell line descends from the cap cell line of the TEB structure. Morphometric analysis of the 4 major cell types show that the undifferentiated cap cell and the intermediate cell are the largest cells in the TEB. In contrast, the fully differentiated myoepithelial and luminal cells are the smallest cells in the TEB (Table 2.1).

No direct contact or distinct intercellular junctional complexes were found between cap cells and adjacent intermediate cells. However, large intercellular spaces between cap cells and the adjacent intermediate cells were common and intercellular processes of various size and shape often protruded into the intercytoplasmic spaces. The inner most layer of intermediate cells and the adjacent myoepithelial and luminal cells displayed an array of junctional complexes which reflected their function and degree of differentiation. No gap junctional complexes were positively identified in any of the cells in the TEB structure. However, the production of endo- and/or exo-micropinocytotic vesicles by all of the various cell types indicates that this is one potential mechanism of intercellular communication acquired at an early stage of differentiation and maintained throughout the differentiation process.

CHAPTER 3

HISTOLOGIC AND ULTRASTRUCTURAL INVESTIGATION OF INTERCELLULAR COMMUNICATION BETWEEN CAP CELLS AND ADJACENT STROMAL CELLS IN THE MOUSE MAMMARY GLAND

Abstract

The type of intercellular communication that exists between the cap cells and adjacent stromal cells (adipocytes and fibroblasts) and ductal epithelial cells, varies according to the type of neighboring cell and the size and character of the TEB. In the majority of TEBs, the adipocytes and/or fibroblasts border the basal lamina. However, in many of the larger more mitotically active TEBs, where there is prominent intercellular spacing between the cap cell layer and the intermediate cell layer, a clear space of variable width, termed the "clearance zone", by this author, is present between the tip of the TEB and the ECM. The clearance zone, as well as the intercellular spacing within the TEB, are believed to be associated with hyaluronate secretion by the cap cell in order to facilitate ductal migration throughout the mammary gland fat pad.

The dynamic basal membrane of the cap cell lies adjacent to a thin, mostly continuous basal lamina at the tip of the TEB. The cap cell membrane engages in extensive endocytotic and exocytotic activity with adjacent epithelial cells (cap cells and intermediate cells) as well as with the extracellular matrix. The exchange of substances with the extracellular matrix results in focal discontinuity of the basal lamina. However, these small openings in the basal lamina appear to be promptly sealed and at no time does the

cap cell membrane come in direct contact with the adjacent adipocytes or fibroblast membranes, which also engage in extensive exocytotic activity. The exchange of cellular and extracellular material, via the endo- and/or exo-micropinocytotic vesicles, appears to be the primary morphologically distinct mechanism of intercellular communication between these cells.

The lateral and luminal membranes of the cap cells lie adjacent to either cap cell, intermediate cell or myoepithelial cell membranes and have irregular cytoplasmic borders that project into intercellular spaces. Unlike the stromal cells, direct contact was visible between the cap cell membranes and adjacent epithelial cell membranes but no junctional complexes were present.

Introduction

There are several mechanisms by which cells communicate with one another. Most of the mechanisms are not morphologically distinct on light or electron microscopic examination. However, some mechanisms of communication, such as gap junctional communication, and micropinocytosis, do possess morphologically distinct features.

Gap junctions are specialized membrane structures which allow the direct exchange of substances through the cell membrane. The membrane structure is composed of small tubules called connexons, that permit intracellular substances of ≤ 1000 Mr (molecular mass) to pass from one cell to another (Finbow et al., 1986; Sosinsky, et al., 1988; Unwin P.N.T., 1986). This form of intercellular communication is extremely important to cell homeostasis and when disrupted, has been shown to be associated with cell autonomy and neoplastic transformation (Trosko et al., 1990).

Micropinocytosis involves the exchange of intracellular and extracellular substances across the cell membrane. This process requires energy, and is often receptor driven (Robbins et al., 1990). Distinct endo- and exo-micropinocytotic vesicles are readily apparent along cell membranes in electron micrographs (Rhodin, 1977).

The type and degree of intercellular communication between the peripheral undifferentiated cap cells and the

adjacent stromal cells, i.e., adipocytes and fibroblasts, depends not only on the ability of the cell membrane to engage in micropinocytotic activity or to form specialized junctional complexes with the adjacent cells but is also influenced by the presence of the basal lamina and the chemical composition of the extracellular matrix. The TEB migrates through the mammary gland at a rate of 0.5 mm per day (Williams and Daniel, 1983). The primary substance believed to permit this migration is hyaluronate. Hyaluronate is a salt or ester of hyaluronic acid which is a mucopolysaccharide found in tissue spaces, acting as an intercellular cement substance (Stedman, 1990). The major function of hyaluronate in the TEB is to decrease cellular adhesion thereby allowing for cellular expansion within the TEB, as well as migration of the TEB throughout the mammary gland fat pad. This decrease in adhesion is morphologically distinct outside the TEB and within the TEB between cap cells and between the cap cell and intermediate cell layers. The decreased cellular adhesion results in less direct contact between adjacent cells and decreases the likelihood for direct exchange of information via gap junctional complexes.

Ironically, hyaluronate is also an integral part of the basal lamina surrounding the TEB (Gordon and Bernfield, 1980; Silberstein and Daniel, 1982a) which serves as another barrier to direct communication. However, this barrier lies between the extracellular matrix and cap cell layer. The basal lamina adjacent to the tip of the TEB is very thin, 104 nm, and is

composed of hyaluronate and chondroitin sulfate (Gordon and Bernfield, 1980; Williams et al., 1982). Unlike the rat, the basal lamina in the mouse has never been shown to be discontinuous (Dulbecco et al., 1982; Williams and Daniel, 1983). The role of hyaluronate and the basal lamina in intercellular communication, as well as the type of intercellular communication between cap cells and adjacent stromal cells, will be presented in this study.

Materials and Methods

Animals. One hundred and eighteen mice, consisting of Balb/c and athymic nude +/- strains, were used in this study. They ranged in age from 28 to 42 days old. Prior to euthanasia, the mice were housed in a temperature controlled environment at $21^0 \pm 1^0C$ on a 12 hour light, 12 hour dark exposure cycle. They had unlimited access to water and were fed a standard laboratory chow diet.

In Vivo Terminal End Bud Identification. The standard identification procedure most often cited in the literature for visualization of ductal epithelium in the mammary gland is the intralactiferous duct infusion technique using aqueous Trypan Blue dye (Humason, 1979). This technique requires a great deal of skill and is difficult in young mice with small openings in the nipple. In addition, the pressure necessary for complete infusion of the entire mammary gland tree via intralactiferous duct infusion can be associated with internal

epithelial damage. Therefore, a less invasive technique, the SIVS technique, was developed from a supravital staining technique described by Buehring and Jensen (1983). This technique was previously described in Chapter 2 and the reader should refer to the section on "SIVS Technique" for further details.

Transmission Electron Microscopy Sample Fixation. Control tissue samples were collected "blind" (unstained) from the No. 4 gland, and SIVS tissue samples, stained light blue, were collected from the No. 2, No. 3 and No. 4 glands. All samples were placed in a modified Karnovsky's fixative consisting of 2.0% glutaraldehyde - 2.0% formaldehyde - 1mM calcium chloride - 0.2 M cacodylate (Karnovsky, 1965; Glauert, 1975) immediately upon excision. The samples were fixed at room temperature for 2 to 3 hours and washed in 0.1 M cacodylate buffer for a total of 3 15 minute washes. Prior to post-fixation, using a dissecting microscope, the SIVS samples were trimmed into triangular shapes. This procedure resulted in 1 to 3 TEB structures per sample placed in longitudinal or cross-sectional orientation. The buffer washed samples were post-fixed in a 50:50 solution of 2.0% osmium tetroxide - 0.2 M cacodylate buffer for 2 hours at room temperature.

In addition to the Karnovsky's fixative, an additional fixation technique consisting of alcian blue - lanthanum nitrate (Shea, 1971) was used to delineate the surface coat of cell membranes and aid in the identification of intercellular junctional complexes. Alcian blue (0.1 or 0.5%) was added to

a solution of 2.0% glutaraldehyde - 2.0% formaldehyde - 1mM calcium chloride in 0.1 M cacodylate buffer (Ph 7.2). The samples were fixed for 2 hours at room temperature and rinsed in 0.1 M cacodylate buffer. Post-fixation consisted of placing the samples in a solution of 1% osmium tetroxide - 1% lanthanum nitrate in 0.1 M of s-collidine (pH 8.0) for 2 hours at room temperature. The remainder of the procedure follows the basic TEM technique outlined below. However, the alcian blue - lanthanum nitrate samples did not require staining with UA or Pb after ultrathin sectioning.

All post-fixed samples were washed in 0.1 M cacodylate buffer for a total of 2 15 minute washes and one 15 minute wash in triple distilled water. In order to increase the contrast in the samples, the tissues were <u>en bloc</u> stained in 0.5% uranyl acetate for 8 hours or overnight and washed in triple distilled water for up to 1 hour. Samples were dehydrated using a graduated series of ethyl alcohol solutions beginning at 25% ETOH up to 100% ETOH for 15 minutes each (25%, 50%, 75%, 95%, and 100% (2 times)). The dehydrated samples were then placed in a graduated series of ethanol:propylene oxide (EtOH:PO) solutions (3:1, 1:1, and 1:3), a transition solvent, for 15 minutes each and transferred to 100% PO for two 30 minute washes. In order for the samples to be compatible with the Epon-Araldite-Spurrs resin, they were placed in a graduated series of PO:resin solutions (2:1 and 1:2) for 3 hours each at room temperature and then transferred to 100% resin for 8 hours or overnight

(Dawes, 1971; Klomparens et al., 1986) on a rotation device to aid in the infiltration or extraction of chemicals across the mammary gland fat pad. The resin infiltrated samples were placed in capsular molds and oriented so the longitudinal or cross-sectional axis of the TEB was adjacent to the block face. The capsules were filled with 100% resin and baked in a convection incubator at 65^{0}C for 48 hours.

Serial Sectioning and Positive Staining. The procedures for serial sectioning and positive staining were presented in Chapter 2 and the reader should refer to the section on "Serial Sectioning and Positive Staining" for review of these techniques.

Freeze Fracture Technique. The TEBs used in the freeze fracture procedure were identified and fixed using the same SIVS and modified Karnovsky's fixation techniques previously described. To protect the post-fixed samples from forming large ice crystals, they were placed in a graded series of glycerol (5% - 25%) for 30 minutes each prior to freezing (Hudson et al., 1979). Using a dissecting microscope, the glycerol treated samples were trimmed, orientated, and placed on metal supports. The support containing the sample was then immediately frozen in liquid propane for 2-3 seconds and placed in liquid nitrogen. The frozen samples were then transferred to a plastic vial and stored in a liquid nitrogen storage container.

Sample cleaving and replication were performed on a Balzers Freeze-Etch unit. The frozen sample was quickly

transferred from the storage unit to a prechilled stage located in a vented bell jar. A cleavage plane was made using a razor blade mounted on a rotating arm inside the bell jar. Once the cleavage plane had been made the freeze-fracture replica was prepared by electron-beam evaporation of platinum. The platinum layer was immediately covered with a layer of carbon resulting in a platinum-carbon replica over the frozen tissue sample.

The platinum-carbon replica and tissue sample were removed from the bell jar and allowed to thaw at room temperature in a 30% glycerol solution. As the sample thawed the tissue separated from the replica and the replica floated to the surface where it was transferred into a series of cleaning solutions prior to being mounted on grids. The first set of solutions was composed of decreasing concentrations of glycerol (30%, 20%, 10%, and 5% - 2 minutes each) followed by 3 washes in distilled water. The replicas were then transferred into a 1% solution of sodium hypochlorite for 30 minutes, undiluted bleach for 1 hour (3 washes at 20 minutes each), followed by decreasing concentrations of bleach and finally into multiple washes in distilled water. Bleaching is normally followed by digestion of any remaining tissue using increasing concentrations of chromic acid (Hudson et al., 1979). However, in this particular study, due to the high fat content of the mouse mammary gland samples, lipase (Sigma Chemical Co.) dissolved in a phosphate buffer solution was used prior to chromic acid for 6 to 8 hours. The cleaned

replicas were then transferred through several distilled water washes and mounted on precleaned copper grids for viewing on the transmission electron microscope.

Ultrastructural Analysis. Thin bar hexamesh grids containing representative ultrathin sections and 200 - 400 mesh copper grids containing freeze fracture replicas of TEB structures were photographed on a Philips 201 transmission electron microscope. The micrographs were then used to study the ultrastructural characteristics of the TEB cap cells and their relationship to adjacent stromal epithelial cells.

Histologic Analysis. One micrometer thick sections from resin blocks were stained with 1.0 % toluidine blue (Kiernan, 1990). Serial micrometer sections from paraffin embedded whole mount specimens were stained with hematoxylin and eosin and viewed under a light microscope in order to further investigate the degree of intercellular communication between cap cells and stromal cells.

Results

Approximately 150 TEB structures were thick sectioned (1 micrometer) from a total of 120, 4 to 6 week old, Balb/c and athymic nude (Nu/+) mice. Of the 150 structures thick sectioned, 60 were ultrathin sectioned (between 80 - 100 nm) and examined on a Philips 201 transmission electron microscope. In examining the relationship between cap cells and adjacent stromal and ductal epithelial cells,

morphologically distinct characteristics were observed using both methods of sectioning, i.e., thick and thin. Unique morphologic characteristics associated with TEB migration were first recognized in serial thick sections. In the majority of TEB structures, the adipocytes were adjacent to an intact basal lamina produced by the peripheral cap cells (Figure 3.1). However, a clear space, containing an occasional migratory cell, i.e., leukocyte, macrophage or fibroblast, and ranging from approximately 15 - 100 micrometers in width, was often present anterior to the tip of the larger TEB structures (Figure 3.2). This clear space has been termed the "clearance zone" by the present author. To confirm that the clearance zone was not an artifact associated with the TEM fixation procedure or SIVS technique, control blocks (TEBs not stained with methylene blue chloride), and whole mount mammary glands were serial sectioned at 10 to 15 microns and 5 microns, respectively, and analyzed. Both the control block and whole mount sections revealed the presence of a clearance zone, of variable width, anterior to the larger TEB structures (Figures 3.3, 3.4a and 3.4b).

Ultrathin sections, examined under the transmission electron microscope, revealed 1) the relationship between stromal cells and cap cells in the presence or absence of a clearance zone, 2) the integrity of the basal lamina at the tip of the TEB structure and 3) the absence of intercellular junctional complexes associated with cell-cell communication.

Ultrastructural micrographs showed that when the

Figure 3.1. Histologic cross-section (1 μm) of a TEB from a mouse mammary gland. The TEB was identified in vivo using the SIVS technique. Note the close proximity of the adipocytes to the tip of the TEB (arrow). Toluidine blue-1% staining. X19.

Figure 3.2. Histologic cross-section (1 μm) of a TEB from a mouse mammary gland. The TEB was identified in vivo using the SIVS technique. Note the presence of a "clearance zone" near the flank region of the TEB (arrow). Toluidine blue-1% staining. X31.

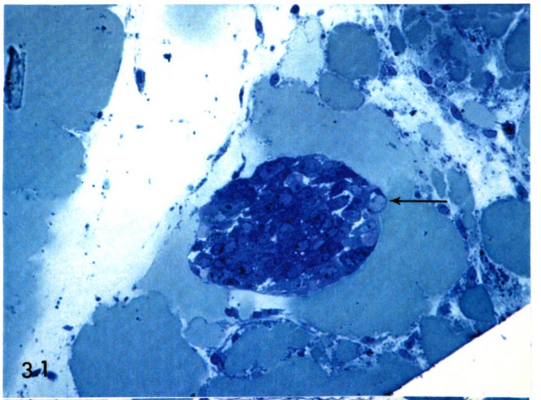

3-1

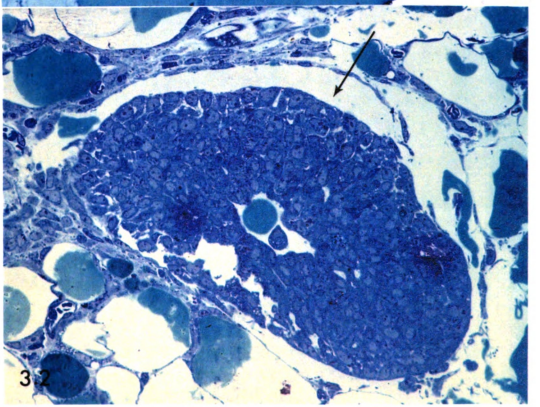

3-2

Figure 3.3. Histologic oblique section (1 μm) of a TEB from a mouse mammary gland near the flank region. The TEB was a control specimen (not stained in vivo with MBC) and was oriented "blind". Note the presence of a "clearance zone" adjacent to the cap cells with prominent ICs (arrow). On the opposite border the adipocytes and fibroblasts are in close proximity to the basal lamina in the presence of CCs without prominent ICS and in the absence of cap cells (double arrow). Toluidine blue-1% staining. X16.

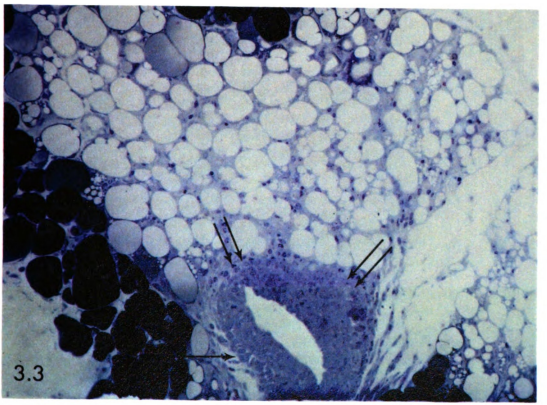
3.3

Figure 3.4a. Histologic section (5 μm) of a whole mount preparation from a Nu/+ mouse mammary gland showing two large TEB structures in the fat pad. Note the distinct variable sized "clearance zones" present at the tip of each of the TEBs (arrows) and the large number of fibroblasts and deposition of collagen surrounding the flank (Fk), neck (Nk) and duct (Dt) regions. In addition, the TEB with the smaller "clearance zone" has less separation between the cap cell layer and underlying ICs. H and E. X6.6.

Figure 3.4b. Close up of the larger TEB in Figure 3.4a. Note the "clearance zone" is much larger in the featured TEB than in the adjacent TEB (above) and that the separation between the cap cell layer and the underlying IC layer is also more prominent (double arrow) indicating active hyaluronate secretion. In addition, the featured TEB has migrated through the fat pad and lies adjacent to cutaneous muscle and fascia which is partially responsible for the larger zone. H and E. X16.

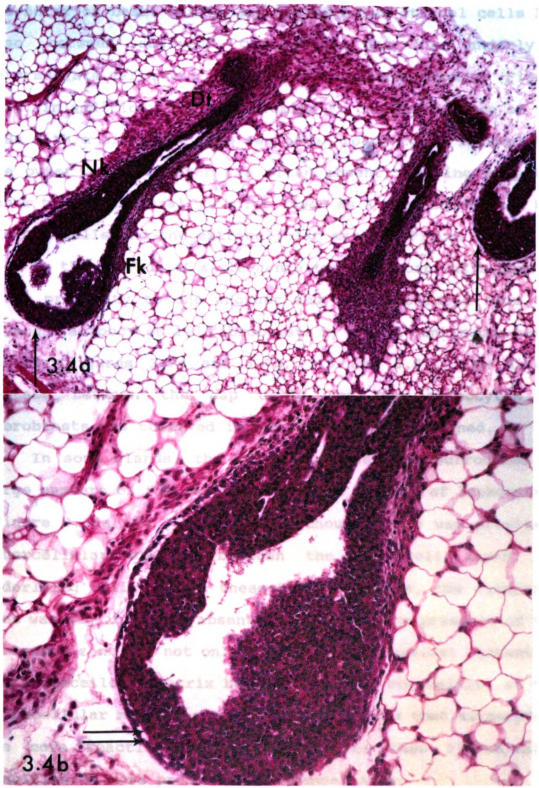
Dk
Nk
Fk
3.4a
3.4b

clearance zone was present, not only was there a space between the anterior basal lamina and the adjacent stromal cells but also between adjacent cap cells and the underlying intermediate cells on their lateral and apical borders (Figure 3.5). In addition, the basal lamina at the tip of some of the TEBs with a clearance zone was often found to be incomplete. The outer anionic layer was often absent, leaving only the inner two-dimensional globular layer as a barrier between the TEB cap cells and the extracellular matrix (Figure 3.6).

In the absence of a clearance zone, the cap cells were in close proximity to one another and were separated from the adjacent adipocytes and fibroblasts by a thin continuous basal lamina (Figures 3.7a and 3.7b, 3.8 and 3.9). No direct contact between the cap cells and the adipocytes or fibroblasts was observed in any of the TEBs examined.

In some glands, the TEB structures were surrounded by large numbers of fibroblasts and small numbers of leukocytes (Figure 3.10a and 3.10b). Even though there was prominent intercellular spacing between the cap cell layer and underlying cells within these TEB structures, the clearance zone was negligible or absent. Therefore, the presence of the clearance zone may not only depend on the chemical content of the extracellular matrix but the cellular composition of the extracellular matrix as well. It is possible that adipocytes are more reactive to the hyaluronate than fibroblasts, resulting in more prominent clearance zones.

In the presence or absence of a clearance zone, the inner

Figure 3.5. Transmission electron micrograph of the tip of a TEB structure in a mouse mammary gland (a longitudinal ultrathin section). Note the small "clearance zone" (Cz) between the adipocyte (A) and the underlying CCs and "myocap cells" (MCC). Prominent intercellular spaces and processes are present between adjacent CCs and MCCs (arrow) and between the CC and IC layers (double arrows). The sample was prepared using a standard TEM procedure consisting of a modified Karnovsky's fixative, followed by O_sO_4 and an *en bloc* UA. Scale bar = 1.0 μm.

Figure 3.6. Transmission electron micrograph of a cap cell (CC) membrane in the TEB of a mouse mammary gland (a longitudinal ultrathin section). Note the variation in the morphology of the basal CC membranes adjacent to the basal lamina (Bl) in the presence of a "clearance zone" (Cz). The basal lamina is complete (arrow) and incomplete (outer anionic layer is absent) (double arrow) and a small round piece of membrane bound cytoplasm is present adjacent to the incomplete lamina (open *). Intracytoplasmic spaces (ICS) and ribosomes (R) are also labelled. Scale bar = 0.5 μm.

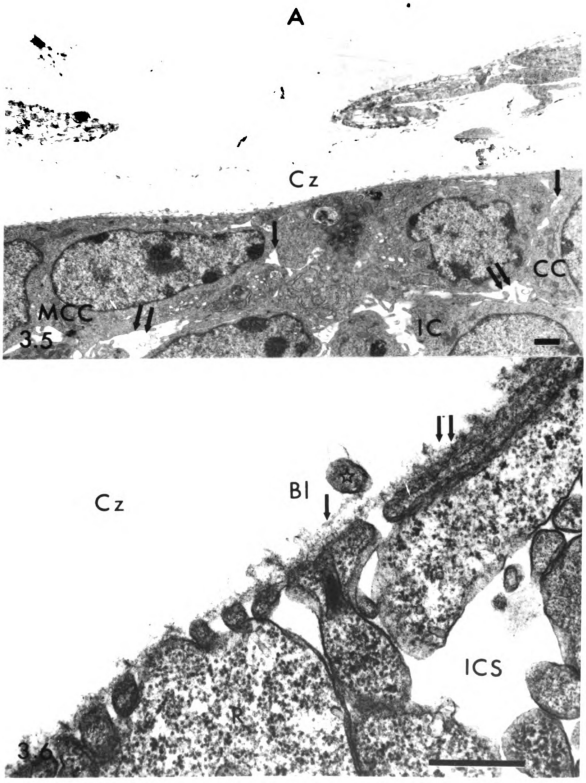
A
Cz
CC
MCC
IC
3.5
Cz
Bl
ICS
3.6

Figure 3.7a. Histologic longitudinal section (5 μm) of a whole mount preparation from a No. 4 inguinal Nu/+ mouse mammary gland. Note the more linearly shaped TEB structures (characteristic of this gland) at the leading edge of ductal migration through the mammary gland fat pad (arrow). The inguinal lymph node is also visible (double arrow) in addition to the ducts. H and E. X4.

Figure 3.7b. Close up of a linear TEB in Figure 3.7a. Note the absence of a "clearance zone" (arrow) and a lack of prominent intercellular spaces between the CC layer and underlying IC layer (double arrow). The adipocytes (A) are directly adjacent to the cap cell layer and a mild to moderate collagen-fibroblast collar is present in the flank (*) and neck (**) regions. H and E. X20.

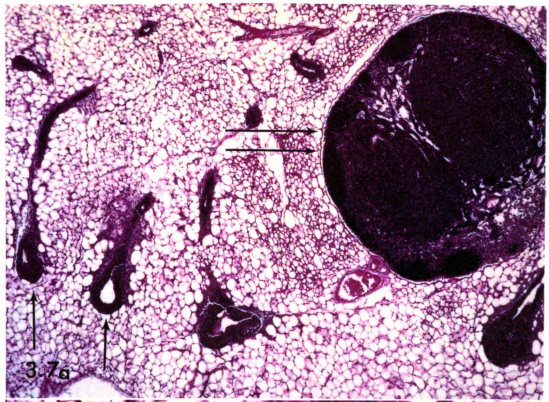

3.7a

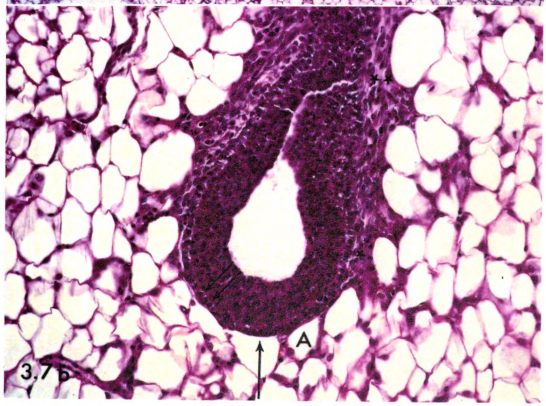

3.7b

Figure 3.8. Transmission electron micrograph of a TEB structure without a "clearance zone" in a mouse mammary gland (a longitudinal ultrathin section). Note the adipocyte (A) is separated from the cap cell membrane by an intact basal lamina (Bl). In addition, focal endomicropinocytotic vesicles (En-mv-arrow) are present along the CC membrane and along the adipocyte (A) cell membrane (En-mv-arrow). The sample was prepared using a standard TEM procedure consisting of a modified Karnovsky's fixative, followed by O_sO^4 and an *en bloc* UA. Scale bar = 1.0 μm.

Figure 3.9. Transmission electron micrograph of the cap cell (CC) membrane in a mouse mammary gland (a longitudinal ultrathin section). Note the intact basal lamina (Bl-arrow) in the absence of a "clearance zone" separating the adjacent adipocyte (A) from the underlying cap cell membranes. Endoplasmic reticulum (ER), endomicropinocytotic vesicles (En-mv-arrow), membrane bound microvesicles (mv), mitochondria (M), and ribosomes (R) are also labelled. Scale bar = 0.5 μm.

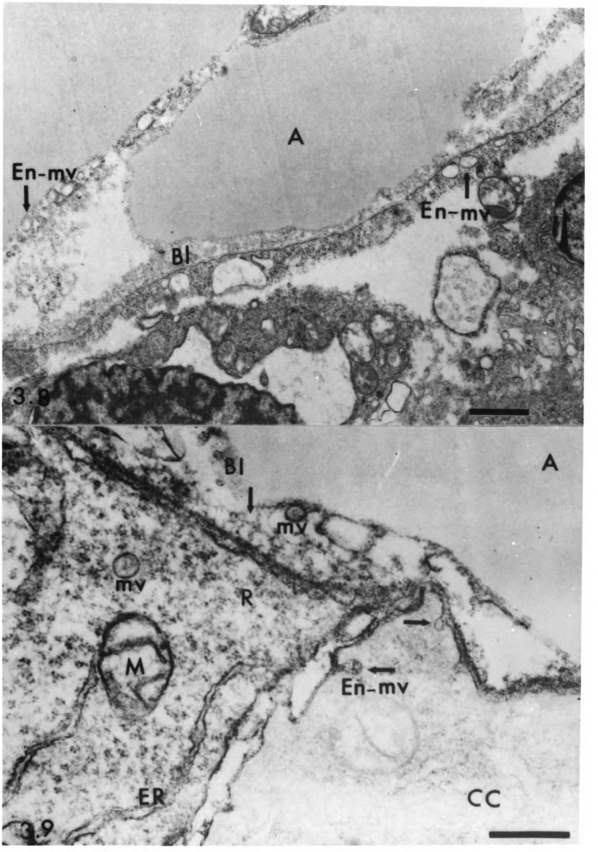
A
En-mv
En-mv
Bl
3.8
Bl
A
mv
mv
R
M
En-mv
ER
CC
3.9

layer of the basal lamina along with the cap cell and stromal cell membranes, contained endo- and exo-micropinocytotic vesicles consistent with pinocytotic activity. However, in order for exo-micropinocytosis to occur in the basal membrane of the cap cell there must be discontinuity of the basal lamina. Figure 3.11 shows an exo-micropinocytotic vesicle on the outer surface of a cap cell basal membrane and a break in the basal lamina of the mouse mammary gland. From a morphologic standpoint, this appears to be the primary mechanism of informational exchange between cap cells and the extracellular environment; which includes adipocytes and fibroblasts.

To support the hypothesis that cap cells are the stem cells of the mammary gland, several cap cells were examined for the presence or absence of gap junctions. Micrographs of cap cells from both modified Karnovsky's and alcian blue - lanthanum nitrate fixation protocols were examined. The latter fixative is used for delineating the surface coat of cell membranes and junctional complexes residing in those membranes. No junctional complexes of any kind, including gap junctions, or specialized membrane structures were found in any of the cap cells examined. Therefore, the lack of gap junctional complexes in the cap cells of the TEB, supports the hypothesis that the cap cells are the stem cells of the mammary gland.

Figure 3.10a. Histologic longitudinal section (5 μm) of a whole mount preparation from a Nu/+ mouse mammary gland showing two large TEBs surrounded by fibroblasts and abundant collagen. Note the tremendous numbers of fibroblasts and collagen (FC), cutaneous musculature (*), and the small aggregates of adipocytes (A) in the extracellular matrix (ECM). There is prominent intercellular spacing between cap cell and intermediate cell layers (double arrow) but a total absence or minimal presence of a clearance zone (arrow). The cutaneous muscle is labelled (*). H and E. X10.

Figure 3.10b. Close up of one of the TEB structures in Figure 3.10a. Note the prominent intercellular spacing between the CC layer and the IC layer (double arrow) and the minimal "clearance zone" (arrow). In addition to the fibroblasts and collagen, the ECM also contains mild to moderate numbers of leukocytes and mononuclear cells (*) H and E. X20.

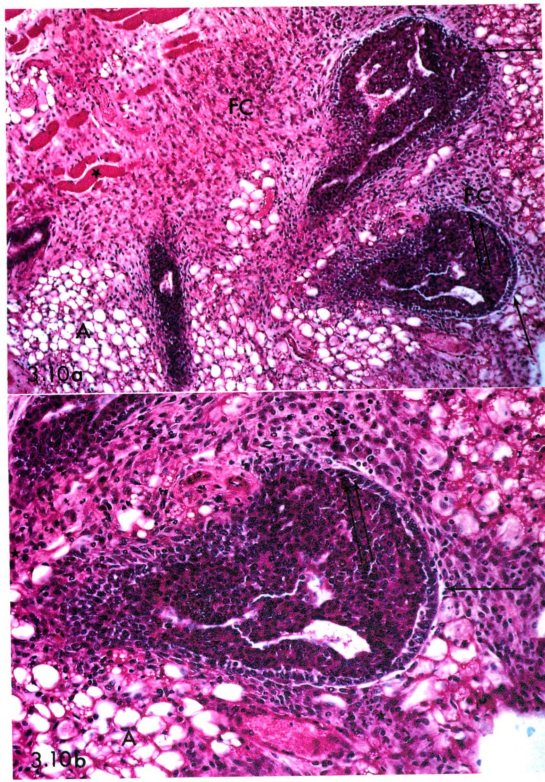
FC
FC
A
3.10a
A
3.10b

Figure 3.11. Transmission electron micrograph of a cap cell membrane in the TEB of a mouse mammary gland (a longitudinal ultrathin section). Note the endo- and exo-micropinocytotic vesicles (En-mv-double arrow and Ex-mv arrow) along the basal membrane border. There is a distinct break in the basal lamina (arrow) as the exo-micropinocytotic vesicle protrudes out into the ECM. The sample was prepared using a standard TEM procedure consisting of a modified Karnovsky's fixative, followed by O_sO_4 and an <u>en bloc</u> UA. Scale bar = 0.25 μm.

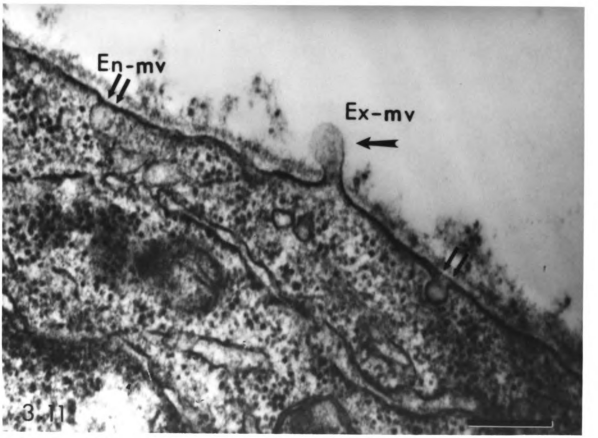
En-mv
Ex-mv
3-11

The cap cell layer was also examined using freeze fracture analysis. By splitting the lipid bilayer, freeze fracture provides more detailed information about the macromolecular structure of the cell membrane. For example, using basic TEM, the pentalaminar configuration of the tight junction can be difficult to differentiate from the septilaminar configuration of the gap junction, but the freeze fracture replica of these two junctional complexes are very different (Ryerse and Nagel, 1991; Wolfe, 1985) (Figures 3.12 and 3.13).

Over 40 TEBs were fractured and examined under the transmission electron microscope. Unfortunately, none of the samples examined could be positively identified as cap cell - cap cell or cap cell - adipocyte fracture sites. The inability to define these specific sites was due to: 1) a lack of specific morphologic cell markers which could distinguish the cap cell from other TEB epithelial cells, 2) the technical difficulty associated with fracturing a specific cell layer in a minute structure, and 3) the lack of a special fracturing device capable of fracturing specific areas within the TEB. Unfortunately, the orientation of the cells within the TEB was not sufficient in differentiating between these regions and therefore no statement can be made regarding the cap cell - stromal cell or cap cell - cap cell intercellular relationship based on freeze fracture results. However, based on ultrastructural analysis of the cap cell region (which was negative for gap junction complexes), and the results of

Figure 3.12. Transmission electron micrograph of a freeze fracture replica from the tip of a TEB in a mouse mammary gland. Note the tight junction (T) present in the luminal cell (LC) membrane and numerous microvilli (Mv) which project into the lumen of the TEB. The sample was prepared using a standard freeze-fracture procedure and a modified Karnovsky's fixative. Scale bar = 0.5 μm.

Figure 3.13. Transmission electron micrograph of a freeze fracture replica from a liver sample taken from a Nu/+ mouse. Note the tight (T) and gap junctions (GJ) in the endothelial plasma membrane of the liver sinusoids. Endothelial pores (EP) and the cytoplasm (Cy) are also labelled. Scale bar = 1.0 μm.

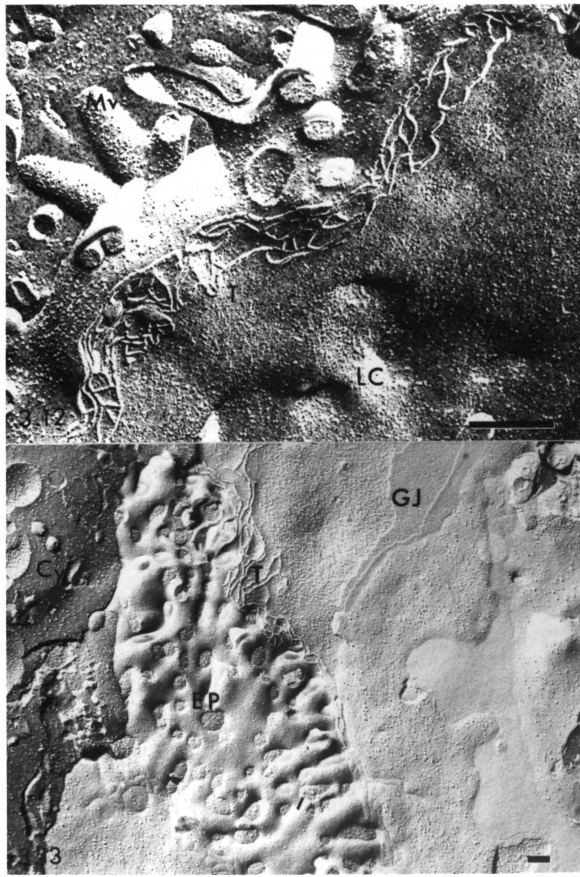
Mv
T
LC
2
GJ
C
T
LP
3

previous research which points to the cap cell as the stem cell of the mammary gland even if the technology and equipment had been available, it is unlikely that gap junctions would have been found in the cap cell population since stem cells do not possess gap junctions.

The replica preparation technique developed in this study in which lipase was used in place of bleach to clean the replicas, proved to be successful in providing high quality freeze fracture replicas of the mouse mammary gland. Figures 3.14 and 3.15, of the extracellular matrix, reveal the high quality of the replicas.

Discussion

The type of intercellular communication between cap cells and between cap cells and adjacent stromal cells was explored by using the light microscope and transmission electron microscope. The cap cells in the larger, more mitotically active TEBs were surrounded by large intercellular spaces containing cytoplasmic projections of various size and shape. The cap cell membranes had numerous sites of micropinocytotic activity. However, no gap junctional complexes or specialized membrane structures were found. Because stem cells do not possess gap junctions, the lack of gap junctions in the cap cells supports the theory that the cap cells are the stem cells of the mammary gland.

In addition to the intercellular spaces between cap

Figure 3.14. Transmission electron micrograph of a freeze fracture replica from the tip of a TEB in a mouse mammary gland. Note the narrow intercellular space (ICS) between the cytoplasm (Cy) of two adjacent adipocytes (A) containing lipid. Collagen fibrils (Cf) are visible in the ICS and numerous microvesicles (Mv) are present in the cytoplasm. The sample was prepared using a standard freeze-fracture procedure and a modified Karnovsky's fixative. Scale bar = 1.0 μm.

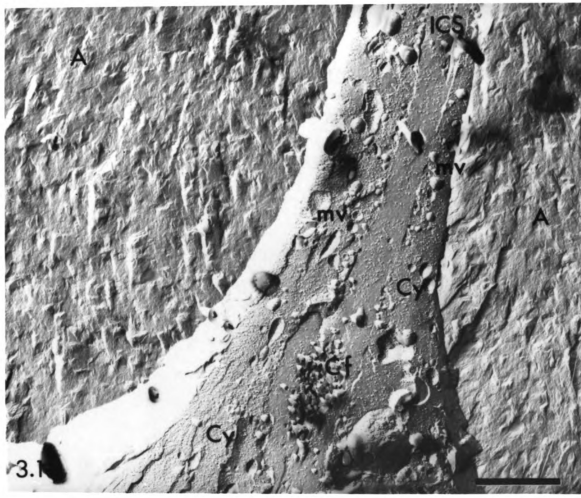

3.1

Figure 3.15. Transmission electron micrograph of a freeze fracture replica from the tip of a TEB in a mouse mammary gland. Note the endothelial cell (EC) lining the central lumen (Cl) of a blood vessel in the upper left hand corner. An adipocyte (A), collagen fibrils (Cf) in the intercellular spaces (ICS), and various cytoplasmic projections (Cy) from extracellular matrix cells containing microvesicles (mv) are also labelled. The sample was prepared using a standard freeze-fracture procedure and a modified Karnovsky's fixative.
Scale bar = 0.5 μm.

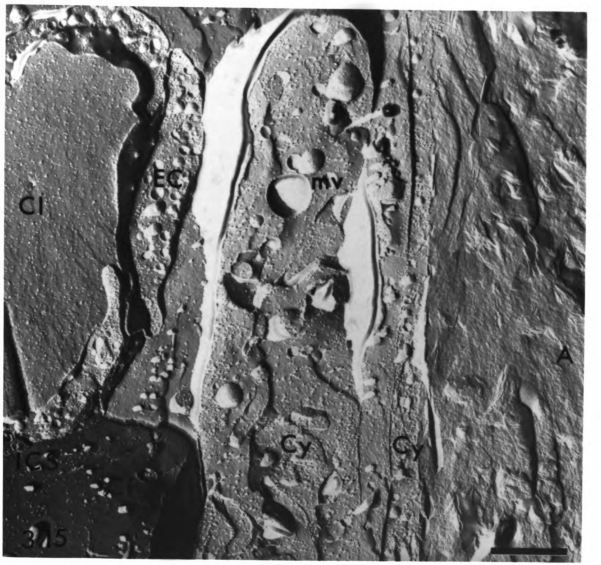
Cl
EC
mv
A
Cy
Cy
IC3
3.5

cells, some of the larger TEBs had a similar space between the cap cell basal lamina and adjacent stromal epithelial cells, i.e., adipocytes and fibroblasts. This space, termed the "clearance zone", varied in width ranging from approximately 15 to 100 micrometers. The zone has a crescent shape and spans the tip of the anterior TEB from flank to flank. Silberstein and Daniel (1982a) believed that the presence of intercellular spaces between cap cells is associated with hyaluronate secreted by the cap cells. Since hyaluronate is a component of the basal lamina, it is likely that the clearance zone, when present, as well as the intercellular spaces between cap cells are associated with significant hyaluronate production by the cap cells. This theory is supported by the observation that the small to medium sized TEBs, whether surrounded by adipocytes or fibroblasts, did not possess clearance zones or significant intercellular spaces between cap cells (suggestive of minimal or no hyaluronate production). In those glands where the TEB structures were surrounded by excessive fibroblasts, no clearance zones or negligible clearance zones were present in spite of prominent spaces between cap cells. Therefore, it is possible that the adipocytes are more sensitive to hyaluronate than fibroblasts and/or possible excrete a substance that interacts with hyaluronate resulting in the formation of a clearance zone.

In TEBs where clearance zones were not present, the basal cap cell membranes were separated from adipocyte and/or fibroblast membranes by an intact basal lamina. Unlike the

basal lamina in some of the larger TEBs with clearance zones, those without clearance zones had no discontinuity in the outer layer of the basal lamina. However, small breaks in the basal lamina, allowing exo-micropinocytotic vesicles to migrate in the ECM, were positively identified and confirm that points of discontinuity exist in the basal lamina of the mouse mammary gland as well as in the rat mammary gland. In addition, no direct cap cell - stromal cell contact was observed in any of these TEB structures but endo- and exo-micropinocytotic activity was present in both the cap cell and stromal cell membranes.

In conclusion, the results of this study suggest that TEBs are morphologically similar yet unique. Tremendous variation in TEB size is just one morphologic characteristic which reflects a difference in mitotic activity and cytodifferentiation amongst the cells composing the TEB structure. The degree of intercellular spacing and the presence or absence of a clearance zone is another morphologic characteristic that most likely is a direct reflection of hyaluronate secretion by the cap cells; which in turn is most likely associated with 1) the number and/or metabolic activity of the cap cells and 2) the age of the mouse, i.e., as the mouse matures, the size and number of TEBs per gland decreases (Chapter 3).

Ultrastructurally, the undifferentiated appearance of the cap cell along with the lack of gap junctional complexes, supports the hypothesis that the cap cells are in fact the

stem cells of the mouse mammary gland (Bennett et al., 1978; Dulbecco et al., 1982; Williams and Daniel, 1983; Dulbecco et al., 1983). In addition, the cap cell membranes, while engaging in micropinocytotic activity, which in itself is a form of intercellular communication, do not come in direct contact with adjacent stromal cell membranes. The primary reason for this is that the basal lamina while lacking a lamina externa in some instances is never totally absent; even in the region where exo-micropinocytosis is occurring, small breaks in the basal lamina appear to be quickly sealed by the adjacent lamina.

CHAPTER 4

ASYNCHRONOUS DEVELOPMENT OF THE TERMINAL END BUD IN THE MOUSE MAMMARY GLAND

Abstract

Asynchronous development of the prepubertal-pubertal mouse mammary gland and differential growth in the size and number of the terminal end bud (TEB) structures are influenced not only by the age of the mouse but by the gland of origin and the location of the TEB within the gland. The left and right, No. 2 and No. 3 thoracic and the No. 4 inguinal, glands were collected from athymic nude (Nu/+) mice weaned at 21 days of age and fed a high caloric non-restricted intake diet for 2 and 3 weeks post-weaning. The mean maximum terminal end bud (MTEB) area was calculated in mm^2 from the 5 largest TEB areas measured in each gland and these data were used to compare glands within and between mice of the same and different age groups. At 5 weeks of age the size and number of TEB structures in the No. 2 and No. 3 thoracic glands were significantly greater than those found in the No. 4 inguinal gland. By 6 weeks of age the mean MTEB area and the number of TEBs in the No. 2 thoracic glands significantly decreased, indicating that for this particular gland the largest and greatest number of TEB structures is present at approximately 5 weeks of age. In contrast, the mean MTEB area and the number of TEBS in the No. 3 thoracic and No. 4 inguinal glands remained relatively constant between 5 and 6 weeks of age. However, consistent numerical decreases in range, mode, and maximum TEB area indicate that there is an overall decline in

the size of these TEB structures by 6 weeks of age in the mouse.

Introduction

The mammary gland is one of the few organ systems in mammals that completes its morphologic development postnatally. Because of this unusual developmental property, it serves as an excellent model for studying ductal morphogenesis beyond embryologic life. A detailed account of the embryological development of the rodent mammary gland was first published by Turner and Gomez (1933). The work done by Turner and Gomez on the prenatal development of the rodent mammary gland served as a basis for future research in the area of embryogenesis (Balinsky, 1950; Raynaud, 1961; Kratochwil and Schwartz, 1976; Sakakura et al., 1982), and postnatal development (Pitelka and Hamamoto, 1977; Silberstein and Daniel, 1982a; Williams and Daniel, 1983). For the past seven decades, rodent mammary gland models have been widely used for studying ductal morphogenesis and mammary gland carcinogenesis (Medina et al., 1990). However, it has only been in the past decade that researchers have developed a better understanding of the basic structure that drives ductal proliferation and plays a key role in mammary gland tumorigenesis, namely the terminal end bud. During the 1980's, a significant amount of information was published regarding ductal morphogenesis and tumorigenesis in the

postnatal rodent mammary gland. The majority of information focused on the cellular composition of the TEB structure, the effect of carcinogens on the TEB structures in relationship to tumor incidence, and the interaction of the TEB with the surrounding extracellular matrix (Gordon and Bernfield, 1980; Silberstein and Daniel, 1982a and 1982b; Dulbecco et al., 1982 and 1983; Williams and Daniel, 1983; Russo and Russo, 1987; Coleman et al., 1988; Daniel et al., 1989).

Briefly, the postnatal growth of the rodent mammary gland is divided chronologically into five periods, namely the neonatal, juvenile, prepubertal, pubertal, and mature virgin growth periods. In the mouse mammary gland these periods coincide with 1-3 weeks of age, 3-4 weeks of age, 4-5 weeks of age, 5-7 weeks of age, 7-9 weeks of age and beyond, respectively (Topper and Freeman, 1980). It has been documented that during the neonatal and juvenile growth periods, the rat mammary gland grows isometrically with respect to the animal (Sinha and Tucker, 1966). However, when the rat reaches the prepubertal growth period, the mammary gland grows allometrically, with respect to the animal (Sinha and Tucker, 1966). During this significant period of ductal expansion in the rat the highly mitotic TEB structure is present and drives ductal morphogenesis. A similar allometric growth pattern has been documented in the mouse mammary gland as well (Topper and Freeman, 1980).

In the mouse mammary gland the TEB is present at two

specific time intervals between late gestation and puberty, as marked by the onset of estrous (Sekhri et al., 1967). It first appears between late gestation and 1 week of age in response to maternal hormones (Sakakura, 1987). As the maternal hormonal level decreases, there is a complementary decrease in the size and number of TEB structures. During the remainder of the neonatal period through the juvenile period, the TEB structure is not visible in the mouse mammary gland. With the onset of the prepubertal-pubertal growth period, at approximately 4 weeks of age, the mouse mammary gland becomes increasingly sensitized and responsive to elevations of local and systemic reproductive hormones which coincides with the reappearance of the TEB structures (Topper and Freeman, 1980; Williams and Daniel, 1983). It is during this crucial growth phase that the terminal end bud structures orchestrate the morphologic development of the ductal system throughout the mammary gland fat pad.

The ability of the TEB structures to drive ductal morphogenesis is associated with their cellular content. The TEB contains a very significant population of undifferentiated cells called "cap cells". These cells are believed to be the pleuripotential stem cells of the developing gland and to play a key role in mammary gland carcinogenesis (Williams and Daniel, 1983). The cap cells lie in the outer layer of the TEB structure and have been shown to give rise to the intermediate cells and myoepithelial cells of the advancing duct. If in fact the cap cells are the stem cells of the

mammary gland, then they are subject to the same basic tumorigenic principles as other stem cell populations with respect to initiators and promoters. Russo and Russo (1987) found that exposure of the mammary gland to carcinogens at an early age results in significant mutations associated with malignant transformation in the undifferentiated cell populations of the TEB and increased susceptibility to tumor development. They documented that the intermediate (undifferentiated) cells in the rat had a much shorter G_1 phase and a lower DNA adduct removal rate than the dark (differentiated) cells and that the thoracic glands had a higher number of TEBs per gland than the inguinal glands. Russo and Russo (1987) concluded that these properties, amongst others, were responsible for the increased susceptibility of the rat mammary gland to carcinogenesis, i.e., the rats were exposed to DMBA between 21-55 days of age when the number of TEB structures were at their peak.

The objectives of this study were to 1) investigate the asynchronous development of the prepubertal-pubertal mouse mammary gland 2) document the differential growth of the TEB structure as a function of gland origin, location and prepubertal-pubertal age and 3) define the growth period of maximum TEB size and number for the thoracic and inguinal mouse mammary glands.

Materials and Methods

Animals. Seventy-five haired immune competent, athymic nude (Nu/+) female mice were used in this study. The F_1 generation was obtained from parental strains, consisting of a Nu/Nu male and a Nu/+ female. The in house bred Nu/+ females used in this study were individually caged and housed in a temperature controlled environment at 21±1°C on a 12 hour light, 12 hour dark exposure cycle.

Diet. For maximum TEB growth, a semisynthetic high fat (20% corn oil) diet was used in this study (Welsch et al., 1985; Faulkin et al., 1986). It was prepared on a weekly basis and stored in plastic bags at -20°C prior to use. The high fat diet was composed of 20% corn oil, 20.17% casein, 0.35% DL-methionine, 32.18% dextrose, 16.09% sucrose, 4.13% AIN salt mixture, 1.18% AIN vitamins, and 5.90% cellulose. The mice were fed a pre-weighed amount of the high fat diet daily (usually 5.0 g) and had unlimited access to water. To monitor feed consumption, all unconsumed feed was weighed at the end of every 24 hour interval and recorded. The mice were fed at the same time every day, and body weights were recorded twice a week.

Experimental Design. Two groups of prepubertal-pubertal mice were targeted for this study. The first group consisted of 40 mice, weaned at 21 days of age and fed a high fat non-restricted intake diet for 2 weeks. At the end of this

interval, the then 5 week old mice were anesthetized with ether and euthanatized by cervical dislocation. The right and left No. 2 and No. 3 thoracic mammary glands and No. 4 inguinal mammary glands were removed for whole mount and light microscopic evaluation (Figure 4.1 and 4.2). The second group consisted of 35 mice, weaned at 21 days of age and fed the same high fat diet for 3 weeks. At the end of this interval, the 6 week old mice were euthanatized as previously described and the same mammary glands were removed for whole mount and light microscopic evaluation.

Whole Mount Procedure. At the end of the 2 and 3 week feeding intervals, the left and right No. 2, No. 3, and No. 4 mammary glands were removed and fixed in a 3:1 solution of 100% ethanol:glacial acetic acid for approximately 1 hour. Fixation was followed by a 15 minute wash in 70% ethanol, a 5 minute wash in distilled water, and overnight staining in alum carmine (Sigma Chemical Co.). The next morning, the mammary glands were placed in a graded series of ethanol solutions, 70%, 95%, and 100% respectively, for 15 minutes each. Alcohol dehydration was followed by a 15 minute wash in toluene. The mammary glands were stored in methyl salicylate at room temperature prior to evaluation (Banerjee et al., 1976; Humason, 1979).

Quantitative Analysis of the Terminal End Bud. The maximum growth of the TEB structure was assessed by measuring the area, in mm^2, of the TEBs at the peripheral leading edge of the advancing ductal mass in the No. 2 and No. 3 thoracic

Figure 4.1. Light micrograph of a whole mount preparation from a 5 week old Nu/+ mouse showing the No. 2 (left) and No. 3 (right) thoracic mammary glands. Note the dichotomous branching of the ducts (arrows) and the various sized TEB structures at the peripheral leading edge of the expanding ductal tree (double arrows). H and E. X13.

Figure 4.2. Light micrograph of a whole mount preparation from a 5 week old Nu/+ mouse showing the No. 4 inguinal mammary gland. Note the centric inguinal lymph node (arrow) and the dichotomous branching of the ducts. Various sized TEB structures are present at the peripheral leading edge of the expanding ductal tree (double arrows) and compared to the No. 2 and No. 3 thoracic glands (above), the No. 4 inguinal gland typically has smaller, less bulbous TEB structures. H and E. X13.

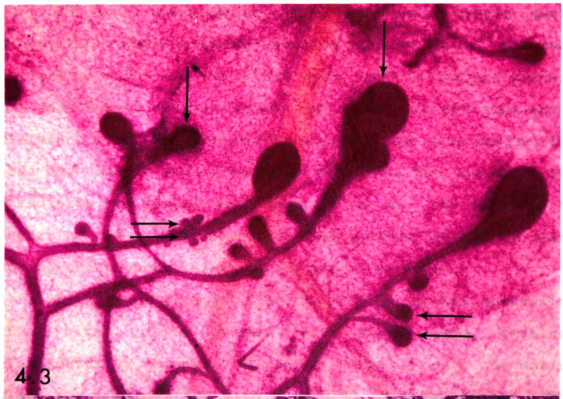

4.3

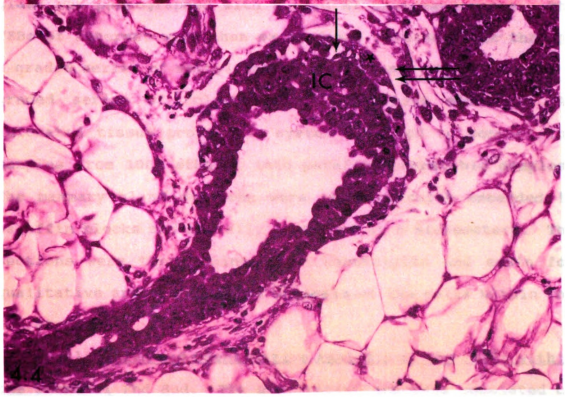

4.4

and No. 4 inguinal mouse mammary glands (Figure 4.1 and 4.2). The TEB area measurements were made using whole mount preparations and a computer-assisted image analyzer. The mean maximal terminal end bud (MTEB) area, used to compare maximum TEB development between glands and animals of the same and different ages, was obtained by averaging the five largest TEB area measures in each gland. In addition, the number of TEB structures per gland, with areas $\geq .03$ mm^2, was recorded to determine the average number of TEBs present in a given gland during the prepubertal-pubertal growth periods.

Light Microscopy. Specific mammary glands containing TEBs with unique shapes and sizes were examined histologically, Figure 4.3. Prior to sectioning, the entire gland was photographed with a Wild M7 photomacroscope. The TEBs of interest were then excised and reversed back through a graded series of methyl salicylate:toluene, 100% toluene, a graded series of toluene:ethanol, to 100% ethanol. An automated tissue processing system was used to convert the samples from 100% ethanol into paraffin compatible samples. The mammary gland sections were longitudinally embedded in paraffin blocks and serially sectioned at 5 micrometers. The sections were then stained with hematoxylin and eosin for qualitative and quantitative analysis of the cells within the TEB structure.

Qualitative and Quantitative Analysis of the Cells within the Terminal End Bud. The qualitative analysis consisted of a subjective description of the shape of the TEB, and the

distribution and character of the cells comprising the structure. Glands containing TEBs with the largest areas were selected for quantitative analysis and were serially sectioned at 5 micrometers. The section containing the TEB structure at its maximum diameter was identified, and the cells from the histologically distinct cap cell layer were counted (Figure 4.4).

Statistical Analysis. The average maximum size of TEB structures per gland, as measured by the mean MTEB area, and the average number of TEB structures, with an area $\geq .03$ mm^2, were analyzed by a one-way analysis of variance at a $p \leq .05$.

Results

The results of the 2 week and 3 week experiments are summarized in Table 4.1. In the 2 week experiment, there was a significant difference in the mean MTEB area between glands in mice of the same age, i.e., 5 weeks old. The mean MTEB area for the No. L3 and R3 (.084 mm^2 and .089 mm^2) and No. L2 and R2 (.073 mm^2 and .077 mm^2) glands was significantly greater than the mean MTEB area for the No. L4 and R4 (.055 mm^2 and .055 mm^2) glands at $p \leq .05$ i.e., No. 3's > No. 2's > No. 4's. At 5 weeks of age, the number of TEBs per gland was significantly greater in the No. 2 and No. 3 glands when compared to the No. 4 glands. There was no significant different in the mean MTEB area or the number of TEBs between right and left glands of the same number.

Figure 4.3. Light micrograph of a whole mount preparation from a 5 week old Nu/+ mouse showing a close up of the TEB structures in the No. 3 thoracic mammary gland of Figure 4.1. Note the unique size and shape of the TEB structures at the peripheral leading edge of the advancing mammary tree (arrows) and the smaller TEBs along the outer wall of the differentiated ducts (double arrows). H and E. X40.

Figure 4.4. Histologic longitudinal section (5 μm) of a whole mount preparation from a Nu/+ mouse mammary gland. Note the "clearance zone" anterior to the TEB (arrow) and the distinct cap cell layer (double arrow). Prominent intercellular spaces are present between the cap cells (*) and between the cap cell and intermediate cell (IC) layers. H and E. X36.

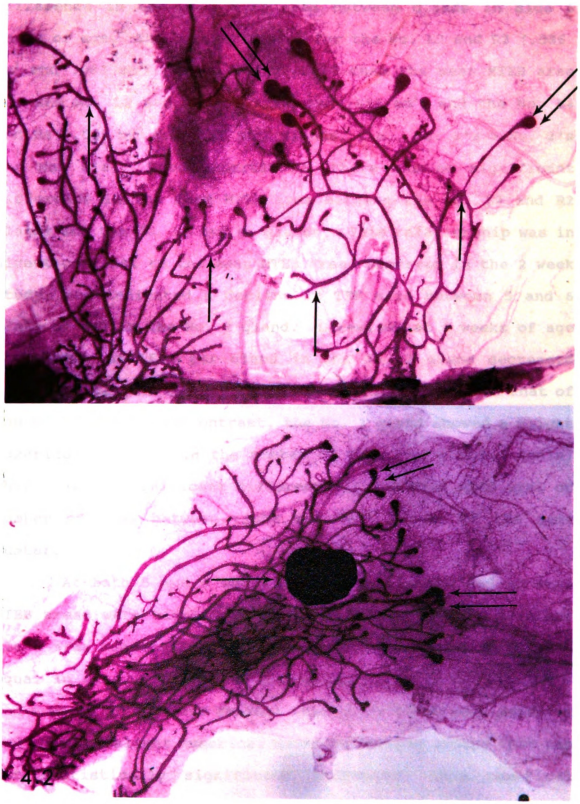

In the 3 week experiment there was a significant difference in the mean MTEB area between glands in mice 6 weeks of age. The mean MTEB area for the No. L3 and R3 (.086 mm^2 and .083 mm^2) glands was greater than the mean MTEB area for the No. L2 and R2 (.050 mm^2 and .056 mm^2) and the No. L4 and R4 (.048 mm^2 and .048 mm^2) glands, i.e., No. 3's > No. 2's and No. 4's. More importantly, there was no significant difference in the mean MTEB area between the No. L2 and R2 glands and the No. L4 and R4 glands. This relationship was in direct contrast to the mean MTEB areas observed in the 2 week study, and indicated a decline in TEB size between 5 and 6 weeks of age in the No. 2 gland. Likewise, at 6 weeks of age the number of TEBs per gland in the No. 2 gland decreased significantly and was not statistically different from that of the No. 4 gland. In contrast, the No. 3 gland showed a slight numerical increase in the number of TEBs per gland. Again, there was no significant difference in the mean MTEB area or number of TEBs between right and left glands of the same number.

At both 5 and 6 weeks of age, the No. L3 and R3 mean MTEB areas were significantly greater than any of the other gland area measures and, at the same time, were virtually equal in size. The No. L4 and R4 mean MTEB areas between 5 and 6 weeks of age were smaller than other gland area measures and showed a slight numerical decrease between groups that was not statistically significant. However, this numerical decrease suggested a decline in TEB size between 5 and 6 weeks

Table 4.1 Mean maximum TEB area (mm^2) and mean number of TEBs per gland in 5 and 6 week old Athymic nude (Nu/+) mice

Gland	Mean maximum TEB area(mm^2)		Mean Number TEBs per Gland	
	5 Week[a]	6 Week[b]	5 Week[a]	6 Week[b]
No. L2[c]	.073 ± .003[d,e]	.050 ± .002[d]	9.77 ± .48[d,e]	6.08 ± .53[d]
No. R2[c]	.077 ± .003[e]	.056 ± .003	10.18 ± .59[e]	6.86 ± .62
No. L3	.084 ± .003	.086 ± .004[f]	10.11 ± .82	11.49 ± .58[f]
No. R3	.089 ± .005	.083 ± .004[f]	10.42 ± .82	10.66 ± .46[f]
No. L4	.055 ± .003[g]	.048 ± .002	6.80 ± .44[g]	6.54 ± .44
No. R4	.055 ± .003[g]	.048 ± .002	6.92 ± .33[g]	6.71 ± .48

(a) Forty athymic nude (Nu/+) mice were fed a high fat diet for 2 weeks and sacrificed at 35 days of age.
(b) Thirty-five athymic nude (Nu/+) mice were fed a high fat diet for 2 weeks and sacrificed at 42 days of age.
(c) R = right gland; L = left gland
(d) Mean ± SE
(e) Significantly different ($p < 0.05$) from 6 week values.
(f) Significantly different ($p < 0.05$) from No. 2 and No. 4 gland values.
(g) Significantly different ($p < 0.05$) from No. 2 and No. 3 gland values.

of age in the No. 4 gland. The most significant change in the mean MTEB area between 5 and 6 week old mice was observed in the No. 2 gland. By 6 weeks of age, the mean MTEB area in the No. L2 and R2 glands had decreased by 27% to 32% when comparing like glands between 5 and 6 weeks of age, respectively. To further support this trend of decreasing TEB size between 5 and 6 weeks of age, a consistent numerical decrease in the range, mode, and maximum TEB area was present.

This trend toward decreasing cell mass and linearity coincided with the normal increase in the number of terminal end ducts and alveolar buds as the expanding mammary gland tree reaches the limits of its fat pad (Williams and Daniel, 1983). A shift from the larger, bulbous, mitotically active TEB to the smaller, linear, mitotically inactive TEDs and ABs is usually observed in the later stages of puberty and is virtually complete in the virgin female (Topper and Freeman, 1980). In this study the average number of TEBs per gland with an area of $\geq .03$ mm^2 were also analyzed. A statistically significant decline was observed in the number of TEBs in the No. 2 glands between 5 and 6 week old mice which corresponded with the observed decrease in mean MTEB area in this gland. In contrast, there was a lack of statistically significant numerical differences in the number of TEBs in the No. 3 and No. 4 glands between 5 and 6 weeks of age. This suggested that these glands either retained their TEB structures longer and/or gave rise to new TEB structures later such that, the

Table 4.2 Number of cap cells per maximum TEB area (mm^2) in 5 and 6 week old Athymic nude (Nu/+) mice

Gland[a]	Maximum TEB area (mm^2)[c]		Number of Cap Cells per MTEB area[d]	
	5 Week	6 Week	5 Week	6 Week
No. L2[b]	.173	.129	62	53
No. R2[b]	.157	.148	61	63
No. L3	.273	.188	100	87
No. R3	.271	.216	107	NA
No. L4	.105	.098	45	32
No. R4	.138	.094	50	41

(a) The left and right No. 2, 3 and 4 glands were removed from 5 week old Nu/+ mice (N=40) and 6 week old Nu/+ mice (N=35).
(b) R = right gland ; L = left gland
(c) Largest TEB area measured per gland from 5 and 6 week old mice.
(d) Number of cells in the peripheral cap cell layer of the TEB.
NA Histologic section not available for analysis.

overall number of TEBs remained relatively constant between 5 and 6 weeks of age.

The quantitative results of the light microscopic evaluation are summarized in Table 4.2. The analysis revealed a linear relationship between the size of the TEB area and the number of cells present in the cap cell layer at the maximum diameter or midpoint of the TEB structure. As the TEB area increased, there was a coinciding increase in cap cell number.

Discussion

The asynchronous development and differential growth of the TEB structure in the prepubertal-pubertal mouse mammary gland, to this author's knowledge, have never been documented in the literature. In 1989, Welsch and O'Connor examined the effect of different types of dietary oils on the development of the immature mouse and made reference to asynchronous development in the mouse. They injected 42 day old ovariectomized mice (ovariectomized at 35 days) with estradiol-17ß plus progesterone prior to euthanasia in order to insure "synchronous development" of the mammary gland. The large degree of variation in TEB size amongst mice of a certain age group was addressed by Silberstein and Daniel, (1982) who reported that the "typical" TEB in a 5 week old mouse ranged in size from 0.1-0.5 mm in diameter and Williams and Daniel (1983) who reported the prepubertal TEB ranged from 0.2-0.8 mm. This large range in TEB size indirectly reflects

the presence of asynchronous growth in the mouse mammary gland. The results of the present study show that not only was there asynchronous development between glands within and between mice of the same and different group, but that a significant differential growth pattern exists in the maximum attainable size and number of TEBs per gland as a function of gland origin, location and age of the mouse.

For the past decade, it has been known that TEB structures have the ability to bifurcate, which leads to dichotomous branching of the mammary ductal tree. In addition, they possess tropic behavior that results in the expansion of the largest TEB structures, at the peripheral leading edge of the advancing mammary gland tree, into the unoccupied mammary gland fat pad (Williams and Daniel, 1983). The mammary gland fat pad is very significant because it is not only mandatory for normal ductal expansion but in part determines the degree of ductal proliferation by its natural borders (Williams and Daniel, 1983).

In this study, the TEB structures at the peripheral leading edge of each advancing mammary gland tree in forty 5 week old mice and thirty-five 6 week old mice were measured using a computer-assisted image analyzer at 40X. The mean maximum terminal end bud (MTEB) area, in mm^2, was used to make comparisons between glands within and between mice of the same and different age groups. The five largest TEB's were selected because 1) they were blatantly bulbous and could not

be confused with terminal end ducts (TED) or "intermediate" terminal end duct structures and 2) they had clearly demarcated neck regions which increased the accuracy of measuring the TEB structures. The null hypothesis of this study stated that the relative size of TEBs between glands in mice of the same age are equal, i.e., the mean MTEB area of gland No. 2 is equal to gland No. 3 is equal to gland No. 4, i.e., $H_o=M_2=M_3=M_4$. By using the mean MTEB area as the comparative unit of measure, a significant variation in TEB size between glands within mice of the same age was found. In both age groups, 5 and 6 week old mice, the mean MTEB area from the No. L3 and No. R3 glands were significantly greater than the mean MTEB area from the No. L4 and No. R4 glands (Table 4.1). This suggested that, at least in part, the gland of origin of the TEB structure determines the maximal size it will obtain. To further support this statement, at 5 weeks of age although the mean MTEB area from the No. L2 and No. R2 glands was not significantly less than No. L3 and No. R3, they were significantly greater than No. L4 and No. R4.

By 6 weeks of age, a significant change in the mean MTEB area of the No. 2 gland was observed. At this age, the mean MTEB area had decreased by 27% and 32% in the No. R2 and No. L2 glands, respectively (Table 4.1). Numerically, the mean MTEB area of the No. 2 glands and the No. 4 glands was almost identical. The decrease in TEB size for the No. 2 gland between 5 and 6 weeks of age was statistically significant and

indicated that the largest TEB structures in this particular gland are observed around 5 weeks of age. These data suggest that the prepubertal-pubertal age of the mouse, as well as the gland of origin and the location of the TEB within the gland (peripheral leading edge vs internal) have a direct influence on the maximum attainable size of the TEB structure. Although the mean MTEB area in the No. 3 and No. 4 glands did not show as dramatic a decrease in size between 5 and 6 weeks of age, as compared to the No. 2 glands, the modest numerical decrease in mean MTEB area, along with the consistent numerical decreases in range, mode and maximum TEB area, suggested that the peak TEB size was reached in all glands during the prepubertal-pubertal growth period prior to 6 weeks of age.

Light microscopic analysis of selected TEB structures, from representative glands in 5 and 6 week old mice, confirmed that the larger TEB structures were located at the peripheral leading edge of the glands and that the larger TEBs had increased numbers of cap cells, as opposed to cellular hyperplasia, when compared to smaller TEB structures (Table 4.2).

The data presented in this study document the asynchronous development of TEB structures in the mouse mammary gland. In theory, the No. 2 thoracic gland at 5 weeks of age and the No. 3 thoracic gland at 5 to 6 weeks of age, as opposed to the No. 4 inguinal gland in the mouse, should be more susceptible to initiation and promotion events during

these specific prepubertal-pubertal growth periods than at any other time prior to maturation. The rationale behind this statement is: 1) they contain the largest number of TEB's during the prepubertal-pubertal growth period, and 2) they have attained their largest size in terms of area and numbers of undifferentiated cells. The undifferentiated cells characteristically have a shorter G_1 phase and lower adduct removal rate thereby increasing their susceptibility to genetic mutations and tumor formation (Russo and Russo, 1987).

In conclusion, it is clear that there are inherent differences in TEB size and number in the mouse mammary gland during the prepubertal-pubertal growth period. These differences are influenced by the gland of origin and the location of the TEB within the gland, and the age of the mouse. The results emphasize the importance of including representative glands from both the thoracic and inguinal regions when studying the effects of initiators and promoters on the TEB structures because of the differential growth in the size and number of TEB structures in the mouse mammary gland. Failure to recognize these inherent differences in TEB size associated with the gland of origin, as well as the age of the mouse, could result in incomplete and biased data. Future studies in the area of prepubertal-pubertal development of the mouse mammary gland are necessary in order to better understand the mechanisms of tumorigenesis initiated during this particular growth period.

CHAPTER 5

THE EFFECT OF BODY WEIGHT AND FEED CONSUMPTION ON TERMINAL END BUD DEVELOPMENT IN THE MOUSE MAMMARY GLAND

Abstract

The effects of body weight and feed consumption on TEB development during the prepubertal-pubertal growth periods between 5 and 6 weeks of age in the Nu/+ mouse are not clearly defined. In this study the correlations between mean maximum TEB area (MTEB) and mean number of TEBs per gland (NTEB/G), the dependent variables, and initial weight (IW), final weight (FW), total weight gained (TWG) and total feed consumed (TFC), the independent variables, were not linear. In addition, neither the weight nor feed consumption independent variables were good predictors of TEB size or number in the glands analyzed.

However, in the 2 week experiment, when litter pairs were conserved and threshold limits were imposed (paired T-test and Wilcoxon matched-pairs signed-ranks test), the mean MTEB area values of the No. 2 and No. 3 thoracic glands were tested and found consistently significant for IW and TFC in the hypothesized direction, i.e., those mice with higher IWs and TFC had larger TEBs. The independent variables of FW and TWG were not consistently significant in either experiment and therefore no definitive conclusions could be made concerning the effect of these variables on TEB development.

The mean NTEB/G values in the No. 3 and No. 4 inguinal glands were significant or approached significance for FW, TWG, and TFC in the negative direction; i.e., mice with lower

FW, TWG, and TFC had larger NTEB/G with areas of ≥ .03 mm^2.

By the end of the 3 week experiment mammary gland development in the 6 week old mice is strongly influenced by hormones (estrogen and progesterone) secreted by the ovary. During this "pubertal" growth period the TEBs are decreasing in number and regressing into TEDs (Chapter 4). This regression is intimately associated with: 1) the onset of estrous, 2) the expanding ductal network, and 3) the spatial limits of the mammary gland fat pad. The ability of these factors to override the influence of weight and feed consumption on mean MTEB area and number TEB/G results in a consistent lack of significance between mean MTEB area and number, and the independent variables in several of the analyses. The lack of significance at 6 weeks of age is also related to asynchronous development of the TEB (Chapter 4). The TEBs in the No. 2, No. 3 and No. 4 glands have already reached their maximum size by 6 weeks of age and therefore, the effect of the independent variables on TEB development is not as strong at 6 weeks of age as it is at 5 weeks of age. Moreover, weight and feed consumption begin to equalize numerically amongst litter mates by 6 weeks of age adding to the homogeneity observed in the numerical data. In the 3 week experiment, the mean NTEB/G showed no consistent trend for direction or significance in the statistical analyses performed.

Analysis of the rate of growth of the Nu/+ mice during the juvenile, prepubertal and pubertal growth periods shows

that the majority of mice reach their greatest rate of growth during the juvenile growth period. This rapid growth rate often extends into the prepubertal growth period and levels off by the pubertal growth period. These results correspond to previously reported growth rates for other species of mice during these particular growth periods.

Introduction

The effect of high and low fat or no fat diets on ductal expansion in the immature and mature mouse mammary gland has been well documented in the literature (Knazek et al., 1980; Miyamoto-Tiaven et al., 1981; Welsch et al., 1985 and Welsch and O'Connor, 1989; and Faulkin et al., 1986.) In all of these studies, it was concluded that linoleate, a polyunsaturated fatty acid, is essential for normal growth and development of the mammary gland. In 1986, Faulkin and his colleagues showed that immature mice (3 to 9 weeks of age) fed hydrogenated cottonseed oil (HCTO), which does not contain linoleate, had slower mammary gland growth, when compared to mice fed corn oil (CO), which contains approximately 60% linoleate. In addition to examining the mammary glands, they also examined the ovaries in these mice and found that the mice fed HCTO did not develop corpora lutea, whereas the mice fed CO did. From this study, Faulkin concluded that the effect of dietary fat on the developing mouse mammary gland was secondary to its primary effect on the maturation of the ovary and hence the secretion of the ovarian hormones, estrogen and progesterone.

In 1989, Welsch and O'Connor not only looked at the effect of different types of dietary oils on the development of the immature mouse mammary gland but also examined the effect of different percentages of dietary oils, individually and in combination, on mammary gland development. In one

experiment, they fed 8 different diets consisting of 5% corn oil, 20% corn oil, 20% olive oil, 19% coconut oil:1% corn oil, 20% lard, 19% beef tallow: 1% corn oil, 19% menhaden oil:1% corn oil to immature mice (21 to 45 days of age). In order to insure synchronous development of the mammary gland in mice ovariectomized at 35 days of age, they gave them estradiol-17ß plus progesterone injections for three consecutive days prior to euthanasia. The results of this study showed that no significant difference in ductal expansion existed between the mice fed vegetable versus animal fat diets. However, a significant decrease in ductal expansion was observed in those mice fed the fish oil diet and a numerical decrease reaching near significance ($p<.07$) was observed in those mice fed a low fat diet (5% corn oil) versus a high fat diet (20% corn oil).

The purpose of the present study was to examine the effect of body weight, specifically, initial weight, total weight gained and final weight, and total feed consumed on TEB development by examining the maximum size and number of TEB structures present at the peripheral leading edge of the expanding ductal tree in the mouse mammary gland during the prepubertal-pubertal growth period.

Materials and Methods

Animals. Sixteen litters of Nu/+ female mice (N = 40 mice) in the 2 week experiment and sixteen litters (N = 35 mice) in the 3 week experiment were used in this study. The

F_1 generation was obtained from parental strains, composed of a Nu/Nu male and a Nu/+ female. The Nu/+ females were individually caged and housed in a temperature controlled environment at 21 ± 1°C on a 12 hour light, 12 hour dark exposure cycle.

Diet. A semisynthetic high fat diet containing 20% corn oil (60% linoleate) was used for maximum growth and development of the mammary gland and ovaries (Welsch et al., 1985; Faulkin et al., 1986). It was prepared on a weekly basis and stored in plastic bags at -20°C prior to use. The high fat diet was composed of 20% corn oil, 20.17% casein, 0.35% DL-methionine, 32.18% dextrose, 16.09% sucrose, 4.13% AIN salt mixture, 1.18% AIN vitamins, and 5.90% cellulose. The mice were fed a pre-weighed amount of the high fat diet daily (usually 5.0 g) and had unlimited access to water. To monitor feed consumption, all unconsumed feed was weighed at the end of every 24 hour interval and recorded. The mice were fed at the same time every day, and body weights were recorded twice a week to monitor growth rate as well as weight gain.

Experimental Design. In both the 2 and 3 week diet experiments the mice were weaned and weighed (initial weight), at 21 days of age and fed a high fat, non-restricted intake diet, consisting of 20% corn oil, for 14 and 21 days, respectively. During the study, individual body weights were recorded for each mouse every 3 days to monitor weight gain. At the end of the 2 and 3 week experiments the mice were weighed (final weight) anesthetized with ether and

euthanatized by cervical dislocation. The right and left No. 2 and No. 3 thoracic and No. 4 inguinal glands were removed for whole mount analysis.

Whole Mount Evaluation. The left and right No. 2, No. 3, and No. 4 mammary glands were removed and fixed in a 3:1 solution of 100% ethanol:glacial acetic acid for approximately 1 hour (Banerjee, et al, 1976). Fixation was followed by a 15 minute wash in 70% ethanol, a 5 minute wash in distilled water, and overnight staining in alum carmine (Sigma Chemical Co.). The following day, the mammary glands were placed in a graded series of ethanol solutions, 70%, 95%, and 100%, respectively, for 15 minutes each. Alcohol dehydration was followed by a 15 minute wash in toluene. The mammary glands were stored in methyl salicylate at room temperature prior to evaluation.

Quantitative Analysis of the Terminal End Bud. The maximum growth of the TEB structure was assessed by measuring the area, in mm^2, of the TEBs at the peripheral leading edge of the advancing ductal tree. The TEB areas were measured from whole mount mammary gland preparations using a computer-assisted image analyzer. The five largest TEB areas in each gland were averaged to obtain the mean maximal terminal end bud (MTEB) area value. This dependent variable value was then used to compare TEB development between glands within animals of the same and different age groups as a function of body weight and total feed consumed. In addition to measuring the TEB area, the number of TEB structures with an area $\geq .03$ mm^2

(the average size of a TED structure in this study was .02 mm^2) at the leading edge of the advancing ductal tree was counted and the mean number of TEBs per gland (NTEB/G) was analyzed for significance against the independent variables.

Statistical Analysis. Analysis of the empirical data gathered in this study consisted of analyzing two major dependent variables, mean MTEB area and number of TEBs per gland, as well as the weight of the number (No.) 4 inguinal gland and the distance of ductal expansion in the No. 4 inguinal gland, against 4 major independent variables, namely, initial weight, total weight gained, final weight and total feed consumed. The dependent variables were analyzed for significance at $p \leq .05$. A Pearson correlation test and multiple regression analyses were used to test the independent variables for linearity. A one way analysis of variance (ANOVA) was used to test for within and between group differences and the paired T-Test and Wilcoxon matched-pairs signed-ranks test were used to analyze paired data from each litter.

Results

Weight Gain During the Prepubertal-Pubertal Growth Period. In both the 2 week and 3 week studies, the greatest post-weaning weight gain in the Nu/+ mice occurred during the juvenile and prepubertal growth periods, at 21 to 35 days of age, respectively.

Growth charts for each litter were made to monitor the rate of growth and weight gain in the juvenile, prepubertal and pubertal growth periods (Figures 5.1 and 5.2). Each line on the growth chart corresponds to the pattern of individual weight gained by a particular mouse in a specific litter. The rate of growth during the juvenile (21-28 days), prepubertal (29-35 days), and the pubertal (36 - 42 days in this study) growth periods was determined by calculating the slope of the line (S_L) for each 7 day growth period (Tables 5.1 and 5.2). The growth period with the greatest rate of weight gain in this study was the juvenile growth period. In the prepubertal growth period, there was a numerical decrease in the overall rate of weight gained but many mice maintained their juvenile growth rate during this period. However, by the onset of puberty, around 5 weeks of age, the slope of the line began to level out and the S_L values became very small. This sudden change in the character of the slope indicates that the rate of weight gain in the majority of Nu +/ mice levels off during the pubertal growth period.

The greatest variation in the rate of weight gain amongst individual mice occurred in the prepubertal growth period. During this growth period, 12/35 mice in the 2 week experiment and 8/35 mice in the 3 week experiment had weight gains equal in magnitude to that of the juvenile growth period. At the opposite extreme, only one mouse of the 35 mice in the 3 week experiment had a weight gain in the pubertal growth period

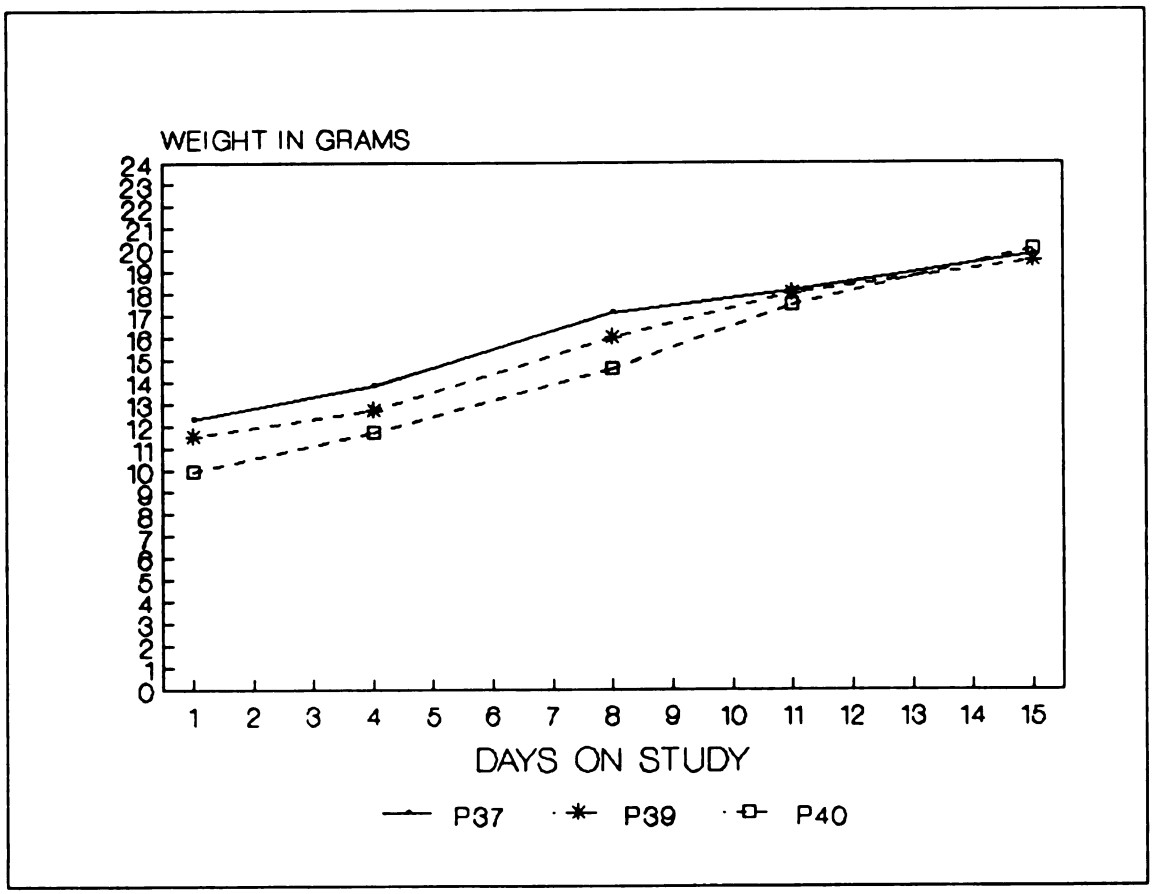

Figure 5.1. A representative growth chart from the 2 week experiment showing the individual weights recorded during the juvenile and prepubertal growth periods for each mouse in the litter. The letter (P) refers to a specific litter and the numbers (37, 3, 40) refer to individual mice in the litter.

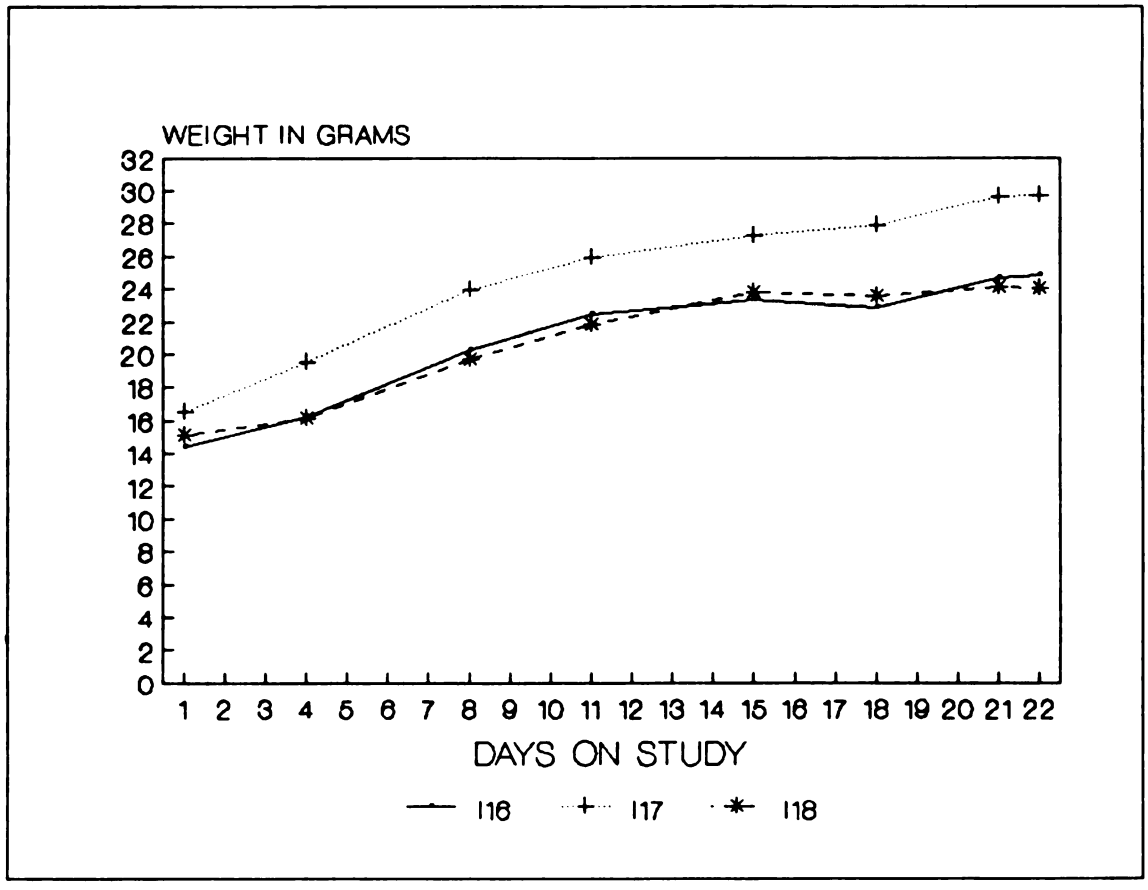

Figure 5.2. **A representative growth chart from the 3 week experiment showing the individual weights recorded during the juvenile, prepubertal and pubertal growth periods for each mouse in the litter. The letter (I) refers to a specific litter and the numbers (16, 17, 18) refer to individual mice in the litter.**

Table 5.1 Rate of Growth for Mice during the Juvenile to Prepubertal Growth Periods

	Litter							
	A	B	C	D	E	F	G	H
Animal-GP								
1 - 1	.69[a]	.79	.71	.96	.73	.41	.40	.76
1 - 2	.67	.69	.66	.71	.64	.47	.70	.90
2 - 1	.56	.74	.53		.71	.20	.50	.64
2 - 2	.87	.88	.44		.71	.47	1.10	.71
3 - 1	.56					.54		.71
3 - 2	.67					.51		.70
								.84
4 - 1	.67							.46
4 - 2	.70							

GP (Growth Period) 1 = Juvenile
GP 2 = Prepubertal
[a] = Slope Values from Individual Growth Charts

Table 5.1 (continued)

	Litter							
	I	J	K	L	M	N	O	P
Animal-GP								
1 - 1	.91[a]	.69	.19	.57	.60	.74	.36	.69
1 - 2	.36	.69	.63	.70	.71	.80	.67	.39
2 - 1		1.01		.51	.63	.47	.32	.66
2 - 2		.63		.71	.60	.77	.70	NA
3 - 1		.71		.61	.79			.64
3 - 2		.94		.50	.71			.50
								.67
4 - 1					.66			.77
4 - 2					1.03			

GP (Growth Period) 1 = Juvenile
GP 2 = Prepubertal
[a] = Slope Values from Individual Growth Charts
NA = Animal eliminated from study
N = 40

Table 5.2 Rate of Growth for Mice during the Juvenile to Pubertal Growth Periods

	Litter							
	A	B	C	D	E	F	G	H
Animal-GP								
1 - 1	1.23[a]	1.00	.66	.50	.31	.60	.49	.81
1 - 2	.36	.70	.41	.41	.64	.52	.57	.42
1 - 3	.20	.11	.44	.10	.34	.20	.17	.25
						.89		
2 - 1	1.06	.80				.44		
2 - 2	.54	.57				.31		
2- 3	.37	.31						
						.79		
3 - 1		.84				.70		
3 - 2		.41				.16		
3 - 3		.06						
						.87		
4 - 1						.56		
4 - 2						.26		
4 - 3								
5 - 1								
5 - 2								
5 - 3								

GP (Growth Period) 1 = Juvenile
GP 2 = Prepubertal
GP 3 = Pubertal
[a] = Slope Values from Individual Growth Charts

Table 5.2 (continued)

	Litter							
	I	J	K	L	M	N	O	P
Animal-GP								
1 - 1	.83[a]	.90	.90	.46	.73	.89	.65	.67
1 - 2	.44	.63	.31	.37	.30	.29	.40	.26
1 - 3	.21	.31	.21	.06	.31	.26	.26	.30
2 - 1	1.06	.73	.87		.73	.89	.79	
2 - 2	.47	.66	.73		.30	.52	.36	
2 - 3	.35	.32	.29		.26	.11	.51	
3 - 1	.66	.83	1.01			.69		
3 - 2	.59	.70	.53			.71		
3 - 3	.03	.16	.19			.20		
4 - 1						.61		
4 - 2						.40		
4 - 3						.30		
5 - 1						.74		
5 - 2						.42		
5 - 3						.24		

GP (Growth Period) 1 = Juvenile
GP 2 = Prepubertal
GP 3 = Pubertal
[a] = Slope Values from Individual Growth Charts
N = 35

which was greater than the prepubertal growth period. Since the 2 week experiment only analyzed growth over the juvenile and prepubertal growth periods, no comparisons could be made between the 2 and 3 week experiments for the pubertal growth period.

The results of this analysis for Nu/+ mice agree with previously reported analyses for other species of mice. Overall 41% of the Nu/+ mice, 10/35 in the 2 week experiment and 25/35 in the 3 week experiment, had their maximum growth spurt during the juvenile growth period (consistent with the onset of allometric growth period). However, 27% of the Nu /+ mice in this study maintained their maximum growth rate throughout the prepubertal period, i.e., 12/35 in the 2 week experiment and 8/35 in the 3 week experiment.

If one compares the mean MTEB area calculated for the prepubertal and pubertal growth periods (Chapter 4) to the slope values for each growth period, there appears to be a linear relationship between maximum TEB size and the rate of weight gained. In this study, the mean MTEB area in all 3 glands measured reach their maximum size at the end of the prepubertal growth period (at approximately 5 weeks of age) followed by a numerical decrease in mean MTEB area between 5 and 6 weeks of age which corresponds to the initial decline in the rate of weight gain by the average mouse.

<u>The Relationship of Mean MTEB Area to Body Weight and Feed Consumption.</u> In this study, the mean maximum terminal end bud area was used to determine the relationship between

TEB size and the independent variables of initial weight (IW), total weight gained (TWG), final weight (FW), and total feed consumed (TFC).

A Pearson correlation test, in which the independent variables IW, TWG, FW, and TFC were correlated with the mean MTEB area for each of the six glands (No. L2, No. R2, No. L3, No. R3, No. L4 and No. R4), showed that none of the independent variables were consistently or strongly correlated with gland area in either the 2 week or 3 week experiments (Table 5.3). However, significant correlation coefficients were found between mean MTEB area and TWG, and nearly significant correlation coefficients were found between mean MTEB area and FW. Here the correlation between the mean MTEB area for the LNo. 2 gland and TWG was significant in the hypothesized direction (positive direction) in both the 2 and 3 week experiments. The correlation between mean MTEB area for the LNo. 2 gland and FW was also significant in the positive direction in the 2 week experiment.

In the 3 week experiment, the correlation coefficient between the mean area for the LNo. 3 gland and IW was significant in the positive direction. The correlation between the mean area for the RNo. 3 gland and TWG was significant opposite the hypothesized direction (negative direction). The overall lack of consistent correlations between the glands and independent variables indicates that the relationship between these independent variables and the mean MTEB area is not linear.

Table 5.3 Pearson Correlation Coefficients of the Mean MTEB Area (mm^2) with Independent Variables in the 2 and 3 Week Experiments

Gland	IW		FW		TWG		TFC	
	2 Week	3 Week	2 Week	3 Week	2 Week	3 Week	2 Week	3 Week
L2	.03	-.15	.23**	.12	.26*	.30*	.06	.02
R2	-.08	-.11	.06	.09	.15	.22	-.03	.04
L3	.01	.22**	.03	.10	.03	-.16	-.04	.15
R3	.12	.20	.14	-.06	.07	-.32*	.03	.04
L4	-.03	.06	-.01	-.09	.02	.17	-.08	-.11
R4	-.08	.21	-.10	.03	-.04	-.21	-.14	.02

N = 39 for 2 week experiment
N = 35 for 3 week experiment
* $p \leq .05$
* * $.06 \leq p \leq .09$

Table 5.4 Multiple Regression Analysis for Independent Variables and Gland Area in the 2 Week Experiment

Variable	Gland L2		Gland R2		Gland L3		Gland R3		Gland L4		Gland R4	
	B	Beta	B	Beta	B	Beta	B	Beta	B	Beta	B	Beta
IW	.177 (.09)	16.2	.14 (.10)	12.1	.16 (.10)	13.8	.16 (.14)	10.5	.12 (.08)	14.0	-.10 (.07)	12.3
FW	-.177 (.09)	-18.5	-.14 (.10)	-13.9	-.16 (.10)	-15.9	-.16 (.14)	-11.9	-.12 (.08)	-16.1	-.11 (.07)	-14.3
TWG	.177 (.09)	16.4	.14 (.10)	12.3	.16 (.10)	13.8	.16 (.14)	10.4	.12 (.08)	14.0	.11 (.07)	12.3
TFC	.00 (.00)	.02	.00 (.00)	-.02	.00 (.00)	.10	.00 (.00)	.09	.00 (.00)	.03	.00 (.00)	.00
K	.067		.12		.12		.08		.08		.10	
$AdjR^2$	.00		-.01		.02		-.06		.01		.06	
F	.99		.94		1.22		.49		1.12		1.60	

() = Standard errors of B.
B = Intercept value of regression line
Beta = Standardized regression coefficient
K = Constant
$AdjR^2$ = Coeffiecient of determination
F = F value
N = 39

Table 5.5 Multiple Regression Analysis of Independent Variables and Gland Area in the 3 Week Experiment

Variable	Gland L2		Gland R2		Gland L3		Gland R3		Gland L4		Gland R4	
	B	Beta	B	Beta	B	Beta	B	Beta	B	Beta	B	Beta
IW	-.05 (.03)	-8.3	-.06 (.04)	-6.9	-.05 (.05)	-4.8	-.05 (.05)	-5.0	.01 (.03)	2.4	.01 (.03)	1.7
FW	.05 (.03)	8.2	.06 (.04)	6.7	-.05 (.05)	4.9	.05 (.05)	4.9	-.01 (.03)	-2.4	.00 (.03)	-1.6
TWG	-.05 (.03)	-6.7	-.06 (.04)	-5.6	-.05 (.05)	-4.3	-.05 (.05)	-4.5	.01 (.03)	1.9	.00 (.02)	1.2
TFC	.00 (.00)	.02	.00 (.00)	-.01	.00 (.00)	.13	.00 (.00)	.08	.00 (.00)	-.07	.00 (.00)	.03
K	.04		.04		.07		.11		.06		.05	
$AdjR^2$	.06		-.01		-.02		.03		-.09		-.06	
F	1.5		.88		.86		1.2		.33		.51	

() Numbers in parentheses are standard errors of B.
B = Intercept value of regression line
Beta = Standardized regression coefficient
K_2 = Constant
$AdjR^2$ = Coefficient of determination
F = F value
N = 35

To further test if one or more of the independent variables were good predictors of TEB area, a multiple regression analysis was done. (Table 5.4 and 5.5) All of the independent variables together only accounted for up to 6% of the variance (adjusted R square values) in the regression equation in the 2 week experiment and up to 9% in the 3 week experiment. In addition, none of the F values, associated with the various gland areas, were significant in either experiment. Therefore, these analyses confirmed that, in addition to not having a linear relationship with mean MTEB area individually, taken together the independent variables are not good predictor variables of TEB size.

A one way ANOVA was used to examine the relationship between mean MTEB area and high, medium and low groups within each independent variable in both experiments. High, medium and low weight groups as well as large, medium and small feed consumption groups were derived from frequency plots obtained for each of the independent variables. Natural breaks between data points and the numerical spread between high and low values within a group were used as guidelines for determining the divisions. None of the ANOVA analyses for IW, FW, TWG, and TFC (Tables 5.6, 5.7, 5.8 and 5.9) were significant at $p \leq .05$ for mean MTEB area. However, consistent numerical trends were observed in both experiments. For example, in the 2 week diet experiment, mice in the medium FW category had the largest mean MTEB area values for all six glands and mice in the high and low FW categories had the lowest mean MTEB areas

Table 5.6 ANOVA of the Mean MTEB Area (mm^2) by the High, Medium, and Low Initial Weight Categories

	2 Week Experiment			3 Week Experiment		
Gland	High	Medium	Low	High	Medium	Low
L2	.074	.070	.077	.048	.048	.056
R2	.074	.078	.075	.054	.053	.062
L3	.085	.085	.087	.095	.081	.085
R3	.091	.090	.084	.080	.079	.091
L4	.053	.056	.057	.049	.048	.046
R4	.052	.058	.061	.052	.049	.044

N = 38 for 2 Week Experiment
N = 35 for 3 Week Experiment

Table 5.7 ANOVA of the Mean MTEB Area (mm^2) by the High, Medium, and Low Final Weight Categories

	2 Week Experiment			3 Week Experiment		
Gland	High	Medium	Low	High	Medium	Low
L2	.073	.077	.064	.056	.046	.050
R2	.069	.084**	.069	.055	.051	.065
L3	.076	.091	.081	.099	.079**	.085
R3	.085	.096	.075	.088	.073	.087
L4	.051	.059	.051	.049	.044	.049
R4	.052	.058	.052	.053	.044	.053

N = 40 for 2 Week Experiment
N = 35 for 3 Week Experiment
** = Group means differ $.06 \leq p \leq .09$ within experiment

Table 5.8 ANOVA of the Mean MTEB Area (mm^2) by the High, Medium, and Low Total Weight Gained Categories

	2 Week Experiment			3 Week Experiment		
Gland	High	Medium	Low	High	Medium	Low
L2	.076	.071	.072	.057	.049	.048
R2	.072	.082	.073	.054	.052	.068
L3	.090	.085	.080	.086	.083	.090
R3	.093	.094	.080	.073	.084	.086
L4	.058	.058	.050	.046	.049	.047
R4	.052	.055	.061	.048	.049	.047

N = 40 for 2 Week Experiment
N = 35 for 3 Week Experiment

Table 5.9 ANOVA of the Mean MTEB Area (mm^2) by the High, Medium, and Low Total Feed Consumed Categories

	2 Week Experiment			3 Week Experiment		
Gland	High	Medium	Low	High	Medium	Low
L2	.073	.071	.076	.054	.049	.054
R2	.081	.070	.082	.057	.056	.056
L3	.081	.088	.083	.084	.081	.096
R3	.085	.089	.093	.086	.079	.087
L4	.053	.054	.060	.044	.050	.048
R4	.053	.055	.059	.048	.048	.050

N = 40 for 2 Week Experiment
N = 35 for 3 Week Experiment

resulting in an inverted "U" distribution. This trend is substantiated by the near significance observed "between groups" for the mean area of the RNo. 2 gland.

In the 3 week experiment, mice in the medium FW category had the smallest mean MTEB area values for all six glands and mice in the low and high FW categories had the highest mean MTEB areas resulting in a "U" distribution. This trend is substantiated by the near significance observed "between groups" for the mean area of the LNo. 3 gland (Table 5.7).

The one tailed paired T-test and Wilcoxon matched-pairs signed-ranks test were selected to examine differences between litter mates using paired data, in which litter pairs were conserved. By conserving litter pairs and using the numerical "difference" between the high and low independent variable values within a specific litter for analysis, the genetic variability between mice was decreased.

In the one tailed paired T-test, the litter mates were divided into high and low weight and feed consumption groups and the differences were analyzed against the mean MTEB area. Of the 32 litters used in the study (16 in the 2 week experiment and 16 in the 3 week experiment), a number were deleted from the analysis because 1) they contained only 1 mouse or 2) there was an insufficient numerical difference between the high and low independent variable group values within the litter. The results of the paired T- test for the 2 week and 3 week experiments for IW are presented in Table 5.10. In the 2 week experiment, 10 litters had sufficient

numerical differences in IW ranging from 0.5 grams to 2.6 grams. The analysis showed that at 5 weeks of age mice with the larger IWs had larger mean MTEB area values in 3 out of 4 of the thoracic glands, compared to mice with lower IWs in the same litter. In the 3 week experiment, the mice in 10 litters were analyzed and none of the mean areas were significantly different for IW. Significant findings were limited due to large standard deviations for some groups, particularly the high IW groups.

In examining the relationship between litter mates with sufficient numerical differences in final weight (FW), the mean MTEB area values were not statistically significant for any of the glands in either the 2 or 3 week experiments (Table 5.10). The lack of significant findings was directly associated with the homogeneity in FW values amongst mice in each litter.

In the paired T-test for total weight gained (TWG), values for mice in 12 out of 16 litters were analyzed in the 2 week experiment and none of the mean MTEB areas were significantly different. In the 3 week experiment, the mice in 10 out of 16 litters had numerical differences in TWG ranging from 0.3 grams to 4.3 grams. The analysis showed a trend toward significance in the mean MTEB area of the No. 2 thoracic glands ($.07 \leq p \leq .09$) but in the negative direction, i.e., the mice with lower TWGs had larger mean MTEB areas when compared to mice with higher TWGs (Table 5.11). This trend in the No. 2 gland may be associated with a curtailment in the

Table 5.10 Paired T-Test Comparison of Mean MTEB Area (mm^2) by IW and FW

Gland	IW				FW			
	2 Week		3 Week		2 Week		3 Week	
	High	Low	High	Low	High	Low	High	Low
L2	.077*	.066	.051	.060	.082	.076	.049	.056
R2	.078	.072	.097	.060	.077	.075	.057	.066
L3	.093*	.076	.089	.091	.087	.085	.087	.083
R3	.098*	.077	.080	.083	.088	.093	.075	.079
L4	.057	.049	.047	.047	.054	.057	.046	.044
R4	.059	.050	.048	.043	.054	.061	.048	.046
	(N = 20)		(N = 20)		(N = 20)		(N = 20)	

* $p \leq .05$
High and Low means differ within week.

Table 5.11 Paired T-Test Comparison of Mean MTEB Area (mm^2) by TWG and TFC

Gland	TWG				TFC			
	2 Week		3 Week		2 Week		3 Week	
	High	Low	High	Low	High	Low	High	Low
L2	.081	.078	.049	.057**	.082**	.071	.044	.059*
R2	.079	.075	.054	.067**	.078	.072	.052	.061*
L3	.087	.092	.079	.084	.082	.083	.080	.083
R3	.097	.100	.080	.077	.093	.097	.077	.077
L4	.057	.060	.044	.046	.057	.053	.041	.047*
R4	.055	.065	.046	.047	.055	.053	.041	.048
	(N = 22)		(N = 20)		(N = 16)		(N = 16)	

* $p \leq .05$
** $.07 \leq p \leq .09$
High and Low means differ within week.

overall maturation and development of the reproductive organs (ovary and mammary glands) as a function of TWG and hence the prolonged appearance and presence of larger TEB structures instead of TEDs.

The last independent variable to be tested, total feed consumed (TFC), was difficult to analyze because of the inability to control inadvertent feed loss, i.e., feed loss due to movement into and out of the feed jars as well as defecation and urination into the feed jars. In the 2 week experiment, the values for mice in 8 out of 16 litters were analyzed and there were no statistically significant differences in mean areas. However a nearly significant result between groups for the mean MTEB area of the LNo. 2 gland was present (Table 5.11). In the 3 week experiment, values for the same number of litters were analyzed and the mean MTEB areas for the No. 2 thoracic glands and the LNo. 4 inguinal gland were significantly different but in a negative direction, i.e., the higher TFC group had smaller mean MTEB areas at 6 weeks of age. As in the 2 week experiment, this trend in the No. 2 gland and the No. 4 gland may be associated with the overall maturation and development of the reproductive organs. At 6 weeks of age those mice which have consumed adequate amounts of feed should be maturing sexually at a normal rate. Therefore, based on Chapter 4 results, one would expect that the group consuming an adequate or increased amount of feed would have a larger number of TEDs, consistent with ovarian maturation and hormone secretion.

The final statistical test used to analyze the effect of the body weight and total feed consumption on TEB size was the Wilcoxon matched-pairs signed-ranks test. The purpose of conducting this test was to impose a threshold value on the independent variables, and examine whether or not a "threshold effect" existed for any of these variables. The threshold value was defined as the numerical difference between high and low litter mates of $\geq$ 10% of the grand mean for the particular independent variable being tested. In the 2 week experiment, the mice in 8 out of 16 litter pairs met the threshold requirement for IW. The mean areas from the LNo. 2, LNo. 3 and RNo. 3 thoracic glands were significantly different and the mean area from the RNo. 2 thoracic approached significance at p=.09 all in the positive (hypothesized) direction (Table 5.12). In the 3 week experiment, there was less variation in IW and only 4 out of 16 litter pairs met the threshold requirement. Therefore, statistical analysis was not applicable for this variable.

A high degree of homogeneity among litter pairs was found for FW in both the 2 and 3 week experiments. The mice in 6 out of 16, and 5 out of 16, litters met the threshold requirements for the Wilcoxon matched-pairs signed-ranks test analysis in the 2 and 3 week experiments, respectively. However, in the 2 week experiment, only the mean area of the LNo. 2 gland was significant in the positive direction. In the 3 week experiment, the mean area for the LNo. 4 gland was significant and the mean area of the RNo. 4 gland approached

significance (p=.065) both in the positive direction (Table 5.12).

In analyzing TWG, the mice in 10 out of 16 litters met the threshold requirement in the 2 week experiment. The results of the analysis showed that there were no statistically significant differences in mean area but the mean area of the RNo. 2 gland approached significance at p=.075 in the positive direction, i.e., the mice with the higher TWGs had larger mean MTEB areas. In the 3 week experiment, mice in 8 out of 16 litters met the threshold requirement and the mean area of the No. 2 thoracic glands were significantly different but in the negative direction, i.e., the mice with smaller TWGs had larger mean MTEB areas (Table 5.13).

In analyzing total feed consumed (TFC), the mice in 8 out of 16 litters met the threshold requirement in the 2 week experiment. A statistically significant difference between high and low feed consumption within a litter was found for the mean area of the LNo. 2 gland and nearly significant results were found in the test of the mean area of the RNo. 2 gland (p=.06); both in the positive direction. In the 3 week experiment, mice in 5 out of 16 litters were analyzed and the mean areas of the No.2 thoracic and LNo. 4 glands were statistically significant but in the negative direction (Table 5.13). The results of the Wilcoxon matched-pairs signed-ranks test bolstered the findings for TFC in the paired T-test even though the sample size was smaller; indicating that

Table 5.12 Wilcoxon Matched-Pairs Signed-Ranks Test of Mean MTEB Area (mm^2) by IW and FW

Gland	IW				FW			
	2 Week		3 Week		2 Week		3 Week	
	High	Low	High	Low	High	Low	High	Low
L2	.075	.062*	.049	.058	.089*	.077	.049	.052
R2	.076	.064**	.055	.062	.081	.074	.056	.066
L3	.089	.075*	.092	.095	.085	.089	.093	.074
R3	.096	.075*	.082	.099	.095	.094	.078	.076
L4	.053	.047	.052	.058	.059	.056	.047	.041*
R4	.054	.049	.046	.051	.052	.059	.053	.043**
	(N_p = 8)		(N_p = 4)		(N_p = 6)		(N_p = 6)	

N_p = Number of pairs
* $p \leq .05$
** $.07 \leq p \leq .09$
High and Low means differ within week.

Table 5.13 Wilcoxon Matched-Pairs Signed-Ranks Test of Mean MTEB Area (mm^2) by TWG and TFC

Gland	TWG				TFC			
	2 Week		3 Week		2 Week		3 Week	
	High	Low	High	Low	High	Low	High	Low
L2	.082	.077	.048	.059*	.082*	.066	.048	.062*
R2	.079**	.073	.054	.071*	.078*	.069	.057	.066*
L3	.087	.092	.076	.086	.082	.083	.089	.086
R3	.100	.097	.080	.079	.093	.086	.084	.083
L4	.059	.057	.046	.049	.057	.053	.044	.052*
R4	.055	.063	.047	.049	.055	.053	.046	.054
	(N_p = 10)		(N_p = 8)		(N_p = 8)		(N_p = 5)	

* $p \leq .05$
** $.06 \leq p \leq .09$
High and Low means differ within the week.

significant differences in mean MTEB area at 5 and 6 weeks of age are more easily distinguishable when threshold values are used.

The Relationship of the Number of TEBs per Gland to Body Weight and Feed Consumption. The results of a Pearson correlation test in which the independent variables IW, TWG, FW and TFC were correlated with the mean number of TEBs per gland are presented in Table 5.14. The mean number of TEBs per gland (NTEB/G) was calculated from the number of TEBs with an area of $\geq .03$ mm^2, at the peripheral leading edge of the expanding ductal tree. Because the average TED measured between .01-.02 mm^2, a minimal value of $\geq .03$ mm^2 for the TEB count was selected. In the 2 week experiment, there was one significant positive correlation between the mean NTEBs in the RNo. 4 gland and one significant negative correlation between mean NTEBs in the RNo. 2 gland and IW. In analyzing FW, TWG, and TFC significant negative correlations were found for the mean NTEBs in the RNo. 2, LNo. 4 and RNo.4 glands respectively. No definitive conclusions could be made from this analysis due to the mixed findings (positive and negative correlations).

In the 3 week study, the mean NTEB/G showed significant or nearly significant positive correlations with IW, FW and TWG in the No. 2 thoracic glands. In contrast significant negative correlations were present with FW and TWG with the mean NTEBs in the LNo. 3 thoracic gland. The positive correlations indicate that mice with smaller initial weight,

Table 5.14 Pearson Correlation Coefficients of the Number of TEBS per gland with Independent Variables in the 2 and 3 Week Experiments

Gland	IW		FW		TWG		TFC	
	2 Week	3 Week	2 Week	3 Week	2 Week	3 Week	2 Week	3 Week
L2	.16	.29*	.01	.40**	.15	.12	-.07	-.03
R2	-.24**	.28*	-.26**	.50*	-.05	.25**	-.08	.00
L3	.17	-.11	.03	-.35*	-.13	-.28*	-.15	-.06
R3	.16	.00	.08	-.05	-.07	-.06	.13	-.03
L4	-.11	.12	-.14	.10	-.26*	-.04	-.09	.02
R4	.27*	.19	-.19	.16	-.47*	-.04	-.40*	.05

N = 38 for 2 week experiment
N = 35 for 3 week experiment

* $p \leq .05$
* * $.06 \leq p \leq .09$

total weight gained, and final weight have a smaller NTEB/G; recall in Chapter 4 that the NTEBs in the No. 2 thoracic glands decreased dramatically between 5 and 6 weeks of age. The significant negative correlation coefficient for FW and TWG in the LNo. 3 thoracic gland is a reflection of the larger number of TEB structures still present at 6 weeks of age in this gland.

A multiple regression analysis was used to further define the relationship between the mean NTEB/G and the various body weight and feed consumption variables. The results of the multiple regression analysis are presented in Table 5.15 and 5.16. In both the 2 and 3 week experiments the independent variables accounted for up to 23 % of the variance (adjusted R squared value) in the regression equation. The mean number of TEBs for the No. 4 inguinal gland had significant or nearly significant F values in the 2 week experiment. In the 3 week experiment, the mean NTEB for the No. 2 thoracic glands had significant or nearly significant F values. The results of the multiple regression analysis indicate that, like the mean MTEB area, none of the independent variables are good predictors of mean NTEB/G. However, in certain cases a linear equation with all four independent variables can be used to predict mean NTEBs in the inguinal glands at 2 weeks and in the No. 2 thoracic glands at 3 weeks.

The paired T-test was used to conserve litter pairs and examine differences within a litter for the mean NTEB/G with each of the independent variables. The results of the paired

Table 5.15 Multiple Regression Analysis for the Independent Variables and Number of TEB per Gland in the 2 Week Experiment

Variable	Gland L2		Gland R2		Gland L3		Gland R3		Gland L4		Gland R4	
	B	Beta	B	Beta	B	Beta	B	Beta	B	Beta	B	Beta
IW	10.4 (14.4)	6.3	7.3 (17.4)	3.6	36.0 (23.2)	12.8	-.58 (24.1)	-.21	29.2 (12.1)	19.3	11.1 (8.3)	9.9
FW	-10.1 (14.4)	-7.0	-7.9 (17.4)	-4.4	-35.8 (23.2)	-14.5	-.90 (24.1)	.37	-29.2 (12.1)	-21.9	-10.9 (8.3)	-11.1
TWG	9.9 (14.4)	6.3	7.6 (17.4)	3.8	34.9 (23.2)	12.5	-1.3 (24.1)	-.46	28.7 (12.1)	19.1	10.6 (8.3)	9.5
TFC	.01 (.13)	.02	.02 (.16)	.02	.04 (.22)	.36	.21 (.22)	.20	.10 (.11)	.17	-.08 (.07)	-.19
K	7.9		20.0		-5.8		.14		6.55		11.1	
$AdjR^2$	-.06		-.03		.05		-.06		.12		.23	
F	.45		.74		1.5		.47		2.22**		3.7*	

() Numbers in parentheses are standard errors of B.
B = Intercept value of regression line
Beta = Standardized regression coefficient
K_2 = Constant
$AdjR^2$ = Coeffiecient of determination
F = F value
N = 39
* $p \leq .05$
** $p \leq .08$

Table 5.16 Multiple Regression Analysis for the Independent Variables and Gland Number in the 3 Week Experiment

Variable	Gland L2		Gland R2		Gland L3		Gland R3		Gland L4		Gland R4	
	B	Beta	B	Beta	B	Beta	B	Beta	B	Beta	B	Beta
IW	-8.7 (6.8)	-5.9	-9.4 (7.4)	-5.5	-3.9 (.10)	7.9	-6.2 (6.6)	-4.9	-1.9 (6.3)	-1.6	-1.2 (6.8)	-.90
FW	9.4 (6.8)	6.3	10.3 (7.4)	6.0	3.4 (7.8)	2.1	6.1 (6.6)	4.8	2.1 (6.3)	1.7	1.4 (6.8)	-1.1
TWG	-8.7 (6.8)	-5.0	-9.2 (7.4)	-4.6	-4.2 (7.8)	-2.2	-6.2 (6.6)	-4.1	-2.0 (6.3)	-1.4	-1.4 (6.8)	-.90
TFC	-.06 (.05)	-.20	-.07 (.06)	-.21	.02 (.06)	.07	.00 (.05)	.03	.00 (.04)	-.02	.00 (.05)	.00
K	-4.6		-9.9		25.2		.08		4.5		2.5	
$AdjR^2$	.14		.23		.05		-.10		-.11		-.09	
F	2.3**		3.6*		1.4		.25		.15		.32	

() Numbers in parentheses are standard errors of B.
B = Intercept value of regression line
Beta = Standardized regression coefficient
K_2 = Constant
$AdjR^2$ = Coefficient of determination
F = F value
N = 35
* $p \leq .05$
** $p \leq .08$

T-test for the 2 and 3 week experiments are listed in Table 5.17 and 5.18. In the 2 week experiment for IW, values from the mice in 10 out of 16 litters were analyzed and significant differences in the mean NTEBs for the LNo. 4 gland were present in the positive direction. None of the mean NTEB/G were significant in the 3 week experiment.

In the 2 week experiment for FW, values from the mice in 10 out of 16 litter pairs were analyzed and significant differences in the mean NTEB for the RNo.3 and RNo. 4 glands were found in the negative direction. The mean NTEBs in the LNo. 4 gland was nearly significant, again in the negative direction. None of the correlations were significant in the 3 week experiment. No definite conclusions could be drawn due to the inconsistent direction of the significant correlations.

In the 2 week experiment for TWG, values from mice in 11 out of 16 litters were analyzed and the mean NTEBs for the LNo. 3 and LNo. 4 glands were significant or nearly significant in the negative direction (Table 5.18). In this analysis, the mice that gained the least weight by 5 weeks of age had a larger number of TEBs per gland. In the 3 week experiment, values from the mice in 10 out of 16 litters were analyzed and only the mean NTEBs for the LNo. 3 gland were significantly different, again in the negative direction.

Finally, in both the 2 and 3 week experiments for TFC, none of the mean NTEBs/gland were significantly different (Table 5.18). However, the mean NTEBs in the RNo. 3 gland in the 2 week experiment and the LNo. 2 gland in the 3 week

Table 5.17 Paired T-Test Comparison of Number of TEBs per gland by IW and FW

Gland	IW				FW			
	2 Week		3 Week		2 Week		3 Week	
	High	Low	High	Low	High	Low	High	Low
L2	9.3	8.4	6.7	6.1	8.8	8.5	5.9	7.5
R2	9.2	9.8	7.6	6.7	9.1	8.5	7.2	8.3
L3	9.8	6.9	12.1	13.5	7.8	10.6	11.1	11.8
R3	10.2	9.1	10.4	10.6	9.4	12.9*	10.2	10.8
L4	7.7*	5.0	7.0	6.4	5.5	6.7	6.9**	5.4
R4	6.6	6.4	6.3	6.4	5.5	7.7*	6.8	6.7
	(N = 20)		(N = 20)		(N = 20)		(N = 20)	

* $p \leq .05$
** $.06 \leq p \leq .09$
High and Low means differ within week.

Table 5.18 Paired T-Test Comparison of Number of TEBs per gland by TWG and TFC

Gland	TWG				TFC			
	2 Week		3 Week		2 Week		3 Week	
	High	Low	High	Low	High	Low	High	Low
L2	9.3	8.7	6.0	7.1	10.6	9.8	5.6	7.5**
R2	9.4	8.8	7.2	8.4	8.8	10.4	6.5	8.1
L3	6.3	10.6*	10.1	12.9*	7.6	11.4**	11.1	9.8
R3	9.2	11.7	11.4	10.2	9.8	13.1**	11.4	11.1
L4	5.5	8.3*	6.5	5.9	6.5	7.6	5.9	6.6
R4	5.9	7.5**	6.7	5.9	6.4	8.1	5.4	7.0
	(N = 22)		(N = 20)		(N = 16)		(N = 16)	

* $p \leq .05$
** $\leq .06$ $p \leq .09$
High and Low means differ within week.

experiment approached significance in the negative direction.

Correlation Between Number 4 Gland Weight, Length, Mean Maximum Terminal End Bud Area, and Number of Terminal End Bud Structures Per Gland. The numerical values for No. 4 gland length (GL) in the 3 week experiment, as measured in mm from the nipple to the leading edge of ductal expansion, correspond with those values reported by Welsch and O'Connor (1989), in 45 day old, immature Balb/c mice fed the same 20% corn oil diet. Therefore, these data suggest that Nu/+ mice have a similar rate of ductal expansion in the absence of estrogen and progesterone injections, as that reported by Welsch and O'Connor (1989) in Balb/c mice ovariectomized at 35 days and given estrogen and progesterone injections 3 days prior to euthanasia; in both studies the mice were fed the same high fat diet from weaning to 21 or 23 days, respectively.

In addition to No. 4 gland length (GL), gland weight (GW) measurements were also gathered in both the 2 and 3 week experiments. A Pearson correlation test showed that there was no significant correlation between No. 4 GW and No. 4 GL in the 2 week experiment. In the 3 week experiment, a significant negative correlation was present between No. 4 GW and GL for the LNo. 4 gland (Table 5.19). The negative "r" value (r=-.46) indicates that on average the heavier weight glands had less ductal expansion than the lighter weight glands. Therefore, while the size of the mammary gland fat pad is one factor which determines the degree of ductal expansion, a heavier mammary gland fat pad does not

Table 5.19 Pearson Correlation Coefficients of Gland Weight with Gland Length in the 2 and 3 Week Experiments

Gland Weight	Gland Length			
	2 Week		3 Week	
	L4	R4	L4	R4
L4	-.27	-.20	-.46*	-.24
R4	-.28	-.20	-.45*	-.21

N = 39 for 2 week experiment
N = 35 for 3 week experiment
* $p \leq .05$

necessarily result in greater ductal expansion.

The relationship between No. 4 GW and mean MTEB area is summarized in Table 5.20. In the 2 week experiment, a significant negative correlation was found between GW and mean MTEB area. The LNo. 4 gland and the RNo. 4 gland had negative Pearson "r" values of -.37 and -.32 respectively. These values indicate that the heavier No. 4 glands contain smaller TEB structures. No significant correlation was present between No. 4 GW and mean MTEB area in the 3 week study.

In examining the relationship between No.4 GL and mean MTEB area, no significant correlation was observed in either experiment. However, a shift in direction from positive correlations in the 2 week experiment (at 5 weeks of age), to negative correlations in the 3 week experiment (at 6 weeks of age), coincides with the decrease in mean MTEB area observed during the pubertal growth period. (Table 5.20)

In examining the relationship between No. 4 GW and mean NTEB/G in the 2 week experiment, a significant negative correlation in the LNo. 4 mean NTEBs ($r=-.56$) and a near significant negative correlation in the RNo. 4 mean NTEBs ($p=.07$, $r=-.30$) was found (Table 5.21). This indicates that the heavier No. 4 mammary glands tend to have a smaller number of TEBs per gland at 5 weeks of age. No significant correlation was present between these variables in the 3 week experiment.

A similar correlation was observed for No. 4 GL and mean NTEB/G (Table 5.21). In the 2 week experiment, a

Table 5.20 Pearson Correlation Coefficients of Mean MTEB Area with Gland Weight and Gland Length in the 2 and 3 Week Experiments

Gland	Weight L4		Weight R4		Length L4		Length R4	
	2 Week	3 Week	2 Week	3 Week	2 Week	3 Week	2 Week	3 Week
L4	-.37*	-.14	-.37*	-.13	.23	-.15	.14	-.21
R4	-.33*	-.13	-.32*	-.04	.16	-.27	.20	-.25

N = 39 for 2 week experiment
N = 35 for 3 week experiment
* $p \leq .05$

Table 5.21 Pearson Correlation Coefficients of NTEB/G with Gland Weight and Gland Length in the 2 and 3 Week Experiments

Gland	Weight L4		Weight R4		Length L4		Length R4	
	2 Week	3 Week	2 Week	3 Week	2 Week	3 Week	2 Week	3 Week
L4	.56*	.04	-.49*	.05	.36*	.02	.38*	-.11
R4	-.24	.08	-.30**	.15	.09	-.39*	.22	-.40*

N = 39 for 2 week experiment
N = 35 for 3 week experiment
* $p \leq .05$
** $07 \leq p \leq .09$

statistically significant positive correlation was found between the LNo. 4 GL (r=.36) and the mean NTEB/G. In the 3 week experiment, a significant negative correlation was present between RNo. 4 GL (r=-.3) and the mean NTEB/G. One possible explanation for this shift in correlation from positive to negative between 5 and 6 weeks is the decreasing number of TEBs $\geq .03$ mm^2; as the mammary gland tree expands and reaches the borders of the fat pad and the hormones of estrous increase, the TEBs regress into TEDs.

Discussion

Determining the effect of weight gain and feed consumption during the prepubertal-pubertal growth periods on TEB development in the mouse mammary gland is of interest for several reasons. First, because the mouse mammary gland is used as a model for studying breast cancer in women, researchers using this model have an obligation to acquire as complete an understanding of the normal developmental biology of this gland as possible. Second, epidemiologic studies in the United States and other countries, such as Japan, have shown that diet and weight appear to influence the incidence of breast cancer in women (Henderson, 1990). And thirdly, epidemiologic data have tied the length and amount of estrogen exposure during a woman's lifetime to breast cancer, i.e., the length and amount of estrogen exposure was directly associated with the onset of puberty (Bernstein et al., 1991). Bernstein

and his colleagues also found that the onset of puberty can be controlled by diet and exercise and appears earlier in young females that are heavier than their female counterparts for any given age and height. Hence, it is imperative that researchers develop an understanding of the effect of weight gain and feed consumption on the mouse mammary gland model during the early stages of TEB development, i.e., prior to puberty.

The results of the present study focus on the prepubertal and pubertal growth periods. No strong linear correlations were found between mean MTEB area or mean NTEB/G and IW, FW, TWG or TFC in either growth period for any of the six glands analyzed. Multiple regression analyses confirmed the nonlinearity between these variables and showed that even when the independent variables were analyzed together, they were not good predictor variables of TEB size or number.

In examining the relationship between high, medium, and low independent variable groups within each experiment (ANOVA) with mean MTEB area, none of the between groups analyses were significant. One possible explanation for this lack of significance is the absence of broad numerical differences between the groups. However, consistent numerical trends were observed in both experimental groups and may be indicators of developmental change nonetheless. One such trend was observed in the FW analyses in which there was a consistent inverted "U" distribution in the 2 week experiment and a consistent "U" distribution in the 3 week experiment for mean MTEB area. It

is this author's opinion that the numerical trends in FW may be partially explained by the maturation of the mammary ductal tree as a function of age and the secretion of estrogen and progesterone by the ovary, in addition to the influence of weight, on the developing mammary gland. In the 2 week experiment, where an inverted "U" distribution was observed, those mice that had gained the least weight, i.e., had low FWs, may not have reached their maximum TEB growth by 5 weeks of age and those mice that gained the most weight i.e., had high FWs, may have surpassed their maximum TEB growth (had an early onset of estrous) and have more TEDs than TEBs in their mammary glands.

By 6 weeks of age, the rate of weight gain dramatically decreases in the mouse and therefore weight gain as a factor in influencing TEB size becomes less significant. However, other factors such as an increase in the release of ovarian hormones, which begin to exert a significant influence on mammary development by 6 weeks of age, may also be partially responsible for the "U" distribution observed in the 3 week experiment. The hormones of estrous result in a cyclical presence of larger TEB structures between 6 and 9 weeks of age. It is important to recognize that, while there are differences in the mean MTEB areas between these weight groups within the same gland, they are minor and the overall trend is toward a decrease in TEB size by 6 weeks of age (Chapter 4).

Additional statistical tests such as the paired T-test and Wilcoxon matched-pairs signed-ranks test used to analyze

the data by conserving litter pairs, decreases the genetic variability factor when comparing high and low independent variable categories within a litter. The paired T-tests for IW, FW, TWG and TFC in the 2 and 3 week experiments showed a variety of trends. In the 2 week experiment, mice with larger IWs and TFC had larger mean TEB areas in the thoracic glands compared to mice with lower IWs and TFC. However, none of the mean values for area in the 3 week experiment for IW were significantly different; due to the fact that the mean TEB area has decreased by 6 weeks of age in all 6 glands and there is very little numerical difference between the gland means at this age.

In both the 2 and 3 week experiments, there were no significant differences in the mean MTEB area for any of the glands when comparing high and low groups for FW and TWG. However, a numerical trend in TWG was present in the 3 week experiment. Here the mice in the group with lower TWG had higher numerical mean MTEB areas in the thoracic glands. The lack of significance in FW and TWG is most likely associated with the absence of numerical differences between litter mates. Many of the litters had mice that gained similar amounts of weight over the 2 and 3 week growth periods, thereby making the difference between high and low groups within a litter very small at times. This author believes that the similar genetic make up of the litter mates played a significant role in the phenotypic expression of weight gain and final weight among litters.

In the 2 week experiment none of the mice had gland areas (mean maximum TEB areas) that were significantly different when analyzed for TFC. In the 3 week experiment, both the mean MTEB areas in the No. 2 thoracic glands and LNo. 4 inguinal gland were significantly different but in the negative direction i.e., the group with higher TFC had smaller mean MTEB area values. The trend at 3 weeks for TFC was similar to the numerical trend for TWG at 3 weeks and is not surprising due to the high correlation between these two independent variables. One possible explanation for these trends is that by 6 weeks of age ovarian hormones may be the primary regulator of TEB size. Therefore, no matter how much weight the animal has gained or feed the animal has consumed, by 6 weeks of age the TEBs are regressing into TEDs due to: 1) the influence of ovarian hormones, 2) the limits of the mammary gland fat pad, and 3) the degree of epithelial density. As a result, in order to detect the influence of weight or feed consumption on TEB development, as measured by the maximum TEB area, experiments must be designed to examine mice prior to sexual maturity (less than 6 weeks of age) due to the effect of ovarian hormones on TEB regression at sexual maturity.

The homogeneity of the paired data was addressed by performing a Wilcoxon matched-pairs signed-ranks test in which threshold values were used. This test analyzed only those litter pairs that had moderate numerical differences between high and low independent variable values. The disadvantage of

this test was that it diluted the data by decreasing the number of litter pairs that were used in the analysis. The advantage was that it uncovered important trends, as supported by the near significant p values of .07 to .09, which were masked in the other tests and can be explored in future studies. In the 2 week experiment testing for IW differences, 4 out of 4 of the mean MTEB areas in the thoracic glands were significantly, or were nearly significantly, different in a positive direction, i.e., the mice with higher IW had larger mean TEB areas. In the 2 and 3 week experiments with FW as the independent variable, there was a significant degree of homogeneity among litter pairs such that only 1/3 of the litter pairs met the threshold value making it difficult to draw any conclusions about the data.

The number of TEBs per gland was a more subjective measure than the mean MTEB area for measuring prepubertal-pubertal mammary gland development against IW, FW, TWG and TFC. In the 2 week experiment the paired T-test used for analyzing the effect of FW on the mean NTEB/G showed the RNo. 3 and RNo. 4 glands were statistically significant in the negative direction; suggesting that mice with larger final weights have smaller numbers of TEBs $\geq .03mm^2$. The results for TWG and TFC in the 2 week experiment were similar to those of FW, i.e., those mice that gained more weight and ate more by 5 weeks of age had a smaller number of TEBs per gland with an area of $\geq .03mm^2$.

In conclusion, the results of this study show that TEB size and number in the prepubertal-pubertal mouse mammary gland are influenced most consistently and significantly by IW and TFC, and FW, TWG, and TFC respectively, during the prepubertal growth period (5 weeks of age) when threshold limits are set. Furthermore, values for certain gland means, namely the thoracic gland means, had the greatest degree of significance and consistency. Therefore, future studies examining the effect of weight and feed consumption on TEB size should focus on the thoracic glands in juvenile and prepubertal mice. At 6 weeks of age, during the pubertal growth period, the TEBs in the mouse mammary gland have surpassed their maximum size in all glands (see Chapter 4) and therefore it is difficult to draw conclusions concerning TEB size and number as a function of the independent variables analyzed in this part of the study.

Future studies are needed to further investigate the effect of body weight and feed consumption on TEB size and number in the juvenile (4 weeks of age) and prepubertal (5 weeks of age) mouse mammary gland. For many decades the scientific community has focused on analyzing the mature virgin and lactating mammary glands. However, with the confirmed presence of stem cells in the TEB of the rodent mammary gland during the juvenile and prepubertal growth periods (Williams and Daniel, 1983; Dulbecco et al., 1983; Chapter 3) and documentation showing that TEB structures are associated with increased susceptibility to carcinogenesis

(Russo and Russo, 1987) it is important to closely examine variables that may affect the development of the gland prior to 6 weeks of age.

SUMMARY

Summary

The primary objective of this work was to investigate the growth and morphologic development of the terminal end bud structure in the prepubertal-pubertal mouse mammary gland. The first two studies consisted of experiments which analyzed the different cell types in the TEB and examined their relationship with cells in the extracellular matrix. The latter two studies analyzed the growth of the TEB structures as a function of gland origin, age, weight and diet.

In Chapters 2 and 3, TEB structures were collected from No. 2 and No. 3 thoracic and No. 4 inguinal glands of Balb/c and Athymic nude (Nu/+) mice between 4 and 5 weeks of age. The four major cell types previously documented in the literature, the cap cell, myoepithelial cell, intermediate cell, and luminal cell were confirmed by ultrastructural analysis. In addition, a fifth cell type the "myocap cell" was also identified without the aid of special markers. Detailed qualitative and quantitative analysis of the epithelial cells comprising the TEB showed that the undifferentiated cap cell, located at the perimeter of the anterior aspect of the TEB, had the largest mean cellular and nuclear areas in the TEB and possessed no specialized intercellular junctions or adhesions. The inability to positively identify gap junctions in over 100 the cap cells in this study, along with other qualitative characteristics, supports the theory that the cap cells are in fact the stem

cells of the mammary gland (stem cells do not possess gap junctions).

The cap cell membranes, while not appearing to possess gap junctions, were found to engage in extensive endo- and exo-micropinocytosis. The basal lamina at the tip of the TEB adjacent to the basal cap cell membrane was found to be discontinuous in the presence of exo-micropinocytotic activity in the mouse mammary gland. This study visually documented, for the first time, discontinuity of the basal lamina this species (discontinuity of the basal lamina has been documented in the rat mammary gland). However, at no time did the exposed cap cell membrane come in direct contact with adjacent ECM stromal cells.

The undifferentiated cap cells were often surrounded by intercellular spaces of various size which separated them from each other, as well as from the underlying intermediate cells. The presence of these spaces is believed to be associated with hyaluronate secretion by the cap cells and is most likely a function of the number and/or metabolic activity of the cap cell and the age of the mouse, i.e., as the mouse matures sexually the TEBs regress into TEDs where the number of cap cells and level of hyaluronate secretion are decreased and eventually lost. The intercellular spaces present between the cap cells and intermediate cells were often associated with a space of variable width in the ECM adjacent to the tip of the TEB. This space, termed the "clearance zone" by the author, was present in many, but not all, of the larger more

mitotically active TEB structures. When present, the clearance zone is crescent shaped and ranges from 15 - 100 micrometers in width (average width 50 μm). The primary function of the clearance zone is most probably to facilitate the migration of the TEB throughout the mammary gland fat pad. The adjacent cap cell basal lamina was frequently incomplete (devoid of the outer anionic layer) but not discontinuous except in the regions where exo-micropinocytosis occurred. In addition, the clearance zone often contained occasional mononuclear cells and fibroblasts In TEBs where the clearance zone was not present, the basal cap cell membranes were separated from adipocyte and fibroblast membranes by a complete intact basal lamina.

The myoepithelial cells, first visualized in the flank region of the TEB structure, are amongst the smallest cells in the TEB. Their membranes possess multiple desmosomes, with an average of 3 to 4 desmosomes in any given plane. These points of adhesion are concentrated at the lateral and internal membrane borders between adjacent myoepithelial cells and underlying intermediate or luminal cells. The lack of such adhesions on the basal lamina membrane between the myoepithelial cells and the basal lamina is most likely a reflection of cap cell to myoepithelial cell differentiation, excess basal lamina and myoepithelial perimeter migration. No hemi-desmosomes, present in mature mouse mammary ducts, were observed in the TEB myoepithelial cells between the basal lamina and the basal membrane border anterior to the neck

region.

The "myocap cell" is present near the flank region, anterior to the MEC. This cell has the nuclear and cytoplasmic characteristics of a cap cell but, in addition, the cytoplasm contains myofilaments found in MECs. Identification of this cell type is supported by previous time-lapse microcinematography experiments and autoradiographic studies in the literature that show the MEC is a direct descendent of the cap cell.

The intermediate cells are a large population of morphologically diverse cells located beneath the cap cell layer and anterior to the luminal cell layer. Their qualitative cellular characteristics vary according to their placement in the TEB. The outer ICs have cellular characteristics similar to the cap cells. The inner ICs are more differentiated and posses many of the cellular characteristics of the luminal cells such as junctional complexes, adhesions and microvilli. The ICs are believed to be "pre-luminal" cells and eventually migrate to an internal luminal position where they become fully differentiated luminal cells.

The differentiated luminal cells have the smallest nuclear and cellular areas of any of the TEB epithelial cells. They possess several specialized membrane alterations such as tight and intermediate junctions as well as desmosomes and abundant microvilli. In addition to the aforementioned membrane specializations, it is important to note that all the

cells within the TEB structure engage in endo- and exo-micropinocytotic activity which indicates that this is one mechanism of intercellular communication acquired at an early stage of differentiation and maintained throughout the differentiation process.

In chapter 4 the development and differential growth pattern of the TEB structures in the prepubertal - pubertal mouse mammary gland was investigated. The results of this study showed that the TEB develops asynchronously with respect to: 1) the gland of origin, 2) the age of the mouse, and 3) the location of the TEB within the mammary gland. The No. 2, No. 3 and No. 4 mammary glands were collected from 5 and 6 week old athymic nude (Nu/+) mice weaned at 21 days of age and fed a high fat non-restricted intake diet (which allowed for optimum growth of the ductal structures) for 2 and 3 weeks respectively. Over 700 TEBs were measured in this study from whole mount preparations using an image analyzer. The mean maximum terminal end bud (MTEB) area, in mm^2, was calculated from the 5 largest TEBs per gland and used to reject or accept the null hypothesis which stated the mean MTEB area of gland No.2 = No. 3 = No. 4 within a mouse. At 5 and 6 weeks of age, the mean MTEB area from the No. L3 and No. R3 glands was significantly larger than the mean MTEB area from the No. L4 and No. R4 glands, suggesting that the gland of origin is a significant factor in determining the maximum attainable size of a TEB structure during this growth period. In addition, the No. L2 and No. R2 gland areas, while not significantly

less than the No. 3 gland areas, were significantly greater than the No. 4 gland areas. By 6 weeks of age the mean MTEB area of the No. 2 glands and No. 4 glands was almost identical. This decrease in TEB size for the No. 2 gland between 5 and 6 weeks of age was statistically significant and indicated that the largest TEB structures in the No. 2 glands occur prior to 6 weeks of age. Numerical decreases in mean MTEB area, range, mode and maximum TEB area for the No. 3 and No. 4 glands between 5 and 6 weeks of age also suggest that the maximum TEB size is reached in all glands during the prepuberal - pubertal growth period prior to 6 weeks of age. Therefore, not only is the gland of origin significant in determining maximum TEB size but the age of the mouse is also significant.

In addition to the mean MTEB area, the number of TEBs per gland was also calculated in this study and showed results similar to the mean MTEB areas, i.e., the No. 2 and No. 3 glands had the greatest number of TEBs at 5 weeks of age. At 6 weeks of age there was a dramatic decrease in the number of TEBs in the No. 2 gland while the No. 3 and No. 4 glands remained relatively stable.

Light microscopic analysis of selected TEB structures confirmed that the larger TEBs were located at the peripheral leading edge of the advancing ductal tree and contained increased numbers of cap cells or "stem cells." Therefore, the results of this study suggest that if the maximum size and number of TEBs (bearing the greatest number of stem cells)

are present in the mouse mammary gland prior to 6 weeks of age, then the No. 2 gland at 5 weeks of age and the No. 3 gland at 5 to 6 weeks of age should be more susceptible to initiation and promotion events during these specific growth periods.

The relationship between the size of the TEB and various weight variables, as well as total feed consumed, was investigated in Chapter 5. The independent variables of IW, FW, TWG, and TFC were tested against the mean MTEB areas and mean NTEB/gland calculated in Chapter 4. Pearson correlation tests and multiple regression analyses showed that no strong linear correlations were present between the 2 dependent variables (mean MTEB area and mean NTEB/gland) and any of the independent variables in either 5 or 6 week old mice. Moreover, the independent variables taken together were shown not to be good predictor variables of TEB size or number. However, further analysis showed that when litter pairs were conserved, in order to decrease genetic variability, and threshold values were imposed, significant relationships between the dependent and independent variables were uncovered. For example, in the 2 week experiment using the paired T-test, mice with larger IWs had larger mean MTEB areas in the thoracic glands compared to mice with lower IWs. In the 3 week experiment, mice with greater TFC had larger mean TEB areas in the No. 2 thoracic glands compared to mice with less TFC. The results of this study suggest that a higher weight at weaning may contribute to the presence of larger

TEBs during the prepubertal growth period (as measured at 5 weeks of age) and during the pubertal growth period (by 6 weeks of age) greater feed consumption may contribute to larger TEBs.

Overall, the statistical tests used to analyze weight and feed consumption in the 3 week experiment (6 week old mice) when litter pairs were not conserved and threshold values were not set were statistically insignificant. One reason for the lack of significance at this age is the dramatic decrease in TEB area and number observed in all of the glands during puberty. In addition to this chronological ovarian-dependent decrease in TEB size and number by 6 weeks of age, the rate of weight gain also levels out in the majority of mice during the pubertal growth period and adds to the lack of statistical significance found in the 6 week data. An important observation obtained from this study was that no matter how much weight the mouse gained or feed the mouse consumed, by 6 weeks of age the TEBs were decreasing in size, i.e. regressing into TEDs, and number and therefore no consistent positive correlations between area and number, and weight and feed consumption were found at this age. Also many of the litters had mice that gained similar amounts of weight (TWG) and had negligible differences in their final weight (FW) values (especially in the 3 week experiment) making the weight differences between high and low groups within a litter extremely small and decreasing the likelihood of finding statistical significance in either experiment.

In the Wilcoxon matched-pairs signed-ranks test where threshold values were imposed, a significant trend between the mean MTEB area in 4 out of 4 thoracic glands for IW was found. While this finding is significant and indicates that IW, i.e., the weight at weaning, may influence the maximum attainable size of TEBs in the prepubertal mammary gland, dilution of the data decreased the overall significance of this positive outcome.

The results of this study showed that TEB size and the number of TEBs per gland in the mouse mammary glands are influenced most consistently and significantly by IW at 5 weeks of age, and by TFC at 6 weeks of age. The study also showed that the thoracic gland means had the greatest degree of significance and consistency compared to the inguinal glands. Therefore, future studies which examine the effect of independent variables on TEB morphology should focus on the juvenile and prepubertal growth periods and on TEB development in the thoracic glands. As opposed to the pubertal growth period when the TEBs are regressing and the cap cell numbers are decreasing.

There is still much to be learned about the cap cell, "stem cell", population present during the prepubertal-pubertal growth period in regards to differentiation, TEB migration, hyaluronate secretion and increased susceptibility to carcinogenesis, i.e., the effect of initiators, promoters, and radiation. The number and types of receptors present on TEB epithelial cell membranes (particularly the cap cells),

their ability to interact with growth factors, the types of proteins they produced and how they interact with the ECM also require further exploration. It is likely that a better understanding of the normal biology and physiology of the prepubertal TEB structure and its cell types will eventually give the research community more insight into the mechanisms of mammary gland carcinogenesis and ultimately breast cancer.

LIST OF REFERENCES

REFERENCES

Abraham, S. Faulkin, L.J., Hillyard, L.A. and Mitchell, D.J. (1984). Effect of dietary fat on tumorigenesis in the mouse mammary gland. J. Natl. Can. Inst. 72, 1421-1429.

American Cancer Society (1992). Cancer Facts and Figures - 1992. Atlanta, GA.

Austin, C.R. and Rowlands, I.W. (1969). Mammalian reproduction. In The L.A.T. Manual of Laboratory Animal Practice and Techniques, eds. D.J. Short and D.P. Woodnott, pp. 340-349. Springfield, Illinois: Charles C. Thomas - Publisher.

Balinsky, B.I. (1950). On the prenatal growth of the mammary gland rudiment in the mouse. J. Anat. 84, 227-388.

Banerjee, M.R., Wood, B.G., Lin, F.K., and Crump, L.R. (1976). Organ culture of whole mammary gland of the mouse. In Tissue Culture Association Manual, Vol.2, pp. 457-462. Tissue Culture Association, Rockville, MD.

Bartley, J.C., Emerman J.T. and Bissell M.J. (1981). Metabolic cooperativity between epithelial cells and adipocytes of mice. Cell Physiol. 10, C204-C208.

Bennett, D.C., Peachey, L.A., Durbin, H. and Rudland, P.S. (1978). A possible mammary stem cell line. Cell 15, 283-298.

Bernfield, M., Banerjee, S.D., Koder, J.E., and Rapraeger, A.C. (1984). Remodeling of the basement membrane as a mechanism for morphogenetic tissue interactions, In The Role of the Extracellular Matrix in Development, pp. 545-572. New York: A.R. Liss.

Bernstein, L., Pike, M.C., Ross, R.K. and Henderson, B.E. (1991). Age at menarche and estrogen concentrations of adult women. Cancer Causes Control 2, 221-5.

Bissell, M. and Hall H.G. (1987). Form and function in the mammary gland: The role of extracellular matrix. In The Mammary Gland: Development, Regulation, and Function, eds. Neville, M.C. and Daniel, C.W., pp.97-136. New York: Plenum Press.

Bonhomme F. and Guenet, J-L. (1989). The wild house mouse and its relatives. In Genetic Variants and Strains of the Laboratory Mouse, eds. Lyon, M.F. and Searle, A.G., pp. 649-662. New York: Oxford University Press.

Buehring, G.C. and Jensen, H.M. (1983). Lack of toxicity of methylene blue chloride to supravitally stained human mammary tissues. Can. Res. 43, 6039-6044.

Carroll, K.K., Gamal, E.B. and Plunkett, E.R. (1968). Diet and mammary cancer. J. Can. Med. Assoc. 98, 590-594.

Ceriani, R.L. (1970a). Fetal mammary gland differentiation in vitro in response to hormones I. Morphologic findings. Dev. Bio. 21, 506-529.

Ceriani, R.L. (1970b). Fetal mammary gland differentiation in vitro in response to hormones II. Biochemical findings. Dev. Bio. 21, 530-546.

Chan, P.C., Head, J.F., Cohen, L.A. and Wynder, E.L. (1977). Influence of dietary fat on the induction of mammary tumors by N-nitrosomethylurea: Associated hormone changes and differences between Sprague-Dawley and F344 rats. J. Natl. Can. Inst. 59, 1279-1283.

Chiquet, M. and Fambrough, D.M. (1984b). Chick myotendinous antigen. II. A novel extracellular glycoprotein complex consisting of large disulfide-linked subunits. J. Cell Bio. 98, 1937-1946.

Chiquet-Ehrismann, R., Mackie, E.J., Pearson, C.A, and Sakaura, T. (1986). Tenascin: An extracellular matrix protein involved in tissue interactions during fetal development and oncogenesis. Cell 47, 131-139.

Chiquet-Ehrismann, R., Kalla, P., Pearson, C.A., Beck, K., and Chiquet, M. (1988). Tenascin interferes with fibronectin action. Cell 53, 383-390.

Christensen, G. C. (1964). The urogenital system and mammary glands. In Anatomy of the Dog, eds. M.E. Miller, G.C. Christensen, and H.E. Evans, pp. 741-806. Philadelphia: W.B. Saunders Co.

Cole, H.A. (1933). The mammary gland of the mouse during the estrous cycle, pregnancy, and lactation. Proc. Royal Soc.Bio. 114, 136-161.

Coleman, D.L., Dagg, C.P., Fuller, J.L., Green, M.C., Kaliss, N., Russell, E.S. and Staats, J. (1975). Biology of the Laboratory Mouse. New York: Dover Publications Inc.

Coleman, S., Silberstein, G. B., and Daniel, C. W. (1988). Ductal morphogenesis in the mouse mammary gland: evidence supporting a role for epidermal growth factor. Dev. Bio. 127, 304-315.

Cotran, R.S., Kumar, V. and Robbins, S.L. (1989). Robbins Pathologic Basis of Disease. Philadelphia: W.B. Saunders Company.

Cowie, A.T. (1949). The relative growth of the mammary gland in normal gonadectomized and adrenalectomized rats. J. Endrocrinol. 6, 147-157.

Daniel, C.W., DeOme, K.B., Young, J.T., Blair, P.B. and Faulkin, L.J. (1968). The in vivo lifespan of normal and preneoplastic mouse mammary glands: A serial transplantation study. Proc. Natl. Acad. Sci. USA. 61, 52-60.

Daniel, C.W. and Silberstein, G.B. (1987). Postnatal development of the rodent mammary gland. In The Mammary Gland: Development, Regulation, and Function eds. Neville, M.C. and Daniel, C.W., pp. 3-31. New York: Plenum Press.

Daniel, C. W., Silberstein, G. B., Van Horn, K. Strickland, P. and Robinson S. (1989). TGF-ß1-induced inhibition of mouse mammary ductal growth: developmental specificity and characterization. Dev. Bio. 135, 20-30.

Dawes, C.J. (1971). Biological Techniques in Electron Microscopy. New York: Barnes and Noble.

Dembinski, T.C., Leung, C.K.H., and Shiu, R.P.C. (1985). Evidence for a novel pituitary factor that potentiates the mitogenic effect of estrogen in human breast cancer cells. Can. Res. 45, 3083-3089.

Dembinski, T.C., and Shiu, R.P. (1987). Growth factors in mammary gland development and function. In The Mammary Gland: Development, Regulation, and Function, pp. 355-373, eds. M.C. Neville and C.W. Daniel. New York: Plenum Press.

DeOme, K.B., Faulkin, L.J., and Bern, H.A. (1959). Development of mammary tumors from hyerplastic alveolar nodules transplanted into gland free mammary fat pads of female C3H mice. Can. Res. 19, 515-520.

Du Bois, M. and Elias, J.J. (1984). Subpopulations of cells in immature mouse mammary glands as detected by proliferative responses to hormones in organ culture. Dev. Bio. 106, 70-75.

Dulbecco, R., Henahan, M., and Armstrong, B. (1982). Cell types and morphogenesis in the mammary gland. Proc. Natl. Acad. Sci. USA 79, 7346-7350.

Dulbecco, R., Unger, M., Armstrong, B., Bowman, M., and Syka, P. (1983). Epithelial cell types and their evolution in the rat mammary gland determined by immunological markers. Proc. Natl. Acad. Sci. USA 80, 1033-1037.

Elias, J.J. (1959). Effect of insulin and cortisol on organ cultures of adult mouse mammary gland. Proc. Soc. Exp. Biol. Med. 101, 500-502.

Ervin, P.R. Jr., Kamiski, M.S., Cody, R.L. and Wicha, M.S. (1989). Production of mammastatin, a tissue-specific growth inhibitor by normal human mammary cells. Sci. 244, 1585-7.

Faulkin, L.J., Abraham, S., Mitchell, D.J. and Hillyard, L.A. (1986). Effects of dietary fat on mammary development relative to age and hormones in balb/c mice (42295). Proc. Soc. Exp. Bio. and Med. 181, 575-585.

Faulkin, J.R., and DeOme, K.B. (1960). Regulation of growth and spacing of gland elements in the mammary fat pad of the C3H mouse. J. Natl. Can. Inst. 24, 953-969.

Festing, M.F.W. (1989). Inbred strains of mice. In Genetic Variants and Strains of the Laboratory Mouse, eds. Lyon M.F.and Searle, A.G., pp. 636-648. New York: Oxford University Press.

Finbow, M.E., Buultjens, T.E.J., John, S. Kam, E., Meagher, L. and Pitts, J.D. (1986). Molecular structure of the gap junctional channel. In Junctional Complexes of Epithelial Cells: Ciba Foundation Symposium 125, pp. 92-107. Chichester: Wiley.

Furlanetto, R.W. and DiCarlo, J.N. (1984). Somatomedin -C receptors and growth effects in human breast cells maintained in long-term tissue culture. Can. Res. 44, 2122-2128.

Gilula, N.B. (1974). Junctions between cells. In Cell Communication, ed. R.P. Cox, pp.1-29. New York: John Wiley and Sons.

Gordon, J.R. and Bernfield, M.R. (1980). The basal lamina of the postnatal mammary epithelium contains glycosaminoglycan in a precise ultrastructural organization. Dev. Bio. 74, 118-135.

Glauert, A.M. (1975). Fixation, dehydration and embedding of biological specimens. In Practical Methods in Electron Microscopy, ed. A.M. Glauert. New York: American Elsevier Publishing Co.

Green, M.C. (1989). Catalog of mutant genes and polymorphic loci. In Genetic Variants and Strains of the Laboratory Mouse, eds. Lyons, M.F. and Searle, A.G., pp. 12-264. New York: Oxford University Press.

Hausman, G.J. and Thomas, G.B. (1984). Enzyme histochemical differentiation of white adipose tissue in the rat. Am. J of Anatomy 169, 315-326.

Henderson, B.E. (1990). Summary report of the sixth symposium on cancer registries and epidemiology in the pacific basin. J. Natl. Can. Inst. 82, 1186-1190.

Heuberger, B., Fitzka, I., Wasner, G. and Kratochwil, K. (1982). Induction of androgen receptor formation by epithelial-mesenchymal interactors in embryonic mouse mammary gland. Proc. Nat. Acad. Sci. USA 79, 2957-2961.

Hollman, K.H. (1969). Quantitative electron microscopy of sub-cellular organization in mammary cells before and after parturition. In Lactogenesis: The Initiation of Milk Secretion at Parturition, eds. M. Reynolds and S.J. Folley. Philadelphia: University Pennsylvania Press.

Hoshino, K. (1964). Regeneration and growth of quantitatively transplanted mammary glands of normal female mice. Anat. Rec. 150, 221-236.

Hoshino, K. (1967). Transplantability of mammary gland in brown fat pads of mice. Nature. 213, 194-195.

Hoshino, K. (1978). Mammary transplantation and its histogenesis in mice. In Physiology of Mammary Glands, eds, A. Yokoyama, H. Mizuno, and H. Nagasawa, pp. 163-195. Baltimore: University Park Press.

Howlett, A.R. and Bissell, M.J. (1990). Regulation of mammary epithelial cell function: a role for stromal and basement membrane matrices. Protoplasma 159, 85-95.

Hudson, C.S., Rash, J.E. and Graham, W.F. (1979). Introduction to sample preparation for freeze fracture. In Freeze Fracture: Methods, Artifacts, and Interpretation, eds. J.E. Rash and C.S. Hudson, pp. 1-10. New York: Raven Press.

Humason, G.L. (1979). Animal Tissue Techniques. 4th ed. San Francisco: Freeman and Co.

Inaguma, Y., Kersakabe, M. Mackie, E.J., Pearson, C.A., Chiquet-Ehrismann, R. and Sakakura, T. (1988). Epithelial induction of stromal tenascin in the mouse mammary gland: From embryogenesis. Dev. Bio. 128, 245-255.

Karnovsky, M.J. (1965). A formaldehyde-glutaraldehyde fixative of high osmolality for use in electron microscopy. J. Cell Bio. 27, 137a-138a.

Kiernan, J.A. (1990). Histological and Histochemical Methods, 2nd Edition. New York: Pergamon Press.

Klomparens, K.L., Flegler, S.L. and Hooper, G.R. (1986). Procedures for Transmission and Scanning Electron Microscopy for Biological and Medical Science. Burlington, VT: Ladd Research Industries.

Knazek, R.A., Liu, S.C. Bodwin, J.S. and Vonderhaar, B.K. (1980). Requirement of essential fatty acids in the diet for development of the mouse mammary gland. J. Natl. Can. Inst. 64, 377-382.

Knight, C.H. and Peaker, M. (1982). Development of the mammary gland. J. of Reprod. Fertil. 65, 521-536.

Kratochwil, K. (1969). Organ specificity in mesenchymal induction demonstrated in the embryonic development of the mammary gland of the mouse. Dev. Bio. 20, 46-71.

Kratochwil, K. and Schwartz, P. (1976). Tissue interaction in androgen response of embryonic mammary rudiment of mouse: identification of target tissue for testosterone. Proc. Natl. Acad. Sci. USA 73, 4041-4044.

Kratochwil, K. (1977). Development and assessment of androgen responsiveness in the embryonic mammary rudiment of the mouse mammary gland. Dev. Bio. 61, 358-365.

Levine, J.F. and Stockdale, F.E. (1985). Cell-cell interactions promote mammary epithelial cell differentiation. J. Cell Bio. 100, 1415-1422.

Lyons, W.R. (1958). Hormonal synergism in mammary growth. Proc. R. Soc. (London) Ser. B. 149, 303-325.

Lyons, W.R., Li, C.H. and Johnson, R.L. (1958). The hormonal control of mammary growth and lactation. Recent Prog. Horm. Res. 14, 219-254.

Medina, D. and Smith, G. H. (1990). In search of mammary stem cells. Protoplasma 159,77-84.

Miyamoto-Tiavin, M.J., Hillyard, L.A. and Abraham, S. (1981). Influence of dietary fat on the growth of mammary ducts in balb/c mice. J. Natl. Can. Inst. 67, 179-188.

Myal, Y., Shiu, R.P., Bhaumick, B. and Bala, M. (1984). Receptor binding and growth-promoting activity of insulin-like growth factors in human breast cancer cells (T-47D) in culture. Can. Res. 44, 5486-5490.

Myers, J.A. (1917). Studies on the mammary gland. II. The fetal development of the mammary gland on the albino rat. Am. J. Anat. 22, 195-223.

Nandi, S. (1958). Endocrine control of mammary gland development and function in the C3H/He Crgl mouse. J. Natl. Can. Inst. 21, 1039-1063.

Nandi, S. (1959). Hormonal control of mammogenesis and lactogenesis in the C3H/He Crgl mouse. Univ. of Calf. Publ. Zoology 65, 1-128.

Newman, C.B., Cosby, H., Friesen, H.G., Feldman, M., Cooper, P. and Kleinberg, D. (1987). Evidence for a nonprolactin, non-growth hormone mammary mitogen in the human pituitary gland. Proc. Natl. Acad. Sci. USA 84, 8110-8114.

Olds, R.J. and Olds, J.R. (1979). A colour atlas of: The Rat - Dissection Guide. London: Wolfe Medical Publications LTD.

Pesce, C.M. (1987). Biology of disease: Defining and interpreting diseases through morphometry. Lab. Invest. 56, 568-575.

Pitelka, D.R., Hamamoto, S.T., Duafala, J.G. and Nemanic, M.K. (1973). Cell contacts in the mouse mammary gland: I. Normal gland in postnatal development and the secretory cycle. J. of Cell Bio. 56, 797-818.

Pitelka, D.R. and Hamamoto, S.T. (1977). Form and function in the mammary epithelium: The interpretation of ultrastructure. J. Dairy Sci. 60, 643-654.

Popesko, P., Rajtova, V. and Horak, J. (1992). A Colour Atlas of Small Laboratory Animals Vol. 2: Rat, Mouse and Hamster. London: Wolfe Publishing.

Propper, A.Y. (1978). Wandering epithelial cells in the rabbit embryo milk line. Dev. Bio. 67, 225-231.

Rao, G.A. and Abraham, S. (1976). Brief Communication: Enhanced growth rate of transplanted mammary adenocarcinoma induced in C3H mice by dietary linoleate. J. Natl. Can. Inst. 56, 431-432.

Raynaud, A. (1961). Morphogenesis of the mammary gland. In Milk: The Mammary Gland and Its Secretion, eds. S. K. Kon and A.T. Cowie, Vol. 1, pp. 3-46. New York: Academic Press.

Rhodin, J.A.G. (1977). Histology: A Text and Atlas. New York: Oxford University Press.

Rugh, R. (1968). The Mouse: Its Reproduction and Development. Minneapolis: Burgess Publishing.

Russo I.H. and Russo J. (1978). Developmental stage of the rat mammary gland as determinant of susceptibility to 7,12-dimethlybenz[a]anthrancene. J. Natl. Can. Inst. 61, 1439-1449.

Russo, J., and Russo, I.H. (1987). Biological and molecular bases of mammary carcinogenesis. Lab. Invest. 57, 112-137.

Ryerse, J.S. and Nagel, B.A. (1991). Gap-junction quantification in biological tissues: freeze-fracture replicas versus thin section. J. Microscopy 163, 65-78.

Sakakura, T., Nishizuka, Y. and Dawe, C.J. (1976). Mesenchyme-dependent morphogenesis and epithelium-specific cytodifferentiation in the mouse mammary gland. Science 194, 1439-1441.

Sakakura, T., Nishizuka, Y. and Dawe, C. J. (1979). Capacity of mammary fat pads of adult C3H/HeMs mice to interact morphogenetically with fetal mammary epithelium. J. Natl. Can. Inst. 63, 733-736.

Sakakura, T., Sakagami, Y. and Nishizuka, Y. (1979). Persistence of Responsiveness of adult mouse mammary gland to induction by embryonic mesenchyme. Dev. Bio. 74, 201-210.

Sakakura, T., Sakagami, Y. and Nishizuka, Y. (1982). Dual origin of mesenchymal tissues participating in mouse mammary gland embryogenesis. Dev. Bio. 91, 202-207.

Sakakura, T. (1987). Mammary embryogenesis. In The Mammary Gland: Development, Regulation, and Function, eds. M.C. Neville and C. W. Daniel, pp. 37-63. New York: Plenum Press.

Sekhri, K.K., Pitelka, D.R. and DeOme, K.B. (1967). Studies of the mouse mammary gland. I. Cytomorphology of the normal mammary gland. J. Natl. Cancer Inst. 39, 459-490.

Shea, S.M. (1971). Lanthanum staining of the surface coat of cells: Its enhancement by the use of fixatives containing alcian blue or cetylpyridinium chloride. J. Cell Bio. 51, 611-620.

Shiu, R.P. (1981). Prolactin, pituitary hormones and breast cancer. In Hormones and Breast Cancer, Banbury Report 8, eds. M.C. Pike, P.K. Siiteri and C.W. Welsch, pp. 185-196. New York: Cold Spring Harbor Laboratory.

Shiu, R.P., Lima, G., Leung, C.K. and Dembinski, T.C. (1986a). Intrinsic and extrinsic factors in estrogen action in human breast cancer. Role of polamines and pituitary factors. J. Steroid Biochem. 24, 133-138.

Silberstein, G.B and Daniel, C.W. (1982a). Glycosaminoglycans in the basal lamina and the extracellular matrix of the developing mouse mammary duct. Dev. Bio. 90, 215-222.

Silberstein, G.B., and Daniel, C.W. (1982b). Elvax 40P implants: sustained local release of bioactive molecules influencing mammary ductal development. Dev. Bio. 93, 272-278.

Sliverstone, H. and Tannenbaum, A. (1950). The effect of the preparation of dietary fat on the rate of formation of mammary cancer in mice. Can. Res. 10, 448-453.

Sinha, Y.N. and Tucker, H.A. (1966). Mammary gland growth of rats between 10 and 100 days of age. Am. J. Physiol. 210, 601-605.

Smith, J.A., Winslow, D.P. and Rudland, P.S. (1984). Different growth factors stimulate cell division of rat mammary epithelial, myoepithelial, and stromal cell lines in culture. J. Cell Physiol. 119, 320-326.

Smith R.L. and Bernfield, M. (1982). Mesenchyme cells degrade epithelial basal lamina glycosaminoglycan. Dev. Bio. 94, 378-390.

Sosinsky, G.E., Jesior, J.C., Casper, D.L.D. and Goodenough, D.A. (1988). Gap Junction structures: VIII. Membrane cross-sections. Biophys. J. 53, 709-722.

Staats, J. (1975). The laboratory mouse. In Biology of the Laboratory Mouse, ed. Green, E.L., pp. 1-9. New York: Dover Publications.

Stedman's Medical Dictionary, 25th Edition - Illustrated, eds. W.R. Hensyl and H. Felscher, (1990). Baltimore, MD: Williams and Wilkins.

Taketani, Y. and Oka, T. (1983b). Epidermal growth factor stimulates cell proliferation and inhibits functional differentiation of mouse mammary epithelial cells in culture. Endocrin. 113, 871-877.

Taketani, Y. and Oka, T. (1983c). The functional receptors of EGF in normal mammary epithelial cells. Proc. Natl. Acad. Sci. USA 80, 2647-2650.

Tonelli, Q.J. and Sorof, S. (1980). Epidermal growth factor requirement for development of cultured mammary gland. Nature 285, 250-252.

Thorpe, D.R. (1968). Dissection guide in color: The Rat (and the sheep's brain). Palo Alto, California: National Press Books.

Toole, B.P. and Underhill, C.B. (1983). Regulation of morphogenesis by the pericellular matrix. In Cell Interactions and Development: Molecular Mechanisms, ed. K.M. Yamada, pp. 203-230. New York: John Wiley and Sons.

Topper, Y.J., and Freeman, C.S. (1980). Multiple hormone interactions in the developmental biology of the mammary gland. Physiol. Rev. 60, 1049-1106.

Trosko, J.E., Chang, C.C., Madhukar, B.V. and Oh, S.Y. (1990). Modulators of gap junction function: The scientific basis of epigenetic toxicology. J. Molecular and Cellular Tox. 3, 9-26.

Turner, C.W., and Gomez, E.T. (1933). The normal development of the mammary gland of the male and female albino mouse. I. Intrauterine. Mo. Agric. Exp. Stn. Res. Bull. 182, 3-20.

Unwin, P.N.T. (1986). Gap junction structure and the control of cell-to-cell communication. In Ciba Foundation Symposium 125: Junctional Complexes of Epithelial Cells, pp. 78-91. New York: John Wiley and Sons.

Warburton, M.J., Mitchell, D., Ormerod E.J., and Rudland P. (1982). Distribution of myoepithelial cells and basement membrane proteins in the resting, pregnant, lactating, and involuting rat mammary gland. J. Histochem. and Cytochem. 30, 667-676.

Welch, D.R., Fabra, A. and Nakajima, M. (1990). Transforming growth factor-ß stimulates mammary adenocarcinoma cell invasion and metastatic potential. Proc. Natl. Acad. Sci. USA. 87, 7678-7682.

Wellings, S.R., Grunbaum, B.W., and DeOme, K.B. (1960). Electron microscopy of milk secretion in the mammary gland of the C3H/Crgl mouse. I. Cytomorphology of the prelactating and the lactating gland. J. Natl. Can. Inst. 25, 393-421.

Welsch, C.W., DeHoog, J.V., O'Connor, D.H. and Sheffield, L.G. (1985). Influence of dietary fat levels on development and hormone responsiveness of the mouse mammary gland. Can. Res. 45, 6147-6154.

Welsch C.W. and O'Connor, D.H. (1989). Influence of dietary fat on developmental growth of the mammary gland in immature and mature female balb/c mice. Can. Res. 49, 5999-6007.

Wicha, M.S., Liotta, L.A., Vonderhaar, B.K. and Kidwell, W.R. (1980). Effects of inhibition of basement membrane collagen deposition of rat mammary gland development. Dev. Bio. 80, 253-266.

Williams, J. M. and Daniel, C. W. (1983). Mammary ductal elongation: Differentiation of myoepithelium and basal lamina during branching morphogenesis. Dev. Bio. 97, 274-290.

Wolfe, S.L. (1985). Cell Ultrastructure. Belmont, California: Wadsworth Publishing Co.

Wynder, E.L. (1968). Current concepts of the aetiology of breast cancer. In Prognostic Factors in Breast Cancer [Proceedings of the First Tenvus Symposium], eds. A. Forrest and P. Kunkler, pp. 32-49. Edinburgh: Livingstone.

Yang, J., Guzman, R. Richards, J., Inagawa, W. McCormick, K. and Nandi, S. (1980). Growth factor and cyclic-nucleotide induced proliferation of normal and malignant mammary epithelial cells in primary culture. Endocrin. 107, 35-41.

Zampighi, G., Corless, J.M. and Robertson, J.D. (1980). On Gap junction. J. Cell Bio. 86, 190-198.

Zhang, L. Ranjana, P.B. and Bruce, W.R. (1987). Proliferative activity of murine mammary epithelium as affected by dietary fat and calcium. Can. Res. 47, 4905-4908.